Communauté
UNIVERSITÉ Grenoble Alpes

THÈSE

Pour obtenir le grade de

DOCTEUR DE LA COMMUNAUTÉ UNIVERSITÉ GRENOBLE ALPES

Spécialité: **Matériaux, Mécanique, Génie civil, Electrochimie**

Arrêté ministériel : 7 août 2006

Présentée par

Zainab KAMMOUNA

Thèse dirigée par **Yann MALECOT** et
co-encadrée par **Matthieu BRIFFAUT**

préparée au sein du **Laboratoire Sols, Solides, Structures, Risques (3SR)**
dans **l'École doctorale Ingénierie - Matériaux, Mécanique Energétique, Environnement, Procédés, Production (I-MEP2)**

Effect of creep strains on the residual mechanical properties of concrete

Thèse soutenue publiquement le **27 Octobre 2016**,
devant le jury composé de :

M. Emmanuel FERRIER
Professeur à l'Université de Lyon 1, Président

M. Farid BENBOUDJEMA
Professeur à l'École Normale Supérieure de Cachan, Rapporteur

M. Ismail YURTDAS
Maître de conférences -HDR à à l'Université de Reims Champagne-Ardenne, Rapporteur

M. Yann MALECOT
Professeur à l'Université de Grenoble Alpes, Directeur de thèse

M. Matthieu BRIFFAUT
Maître de conférences à l'Université de Grenoble Alpes, Co-encadrant de thèse

ACKNOWLEDGMENT

I would like to express my sincere gratitude to my supervisor Yann Malecot for his guidance, advice, critical reflection and encouragement throughout this thesis.

I am very thankful to my co-supervisor Matthieu Briffaut for all the help, advice and numerous discussions which proved to be important to the completion of this work.

I gratefully acknowledge the assistance received from the engineer Jean-Benoît Toni for achieving the experimental part of this study.

Last but not least, I would like to thank my mother for her encouragement and support in spite of being far from me.

ABSTRACT

The objective of this thesis is to study the influence of creep on residual mechanical properties of concrete. The concrete of prestressed structures is primarily subjected to compressive stresses. During the life of the structure, tensile stresses may take place because of the stress relaxation due to creep of the concrete and the applied load. To evaluate the behavior of such structures, it is necessary to know the value of the residual mechanical properties after creep.

The work which concerns only with basic creep (without water exchange with the surrounding environment), includes an experimental part and a numerical part. In the experimental part, compressive and indirect tensile (Brazilian) creep tests were carried out on the concrete using different loading levels that applied at different ages of concrete. At the end of each creep test, a strength test was carried out on the same concrete for determining the creep effect on the residual mechanical properties. In order to distinguish between the effect of creep and that of quasi-instantaneous loading, some Brazilian tests with quasi-instantaneous preloading in compression were realized.

The results revealed that the mechanical properties of concrete after creep depend strongly on the loading age and the loading direction.

Numerically, a mesoscopic model was used for simulating the creep and the mechanical properties after creep. In fact, under a constant loading level, only the cement paste creeps while the aggregate act as an obstacle to this creep. As a result, tensile stresses arise at cement past-aggregate interface leading to microcracks at this zone.

The viscoelastic deformations are correctly reproduced at different levels of loading but the change of the residual mechanical properties of concrete can not only be explained by the microcracking at cement past-aggregate interface.

RESUME

L'objectif de cette thèse est d'étudier l'influence du fluage sur les propriétés mécaniques résiduelles du béton. Le béton des structures précontraintes est essentiellement soumis à des contraintes de compression. Au cours de la vie de l'ouvrage, des contraintes de traction peuvent cependant apparaître en raison de la relaxation des contraintes due au fluage du béton et de la charge appliquée. Pour évaluer le comportement de telles structures, il est ainsi nécessaire de connaître la valeur des propriétés mécaniques résiduelles après fluage.

Le travail se concentre sur le fluage propre (sans échange hydrique avec le milieu environnant) et il comprend une partie expérimentale et une partie numérique. Dans la partie expérimentale, des essais de fluage en compression et en traction indirecte (Brésilien) ont été effectués sur le béton en utilisant différents niveaux de chargement appliqués à différents âges du béton. A la fin de chaque essai de fluage, un essai de résistance a été réalisé sur le même béton pour déterminer l'effet du fluage sur les propriétés mécaniques résiduelles. Afin de distingué l'effet de fluage et celui d'un chargement quasi-instantané, certains essais Brésiliens avec préchargement quasi-instantané en compression ont également été réalisés.

Les résultats ont monté que le comportement résiduel du béton après fluage dépend fortement de l'âge de chargement et du sens de sollicitation.

Numériquement, un modèle mésoscopique a été utilisé pour simuler le fluage et les propriétés mécaniques après fluage. En effet, sous un chargement constant seule la pâte de ciment flue tandis que les agrégats agissent comme un obstacle à ce fluage. Par conséquent, les contraintes de traction se produisent à l'interface pâte de ciment-agrégats conduisant à des microfissures dans cette zone.

Les déformations viscoélastiques sont correctement reproduites à différents niveaux de chargement mais la modification du comportement résiduel du béton ne peut pas être uniquement expliquée par la microfissuration à l'interface pâte de ciment-agrégats.

CONTENTS

LIST OF FIGURES

LIST OF TABLES

GENERAL INTRODUCTION

1. Context

Creep of concrete is generally defined as the strain that occurs in addition to the initial elastic strain under a sustained load. From another viewpoint, for a constant strain, a creep phenomenon appears as a decrease in the stresses with time. This last is generally called relaxation. Most of the time, concrete structural designers do not take into account the creep effects and apply simple approaches (for instance, the use of a degraded Young's modulus as in Eurocode 2) which may lead to an inadequate efficiency of the structure serviceability, durability and long-time safety.

Creep has positive effects on the concrete structure like relaxation the stresses occurred due to restrained shrinkage. However, it has negative effects on the serviceability, durability and long-time safety. The effect of creep that appears clearly and causes a problem from the beginning i.e. during the construction is that in prestress structures. In these structures, the aim is to maintain the main part of the concrete section of a member under compressive stresses even when external loads are applied. Due to theses stresses, creep arises and manifests as a decrease of the prestress (called prestress losses). The reduction in the stresses due to the creep and the applied load, is very dangerous as it can lead to tensile stresses and then to cracking development. In such situation, the durability of a structure is significantly reduced due to the penetration of aggressive.

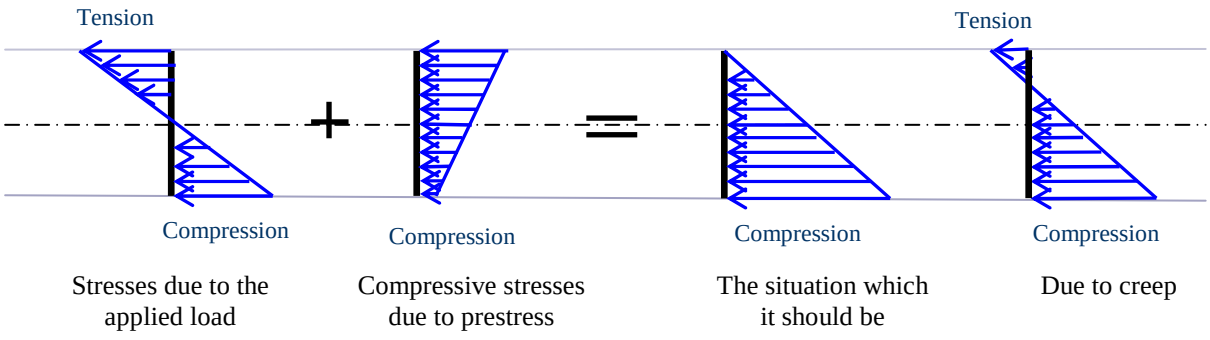

Figure (1): Prestress reduction due to creep

In cases of repairing i.e. increasing the prestress or requalification of the structure (traffic increase for instance), the residual mechanical properties of concrete must be investigated. The effect of creep on the mechanical properties of concrete is not well understood yet in the literature. If creep has negative effects on the mechanical properties of concrete, the amount of prestress increase must be sufficient to overcome this damage in

tension but should not exceed the compressive strength of concrete. Inversely, if creep has benefit effects, the amount of repairing prestress should be reduced to limit the cost.

2. Objective and Scope

In the context of an ageing structural patrimony, it is important to know if creep has negative or positive effects on the evolution of mechanical properties of concrete. The available experimental information about this subject is very limited and not sufficient to conclude clearly as each research is different from the other in terms of curing conditions, age of loading and direction of loading. Moreover very few studied are devoted to concrete properties after sustained load. The main objective of this study is to evaluate the mechanical properties of concrete after it was subjected to creep loading by comparing it with unloaded one. To verify the effect of age, concrete was subjected to creep at both young age and late age, and different loading levels in compression and in tension were used. It should be mentioned here that to achieve creep in tension, an apparatus was designed to hold 3 cylindrical specimens arranged laterally one over the other. The apparatus was installed in the creep device so that the load is applied on these specimens just like the way of Brazilian test in which only 1 cylindrical specimen is used instead of 3, as the case of this study.

To distinguish the effect of creep from the effect of a quasi-instantaneous preloading, some concrete specimens were loaded in compression until a specific level. Immediately after this preloading an indirect tensile test (Brazilian test) was carried out on these specimens until the failure. The tensile strength results of these specimens were compared with the results of specimens that were not subjected to compressive preloading.

For structural members prestressed in two directions, apparent creep Poisson's ratio has an impact on the orthogonal prestress level. Therefore, to understand the effect of compressive creep loading on the lateral strain, the apparent Poisson's ratio was studied.

In addition, to simulate creep and residual mechanical properties numerically, a mesostructural model was developed to represent concrete as a composite material which includes two different components; cement paste and aggregate. These simulations aim to be more representative of the reality than a homogenous approach as under loading only cement paste creeps while aggregate acts as an obstacle to this creep due to its high stiffness. As a result, tensile stresses arise at aggregate-cement paste interface leading to cracking development. The main objective of the mesoscopic simulation is to highlight the phenomena that occur in concrete which could explain the complex behavior observed at macroscopic scale.

3. Outline of the Thesis

The present study is divided into three chapters in addition to the introduction and the conclusion. Chapter one includes a review of previous literatures that are mainly concerned with factors that affect creep, creep effects, creep in tension and in compression, apparent Poisson's ratio and several creep models.

The experimental work devoted in chapter two includes a brief description about the concrete used, apparatus and devices used and the procedure of preparing and testing specimens. In addition, the chapter includes the experimental results with discussion and comparison with the results of the other authors.

Chapter three which concerns the numerical work of this study is based on an article which was recently submitted. It includes the simulation of creep strains in tension and in compression under different stress/strength levels with development of the mechanical properties due to the creep effect. The chapter also includes a numerical calibration of the creep parameters and mechanical properties of concrete used in experimental work for simulating Brazilian creep and to compare the results with the experimental ones. The global layout of this study is presented in a flowchart (see Figure (2)).

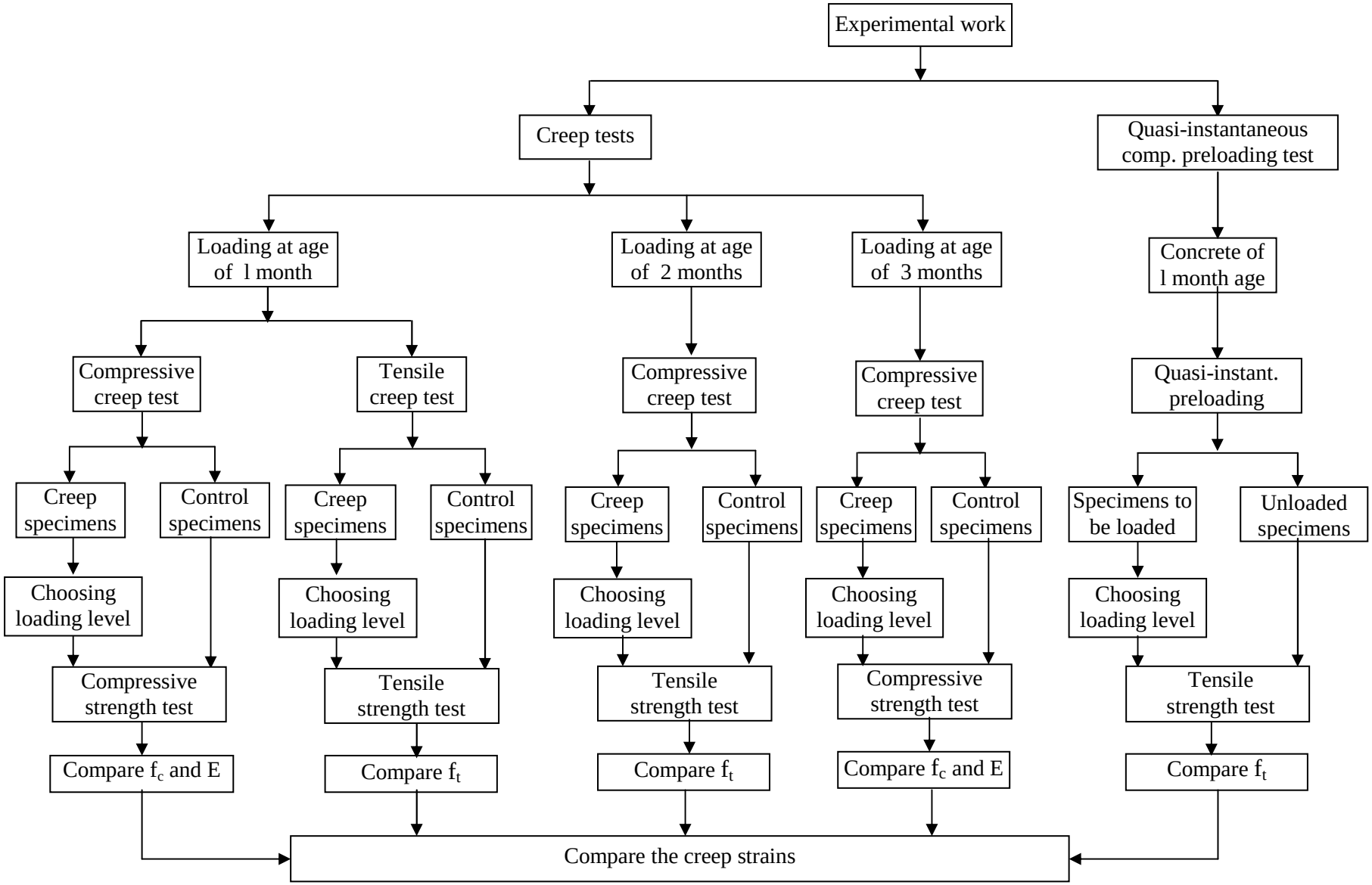

Figure (2.a): Flowchart of the experimental work

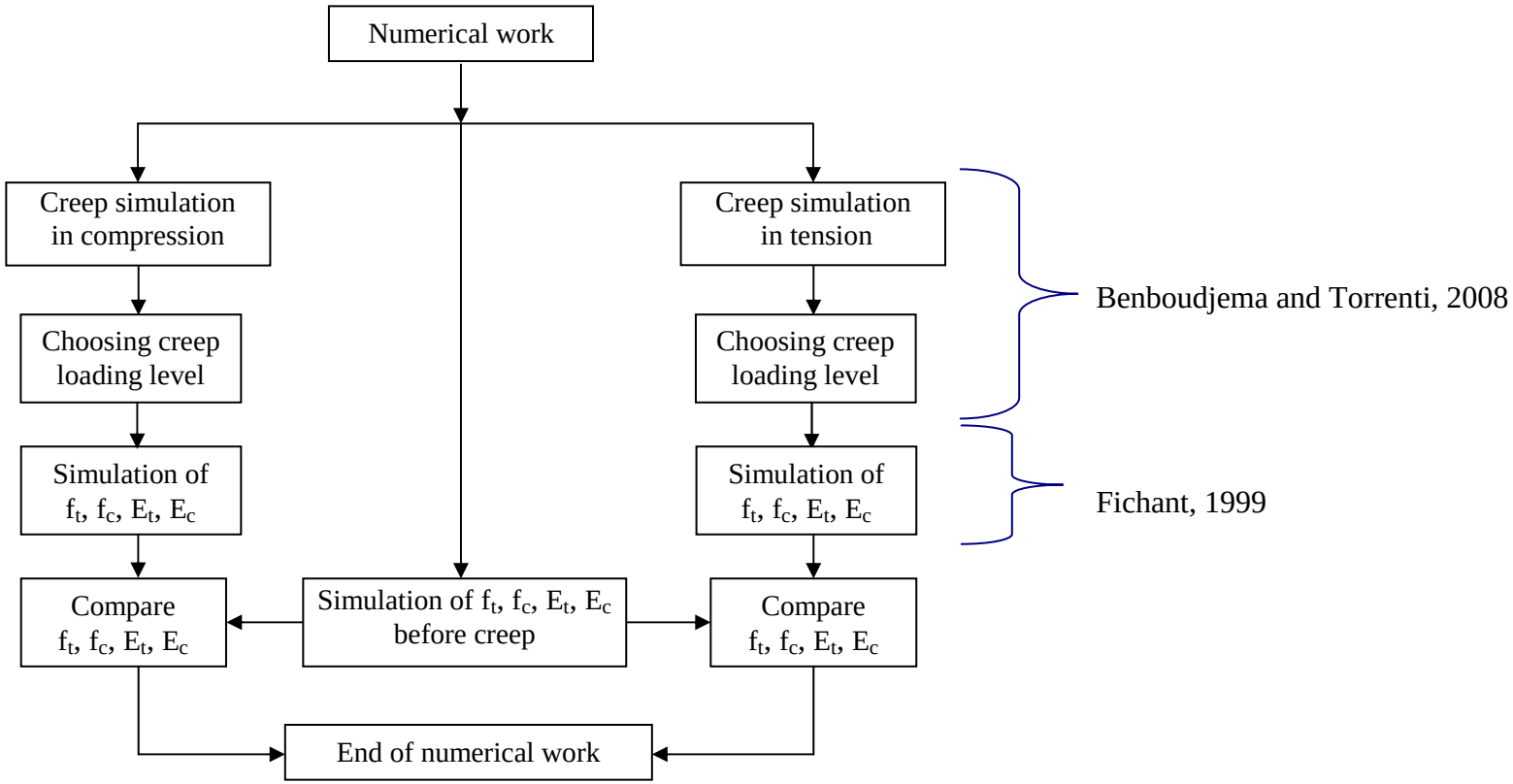

Figure (2.b): Flowchart of the numerical work

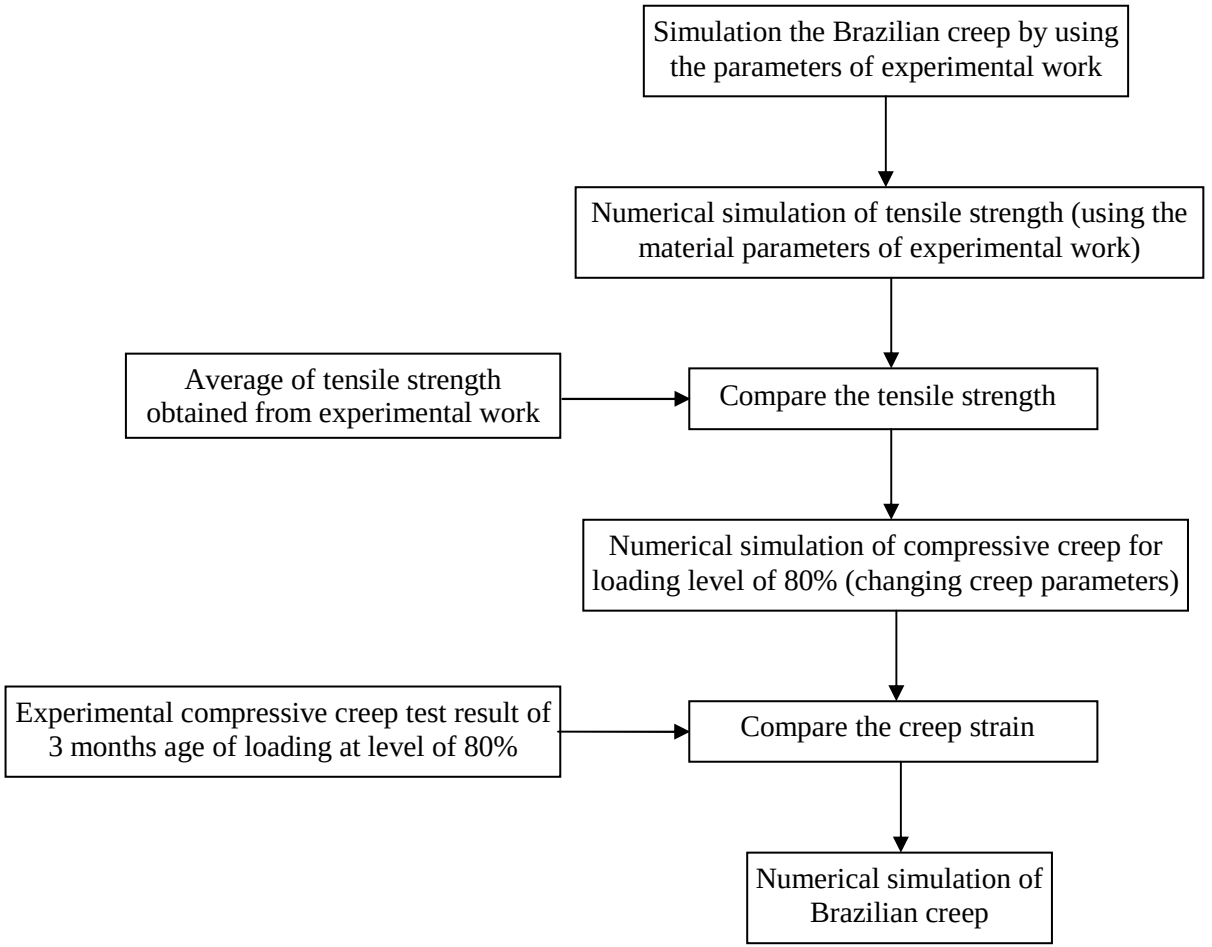

Figure (3.c): Flowchart of numerical simulation of Brazilian creep by using the parameters of experimental work

CHAPTER I: LITERATURE REVIEW

This chapter includes creep terms used, a presentation of experimental studies about factors affecting creep, creep effect and creep Poisson's ratio and a comparison between creep in tension and in compression. Finally, the chapter includes a presentation of models that simulate the creep behavior.

On the one hand, creep of concrete could be defined as a gradual increase in strain due to sustained load. It is the strain which occurs in addition to the instantaneous strain at the time of loading. Creep of concrete could be classified according to the following terms:

- Basic creep is defined as the creep that occurs under conditions where there is no moisture movement between concrete and ambient environment.
- Drying creep is the additional creep that occurs when the concrete is allowed to be drying under load.
- Transitional thermal creep is the additional creep that occurs when there is an evolution in temperature after the load application.
- Total creep is the summation of basic, drying creep and transitional thermal creep (if there is an elevating in temperature after loading).
- Creep recovery is the recoverable strain that occurs after removing the sustained load. This recovered strain must be distinguished from the instantaneous recovery which is equal to the elastic strain at a given age.

On the other hand, the creep of concrete could be expressed in different ways:

- Specific creep is obtained by dividing the creep strain on the corresponding applied stress i.e. creep strain due to a unit applied stress.
- Creep coefficient is defined as the ratio of creep strain to elastic strain.
- Creep compliance function is the summation of elastic and total creep strains that occur due to a unit loading stress.

Until nowadays, there is still an argument about the mechanism of concrete creep phenomena. The water appears to play a fundamental role in the creep mechanism in addition to the flow of cement gel (C-S-H).

As presented by Neville and Dilger (Neville and Dilger, 1970), a number of creep theories have been proposed over the years and it is possible that the actual creep involves two or more mechanisims. These theories are: mechanical deformation theory, plastic theory,

viscous and viscoelastic flow theory, elastic after-effect theory, solid solution theory, seepage theory and contribution of microcracking to creep theory.

Authors [(Reynouard and Pijaudier Cabot, 2005) and (Ulm and Acker, 1998)] revealed that there are two distinct physical mechanisms to explain the basic creep of concrete: at short term and at long term. The most logical and reasonable mechanisms are as follows:

- At short term: The stress resulting from the applied force is transmitted, at a microscopic scale, through amass of the hydration products that surround the capillary pores (see Figure (1.1)). This transfer of a microscopic stress induces a local thermodynamic disequilibrium between the water molecules that are in the free adsorption zone and those in capillary pores. To restore the balance, water molecules diffuse throughout the adsorbed water layers to the capillary pores, resulting in the deformation of solid skeleton [(Powers, 1968), (Lohtia, 1970), (Wittmann, 1982) and (Ulm and Acker, 1998)].

- At long term: It is considered that the viscosity flow is a function of a tensile microprestress carried by the bonds and bridges crossing the micropores (gel pores) in the hardened cement gel. This microprestress is generated by the disjoining pressure of the hindered adsorbed water in the micropores and by very large and highly localized volume changes caused by hydration or drying. The long-term creep is assumed to originate from viscous shear slips between the opposite walls of the micropores in which the bonds or bridges that cross the micropores (and transmit the microprestress) break and reform. The long-term aging exhibited by the flow term in the creep model is caused by relaxation of the tensile microprestress transverse to the slip plane (Bažant et al., 1997), (see Figure (1.2)).

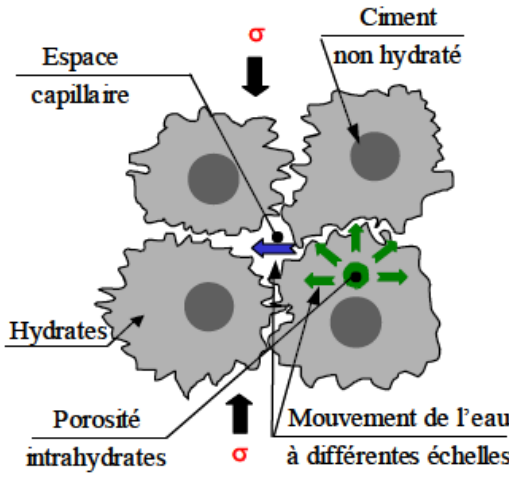

Figure (1.1): Mechanism of basic creep at short time [(Benboudjema, 2002) adapted from (Ulm et Acker, 1998)]

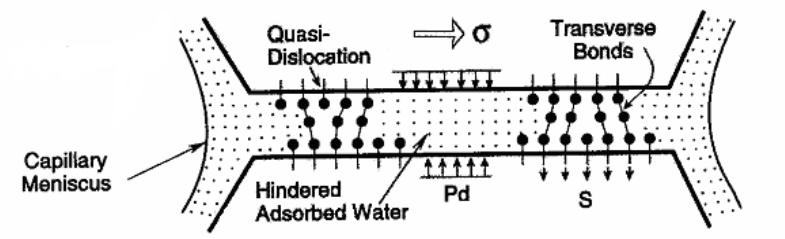

Figure (1.2): Micropore in cement gel, disjoining pressure (Pd) and Microprestress (S) (Bažant et al., 1997)

Summary of Chapter One

1.1 Experimental Studies

This part includes factors influencing creep, a comparison between creep in tension and in compression, apparent Poisson's ratio and creep effects.

1.2 Numerical Models

In this part Regular Models, Analytic Model (Bazant and Prasannan, 1989) and Rheological Models are presented.

In this chapter, creep phenomena have been studied from different aspects by presenting studies that had been carried on, experimentally and numerically.

1.1 Experimental Studies

This part includes a review of experimental studies on the creep behavior under different conditions, effect of loading direction, the strain relation between one direction and the other, and creep consequences on concrete structure.

1.1.1 Factors Influencing Creep

There are many factors that influence the creep of concrete which may be divided into intrinsic factors and extensive factors. Intrinsic factors are related to material characteristics which are fixed once concrete is cast, like the design strength, the fraction of aggregate in the concrete mix and the elastic modulus of aggregate. The extensive are those that can vary after the casting, like temperature, age, degree of hydration, relative vapor pressure in the pores, environmental humidity and the size of specimen (Bažant and Wittman, 1982).

1.1.1.1 Water/Cement Ratio

The water/cement ratio has a major effect on the creep value. In one hand, the strength of concrete is inversely proportional to this factor. In another hand, it has an intrinsic relation

with most of creep theories, especially the seepage and thermodynamic theories, which explain the creep strain occurrence due to water.

When the water/cement ratio increases, the porosity of cement paste increases as there is not enough cement products to fill all the pores that were occupied with water before the hydration threshold. Increasing the porosity leads to decreasing the strength of concrete (Neville and Brooks 2010). Thus, for a constant cement paste content, increasing water/cement ratio results in increasing creep. As given in same reference, this relation was proved by the work of Wagner (Wagner, 1958) which is presented in Figure (1.3). In this figure, creep is expressed as relative to the creep at water-cement ratio of 0.65.

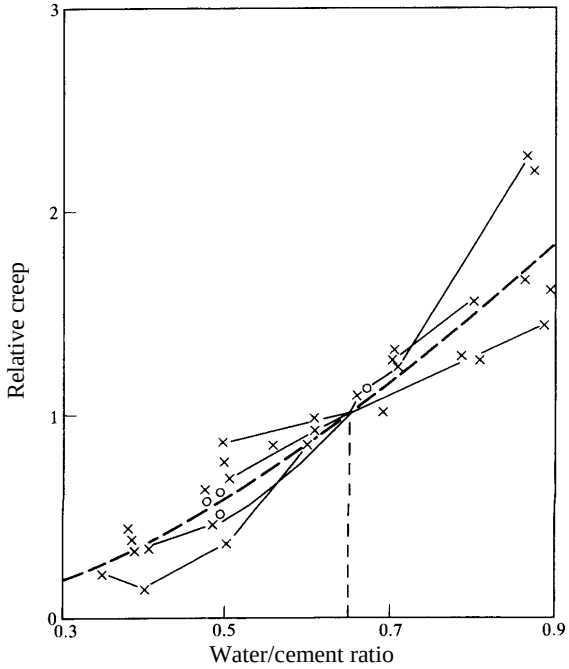

Figure (1.3): Relative creep (creep expressed as relative to the creep at a water/cement ratio of 0.65) vs. water/cement ratio (Wagner, 1958)

According to Cinlar E. as presented by Bazant and Wittmann (Bazant and Wittmann, 1982), the higher the water content, the higher the number of water molecular migrating, and therefore the higher is the rate of creep. When the water content changes, large numbers of water molecules move through the micropores, that gives the sliding particles greater mobility and increase the creep rate.

1.1.1.2 Aggregate

The volumes of aggregate content and the content of hydrated cement paste are complementary fractions of the volume of hardened concrete. So, considering one or the other is strictly equivalent (Neville and Dilger, 1970).

The normal weight aggregates do not suffer creep at the stress level that exists in concrete while the hardened cement paste is the origin of creep. That means that the role of aggregate is restraining the creep of cement paste. So, when the quantity of aggregate increases the creep value decreases. However, this resistance depends on the aggregate type in terms of its elastici modulus. As the elastic modulus of aggregate increases, the restrained offered by the aggregate to the potential creep of cement paste increases too (Neville and Brooks, 2010).

A study by Gudmundsson (Gudmundsson, 2013) was carried out on the correlation between the aggregate porosity and the creep value. The study showed that a reduction in the modulus of elasticity of concrete is observed when porous aggregates are used. The researcher found that an increase in aggregate porosity of 15% can lower the elastic modulus of the concrete up to 40%. As creep of concrete is interlinked to the elastic modulus of the concrete, higher creep strain is observed in concrete made with aggregate of higher porosity.

Hobbs (Hobbs, 1971) studied the decrease of creep strain in concrete (ε_t) with the increase of aggregate volume (D_a). The author represented this relation by the following equation:

$$\frac{\varepsilon_t}{\varepsilon_{tm}} = \frac{1 - D_a}{1 + D_a} \tag{1.1}$$

where creep (ε_t) is the strain in cement paste (ε_{tm}). The author compared equation (1.1) with some creep results plotted versus aggregate volume concentration obtained by Counto (Counto, 1964), as shown in Figure (1.4).

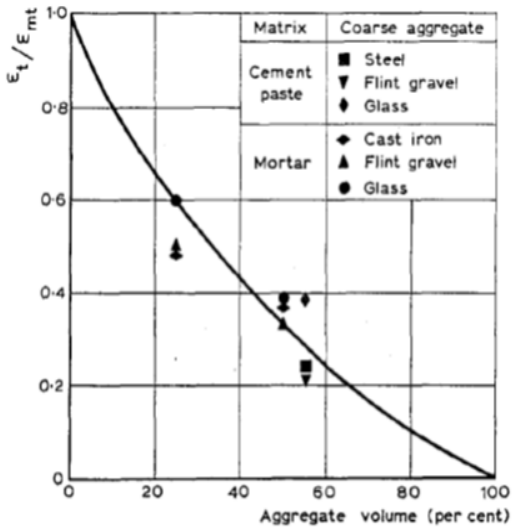

Figure (1.4): Variation of creep ratio or total strain ratio, $\varepsilon_t / \varepsilon_{tm}$, with aggregate volume concentration [(Hobbs, 1971) adapted from (Counto, 1964)]

1.1.1.3 Applied Stress and Strength of Concrete

Creep of concrete increases with the increase of the applied stress and/ or with the decrease the concrete strength (Orchard, 1979).

Creep is related to the movement of water and gel particles (as mentioned previously for the creep mechanism). As well, some of researchers went beyond that to express creep occurrence due to microcracking only (Rossi et al., 2013). Anyhow and whatever was the mentioned causing the reason of creep phenomena, the change of the applied loading level comparing to its strength, affect very largely the creep rate and its value.

As presented by Orchart (Orchart, 1979), Lea and Lee (Lea and Lee, 1947) gave the limit of stress/strength proportion between 25% and 50%. This conclusion is similar to that revealed by the experimental results of Ranaivomanana (Ranaivomanana et al., 2013) on high performance concrete, in which the nonlinearity was arise somewhere between 30% and 50% for creep in tension or in compression. The last limit was confirmed by Illston (Illston, 1965) and Zongjin (Zongjin, 2011) who indicated that creep in concrete is a linear function of stress under a level less than 50% of its strength. For the case of a stress level higher than 50% but lower than 75% of its strength, creep is a nonlinear function of stress. Illston (Illston, 1965) stated that failure can occur under a sustained stress of 75% of the ultimate. While Zongjin (Zongjin, 2011) revealed that for the case of a stress level higher than 75% of the concrete strength, creep will rapidly increase infinitely and will cause structure failure, as shown in Figure (1.5)

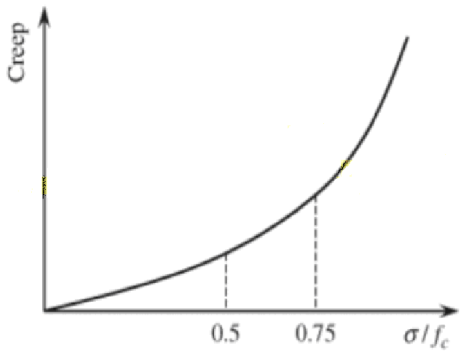

Figure (1.5): Unstable rupture creep (Zongjin, 2011)

As it was revealed by Atrushi (Atrushi, 2003), for sealed concrete loaded at early age of 3 days, relative tensile loadings up to between 60% to 70% the magnitude of creep seems to be linear whereas a non-linear behavior takes place at higher loading levels.

For comparing the creep rate and valus under different loading levels, Roll (Roll, 1964) studied the compressive creep under a wide range of stress/strength levels. The study was achieved on concrete mixture of cement:sand:gravel equals to 1:2:5 submitted to creep loading at age of 28 days. As it is shown in Figure (1.6), creep strain increase as stress/strength level is increased.

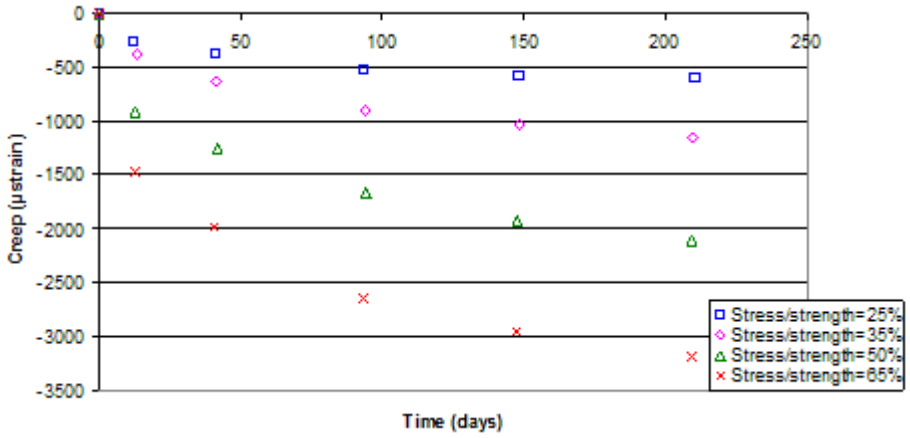

Figure (1.6): Creep strain vs. time of a concrete mixture (Roll, 1964)

To clarify the effect of concrete strength (in addition to the applied stress level) on creep, the study of Smadi et al. (Smadi et al., 1987) was analyzed. The experimental work was carried out on three types of concrete; high-, medium-, and low-strength. The stress/strength ratio was ranging from 40% to 80% for high-strength concrete and from 40% to 75% for medium- and low-strength concrete. As the previous study (Roll, 1964), the results revealed that, for any one of these three types of concrete, compressive creep increases as the

stress/strength ratio is increased. In addition, for the same stress/strength ratio, the creep strain, creep coefficient and specific creep are smaller for high-strength concrete than for medium- and low- strength concrete.

As a part of creep strain is attributed to the movement of adsorbed water within the concrete microstructure, the rate and magnitude of creep associated to this process depend on the relative volume of pores and spaces in the cement gel, and on the amount of water occupying these pores at the time of loading. Smadi et al. (Smadi et al., 1987) related the inverse relation between creep and strength of concrete to that lower strength concrete have higher water-cement ratio which will results in higher porosity and higher capillary as well as adsorbed water, and therefore it will have larger final creep. In addition, high-strength concrete have the lowest aggregate content into the cement paste i.e., lowest heterogeneity of concrete system which is the reason of microcracking (along the aggregate cement interface).

1.1.1.4 Age of Loading

The age of concrete at loading application, is an important factor as in sites the load is generally applied very early to limit the time of the construction process. That means that same loading stress is applied on the structure before the concrete obtains its design strength, and that will result in a higher creep strain.

Browne and Blundell (Browne and Blundell, 1969) measured long term creep on a number of concretes in a sealed state, loaded at 7, 28, 60, 180 and 400 days after casting, for simulating mass concrete conditions in the structure. The results reveals that in general, age reduces the creep rate value as it is expected due to the effective reduction in stress level associated with strength development with time.

In addition to relating the decrease in creep with age due to increasing of concrete strength, De Schutter and Taerwe (De Schutter and Taerwe, 1997) found that this relation between creep and age is true even if the stress/strength ratio is kept constant at the age of loading. Their experimental work was carried out on the basic creep of concrete using three cement types. Creep tests in compression were carried out for different loading ages (1, 2, 3, 7 and 14 days) and by using two different stress levels of 20% and 40% of the ultimate compressive strength at age of loading. The results reveal that, for the same stress/strength ratio, the creep strain decreases as the age of loading is increased. Nevertheless, at the very young ages (1, 2 and 3 days) the relation is inversely related. The experimental results which are presented in Table (1.1), are summarised in another articles by the same author De Schutter (De Schutter, 1999).

Table (1.1): Basic creep experimental results

Age of loading (days)	Stress/strength ratio	Final basic creep strain (m/m)
1	0.2	0.000095
1	0.4	0.000257
2	0.2	0.000097
2	0.4	0.000252
3	0.2	0.000117
3	0.4	0.000290
7	0.2	0.000106
7	0.4	0.000228
14	0.2	0.000084
14	0.4	0.000175

The effect of age was also studied on both basic and total creep in the work of Meyers and Slate (Meyers and Slate, 1970). The experiments were carried on prismatic specimens cured in water for 7 days, and then the specimens prepared for the basic creep test were sealed. The specimens were loaded at different ages (calculated from the end of curing) with different stress levels to achieve the same initial elastic strain. As the previous results, except at 0 day, the age is conversely related with basic and drying creep as they are represented in Figure (1.7) and (1.8), respectively. The authors mentioned that the most important factors that affecting creep are the amount of water present at the start of loading and while the specimens under loading and the amount of microcracking developed in the material before and during the time of loading.

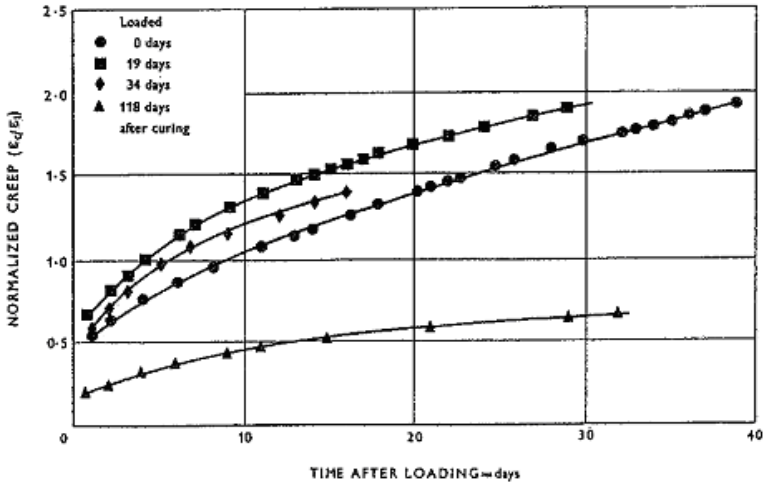

Figure (1.7): Normalized creep of sealed specimens (Meyers and Slate, 1970)

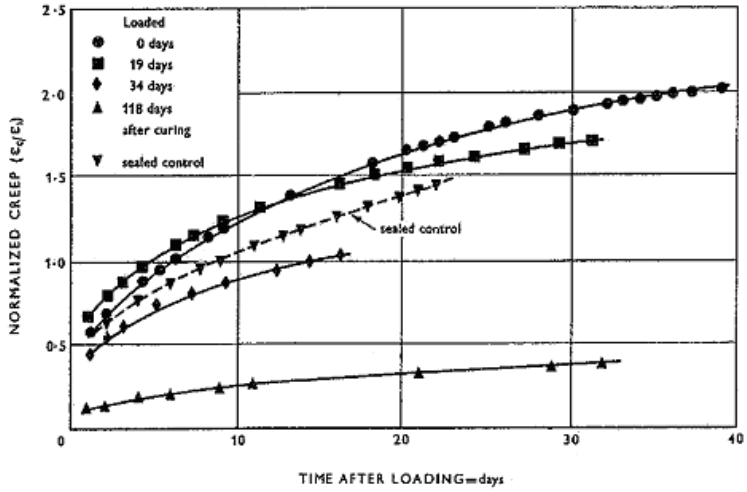

Figure (1.8): Normalized creep of unsealed specimens (Meyers and Slate, 1970)

1.1.1.5 Shape and Size of Specimen

The shape and size of a concrete specimen are expressed in terms of the volume/surface ratio of concrete members. This factor arises only when the specimen is allowed to be drying i.e. when the drying creep takes place (Neville and Diliger, 1970).

Hansen and Mattock (Hansen and Mattock, 1966) studied experimentally the effect of volume/surface ratio on creep of concrete by using different dimensions of cylindrical and I-shape members. They found that the size and the shape of member stored under drying condition affect the rate and final value of creep inversely, i.e. creep decreases when the member becomes larger (see Figure (1.9)).

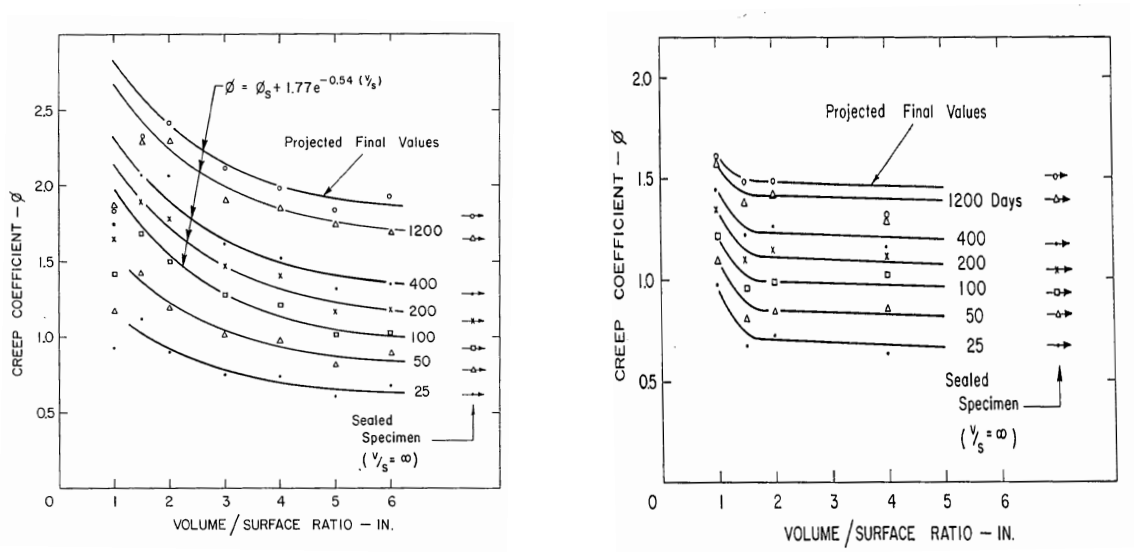

(a) (b)

Figure (1.9): Variation of creep coefficient with volume/surface ratio of cylinders at different ages; (a) using Egine gravel aggregate concrete; (b) using sandstone aggregate concrete (Hansen and Mattock, 1966)

For a very large member, the creep approaches the value of basic creep corresponding to sealed specimen. The reseals also revealed that size and shape of member affect the rate of creep during about the first three months. At greater ages the rate of creep is equal to the rate of creep of sealed specimen.

In the following two sections, the effect of environmental conditions (relative humidity and temperature) was studied due to their considerable importance in the development of creep.

1.1.1.6 Relative Humidity

The humidity of the environment has an important effect on creep as it affects the moisture content of the concrete. If the concrete is dried out before the load application, the creep is very much smaller than if it contained a considerable amount of free water (Orchard, 1979).

The effect of moisture condition on the creep of concrete was studied by Troxell et al. (Troxell et al., 1958). In that work, specimens of 100mm diameter and 350mm length where cured till the age of loaded at 28 days. After 23 years of loading under different moisture conditions (water, fog, 70% and 50% RH), the creep strain of specimens, as presented in Figure (1.10), were 360×10^{-6}, 380×10^{-6}, 800×10^{-6} and 1080×10^{-6} respectively. Thus it is seen that, within this range, the lower is the moisture content of surrounding medium the greater is the creep.

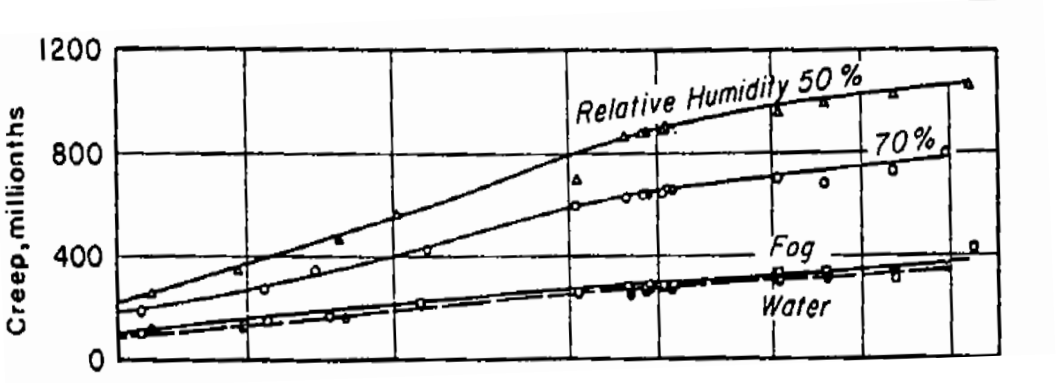

Figure (1.10): Effect of moisture condition of storage upon creep (Troxell et al., 1958)

Hilaire (Hilaire, 2014) presented in his thesis two experimental studies of Wittmann (Wittmann, 1970 and 1973):

- (Wittmann, 1970): 28 days after casting the cement paste, the samples were dried at 105°C for 2 days. Then they were saturated again for 3 months at different humidity. The water/ cement ratio was 0.4.

- (Wittmann, 1973): The samples were first dried under atmosphere P_2O_3 then they were resaturated at different humidity.

The author (Hilaire, 2014) arranged the results in two different figures (Figure 1.11.a and 1.11.b) to show the creep strains obtained for different internal relative humidity. It is clear that the basic creep increases with increasing the internal relative humidity.

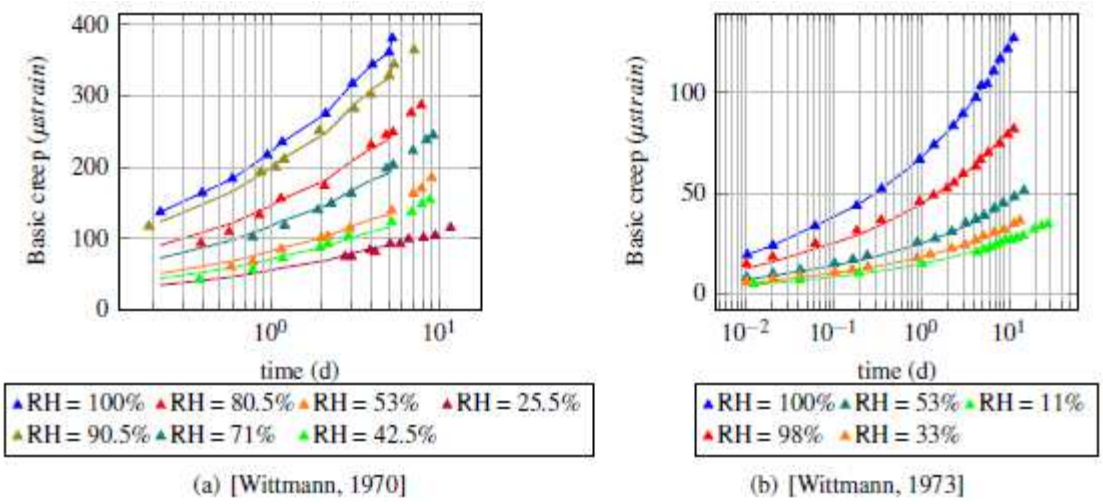

Figure (1.11): Basic creep deformation versus time for different internal relative humidity [(Hilaire, 2014) adapted from (Wittmann, 1970 and 1973)]

Comparing the results of Troxell et al. (Troxell et al., 1958) with those of Wittmann (Wittmann, 1970 and 1973), it could be seen that they are opposite i.e. for the first researcher, the creep strain increases with decreasing the relative humidity while for the second one the creep strain increase with increasing the relative humidity. That is related to the fact that Troxell et al. (Troxell et al., 1958) had studied the effect of relative humidity on the drying creep addition to basic creep. So, when the relative humidity decreases the movement of water out of the loaded specimen increases and the drying creep increases as a consequences. Relating to the study of Wittmann (Wittmann, 1970 and 1973), it was carried on the effect of relative humidity on the basic creep only. So, when the relative humidity increases the movement of water inside the loaded specimen increases.

Other researchers like Hansen (Hansen, 1960) studied the effect of variation of ambient relative humidity on creep. Several series of cement mortar beams were loaded and the deformation was measured during a period of 100 days. After removing them from water at age of 7 days, all the specimens were stored under 70% RH for 21 days before loading. Each series follows a special program. Some of them were exposed to an alternating relative humidity between 50% and 70% while the other stored under a constant relative humidity (50%, 60% and 70%) throughout the time of loading. The results revealed that creep strain of

the cement mortar stored under variable relative humidity (50% and 70%) is larger than under the average of these two humidities (60%), and as large as that stored under a constant relative humidity of lowest limit (50%) (see Figure (1.12)).

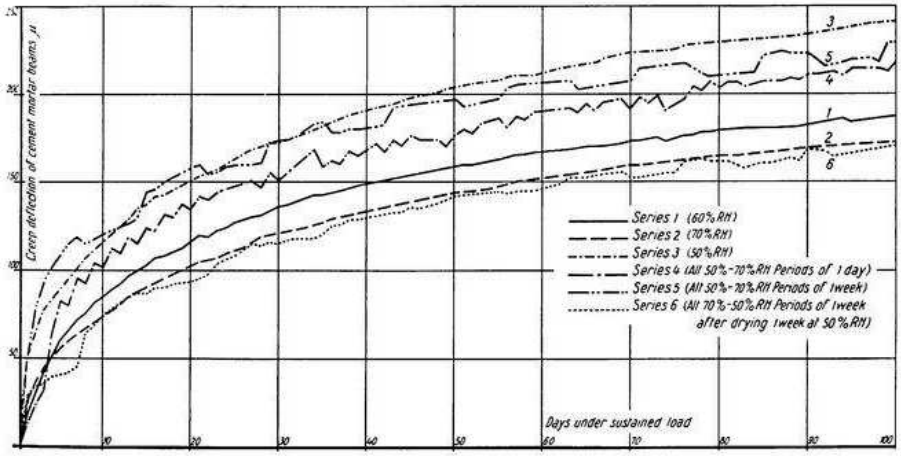

Figure (1.12): Creep curves, series 1 to 6 (Hansen, 1960)

Another work on the effect of variation of ambient relative humidity on creep was achieved by Zou et al. (Zou et al., 2014) but here the objective of the study is to include the influence of seasonal variations of ambient humidity on the creep. The study was carried on concrete shear wall specimen with thickness of 120mm, length of 1500mm and height of 1800mm. The specimen was moist-cured for 90 days and then the shrinkage was monitored for 32 days and then it was loaded with a constant axial loading of 800 KN for 1 year. The results revealed that the variation of ambient humidity has significant impact on the creep of concrete development. Figure (1.13) shows the strain (creep and drying shrinkage) with humidity variation thought one year. Figures (1.13.a, 1.13.b and 1.13.d) show the strains along the loading direction, and Figure (1.13.c) shows the strains perpendicular to the loading direction. The name of strain gages that begin with letter A, are fixed on the surface while those which begin with B are embedded. The shortening strain increases more rapidly when the monthly average ambient relative humidity decreases and vice versa. Consequently, it is not sufficient to describe the time development of creep for a whole year using annual average ambient relative humidity.

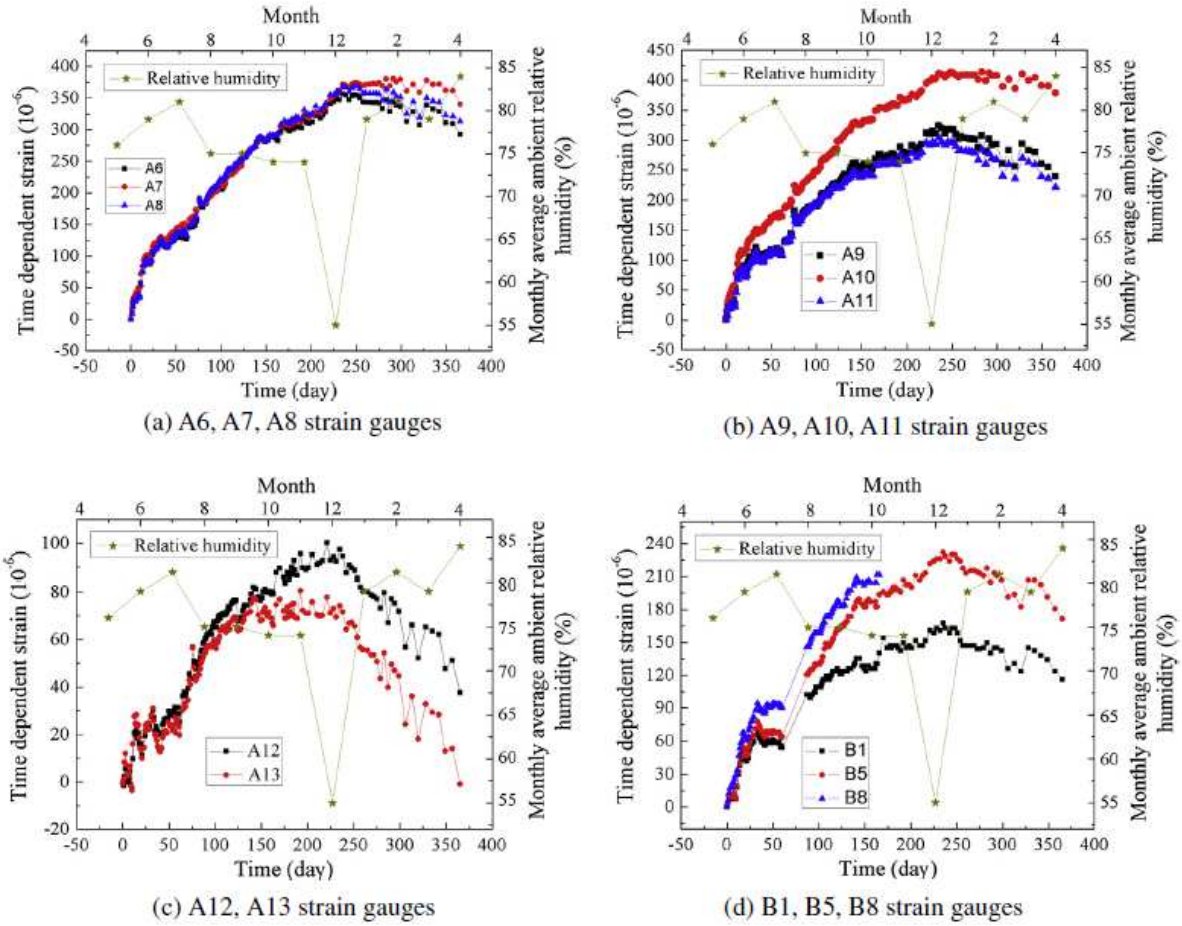

Figure (1.13): Time dependent strains of the shear wall under sustained load,(Zou et al., 2014)

1.1.1.7 Temperature

Another environmental factor that affects profoundly the creep of concrete is the temperature which results in increasing the creep when it is elevated.

To study the effect of temperature on basic creep, Nasser and Neville (Nasser and Neville 1965) submitted the concrete to a wide range of temperature (between 21^{o} C and 96^{o}C), from the age of 1 day and onward. The results showed that the creep rate increases with the elevation of temperature up to 71°C. Neville (Neville, 1962) considered that the temperature increases the mobility of shear flow of gel and of adsorbed water and hence the creep of these two phases. On the other hand, for a temperature higher than 71°C, this factor affects inversely on creep. The authors Nasser and Neville (Nasser and Neville 1965) explained this behavior to be due to desorption of the water from the surface of the gel, so that the gel itself becomes gradually the only deformable phase.

The positive relation between the temperature and the creep of concrete was also validated by a recent study of Vidal et al. (Vidal et al., 2013). The work includes the effect of

moderate temperature on the uniaxial compressive basic creep of four types of High Performance Concretes (with and without fibres and silica fume). Cylindrical specimens (110mm diameter and 220mm high) were cured under water (20°C) until the age of creep loading at 427 days for 50°C test, and at 300 days for 20°C and 80°C tests. The specimens were first heated and the temperature was maintained while they were loaded at 30% of their compressive strength (measured on different samples at 20°C) at the age of creep loading. The results revealed that creep strains at 50°C are approximately twice those obtained at 20°C during 300 days of loading whereas at 80°C, the creep amplitude is multiplied by a value between 4.4 and 9.2 after only 20 days of loading (see Figures (1.14) and (1.15)).

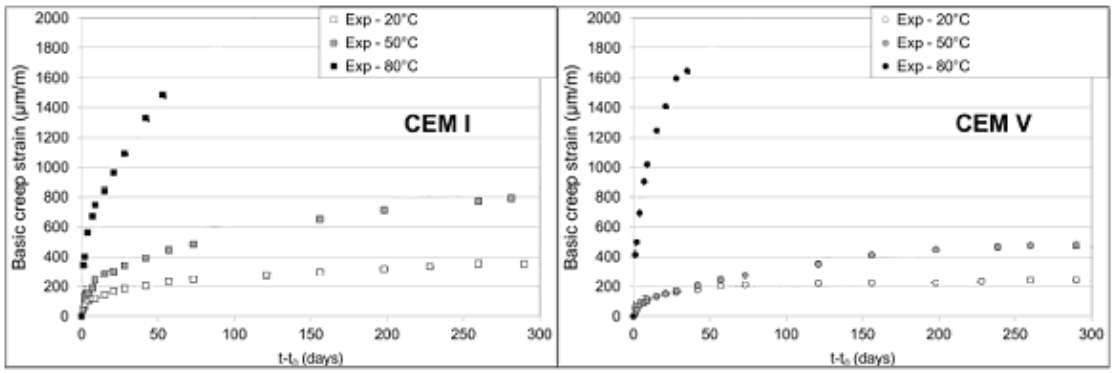

Figure (1.14): Basic creep for CEM I and CEM V at 20°C, 50°C and 80°C (Vidal et al., 2013)

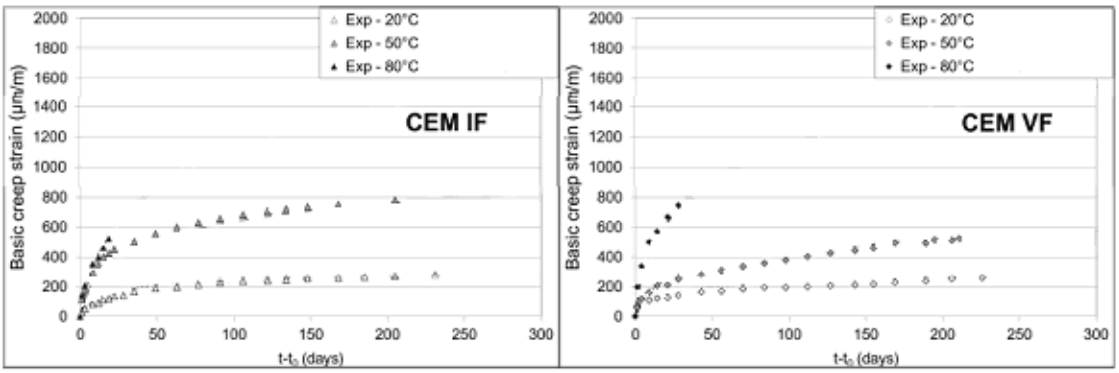

Figure (1.15): Basic creep for high performance cement at 20°C, 50°C and 80°C (Vidal et al., 2013)

However, it must be distinguished between the effect of elevated temperature on creep of concrete before and that after creep loading. This difference is related to the creep component which is called “transitional thermal creep” and that occurs if the temperature is elevated only after loading and to a level which was not reached before (Illston and Sanders, 1973). It should be mentioned that the study of Illston and Sanders (Illston and Sanders, 1973)

was carried on basic creep in shear where the mortar was loaded in torsion. The authors also mentioned that this component does not occur when the temperature decreases under load. The transitional thermal creep was also studied in relation with the compressive basic creep in the work of Hauggaard (Hauggaard et al., 1999). This work includes 2 groups of specimens, the first one was kept in room temperature of 21^{o}C while for the second group, the temperature was elevated from 21^{o}C to 40^{o}C after loading, then reduced again to approach the situation in a massive concrete structure (see Figure (1.16)).

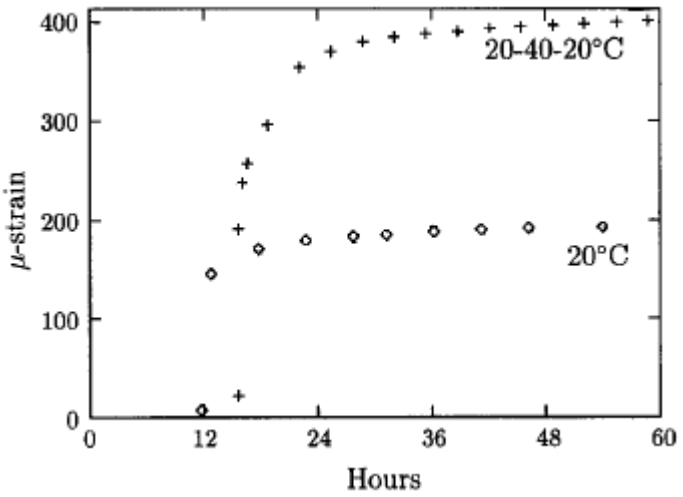

Figure (1.16): Creep of concrete subjected to thermal gradients (Hauggaard et al., 1999)

The study of Kammouna (Kammouna, 2001) was carried out on the total (basic and drying creep) in compression. The results presented in Figure (1.17) revealed that concrete loaded in summer [series (2)] exposes lower creep than that loaded in winter [series (3)] as the transitional thermal creep component occurs later on in summer season. It could be also seen that the creep strain of series (3) approaches to the values of series (1) in which the temperature was elevated just after loading. In the same study and due to this conclusion, the model of (Bazant and Paula, 1979) was developed by making the temperature variable with time under loading.

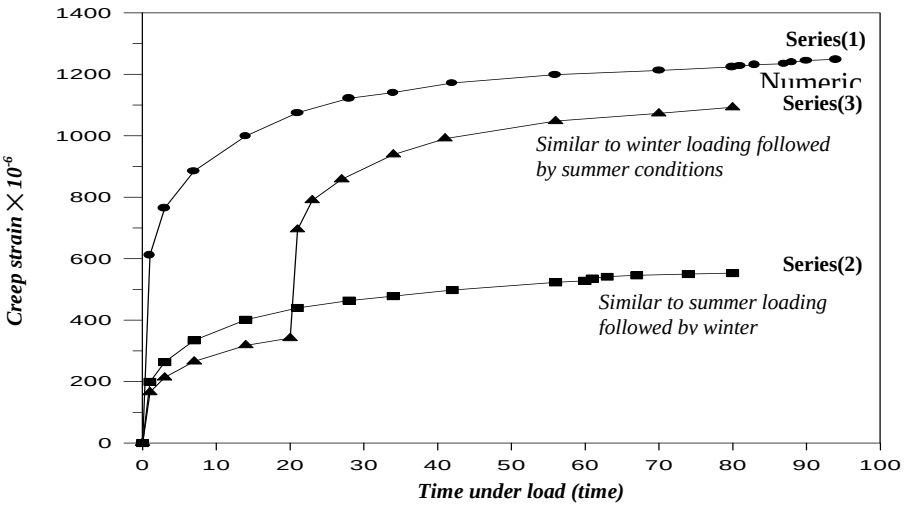

Figure (1.17): Comparison of the observed creep strain vs. time load for series (1), (2) and (3) (Kammouna, 2001)

Illston and Sanders (Illston and Sanders, 1973) attributed the transitional thermal creep to the disturbance that occurs due to the rise in temperature. Bazant and Wittmann (Bazant and Wittmann, 1982) attributed the transient thermal creep to special mechanisms. One of these mechanisms could be related to the thermal gradient that occurs due to the temperature change, which is followed by a moisture gradient resulting in internal stress redistribution which changes the creep rate.

1.1.2 Comparison between Creep in Tension and in Compression

The creep of concrete in tension is considerably important in estimating the allowable tensile stress in concrete beams subjected to flexural loading and when the concrete is subjected to restrained shrinkage.

An experimental work was carried out by Illston (Illston, 1965) to study the effect of different loading levels on creep in tension. The tensile stress levels were 25%, 50% and 75% of the ultimate stress at the time of loading. As for the compressive creep (section 1.2.1.5), the creep strains increase as the loading level increases. The assumption of proportionally of stress and rate of creep is probably justified up to 50% of ultimate stress (see Figure (1.18)).

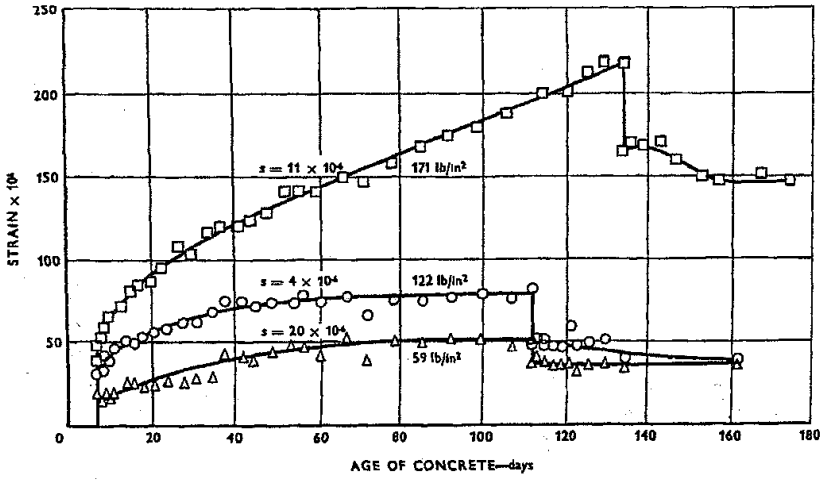

Figure (1.18): Effect of the level of tensile stress on creep of concrete (Illston, 1965)

The strain under sustained tensile stress and that due to an equal compressive stress are compared in Figure (1.19). The actual compressive stress in the test was 6.89 MPa (about 20% of the ultimate) and the strains have been reduced in proportion to the level of the tensile stress 0.9 MPa.

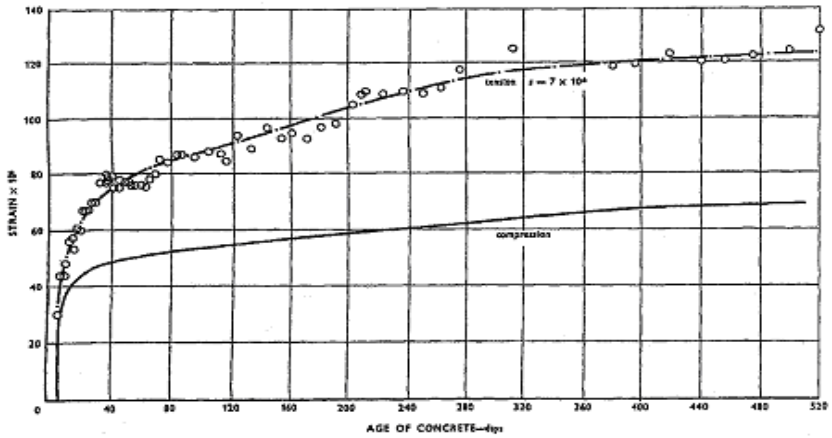

Figure (1.19): Comparative rate of creep for concrete under unaxial tension and compression (Illston, 1965)

The results revealed that both under tensile or under compressive stress, the rate of creep decreases with time under load. Nevertheless, the initial rate of tensile creep is much larger than that of compressive creep, while in the later stages the tensile creep rate decreases so that the compressive rate may become greater (Illston, 1965).

Brooks and Neville (Brooks and Neville, 1977) also compared between tensile creep and compressive creep. Their study involved two ages of loading; 28 days and 56 days. All the specimens were cured in water and thereafter either stored continuously in water (for studying the basic creep) or in air (for studying the basic creep and drying creep). Classification of the Figures which represent the creep strains are as shown in Table (1.2).

Table (1.2): Classification of the Figures of (Brooks and Neville, 1977) according to storage conditions and age of loading

Loading age	28 days		56 days	
Storage conditions	In water	In air from the age of 28 days	In water	In air from the age of 28 days
Type of creep	Basic	Basic and drying	Basic	Basic and drying
Figure No.	1.20	1.21	1.22	1.23

This investigation reveals that for loading at age of 28 days initial rates of basic creep in tension and in compression are similar. Nevertheless, in contrast to basic creep in compression, the rate of basic creep in tension does not decrease with time (see Figure (1.20)). It could be remarked that after unloading, the curve of tensile creep increases instead of decreasing. That may be related to that the concrete was subjected to drying condition. Due to that, when the negative strain value of shrinkage is subtracted from the positive strain value of tensile creep, the result will be the summation of the both previous values and lead to increase the curve of recovered creep.

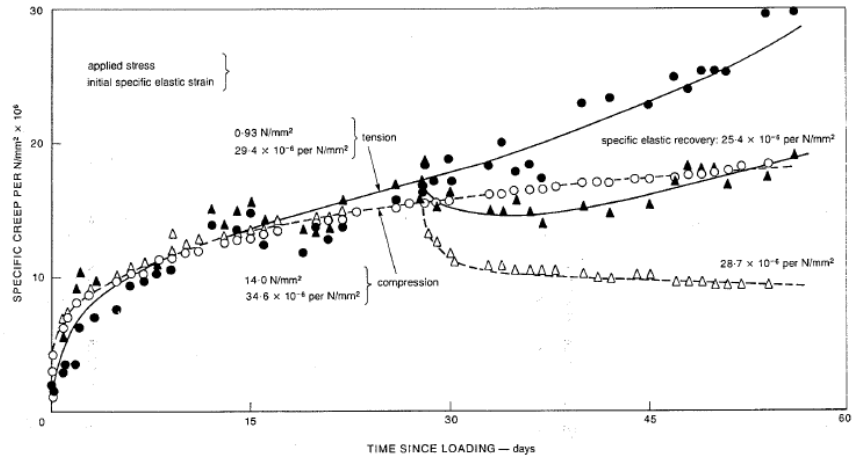

Figure (1.20): Basic creep in tension and compression for concrete loaded at the age of 28 days (Brooks and Neville, 1977)

As shown in Figure (1.21), the rate of total creep in tension is larger than the rate of total creep in compression although at later time the rates are similar. This result about total creep confirms the previous result of Illston (Illston, 1965) i.e. initial rate of tensile creep is higher than that of compressive creep. Even though, Illston (Illston, 1965) mentioned that at later stages, the tensile creep rate becomes much lower than before so that the compressive rate may become the greatest while Brooks and Neville (Brooks and Neville, 1977) mentioned that at late time, the both rates become similar.

Brooks and Neville (Brooks and Neville, 1977) related these results to the extension of the horizontal gel pores under tension promote evaporation which increase the disturbance of

adsorbed water layer. Under compression, contractions of the gel pores reduce the disturbance and hence the creep occurrence.

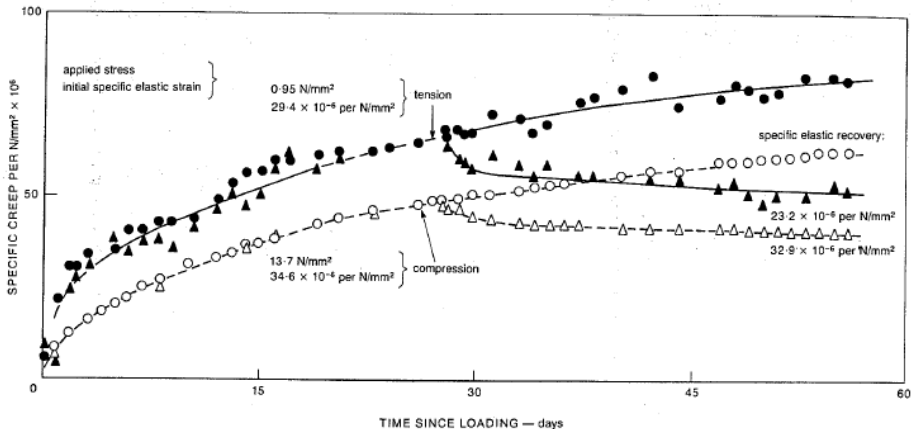

Figure (1.21): Total creep in tension and in compression for concrete loaded at the age of 28 days (Brooks and Neville, 1977)

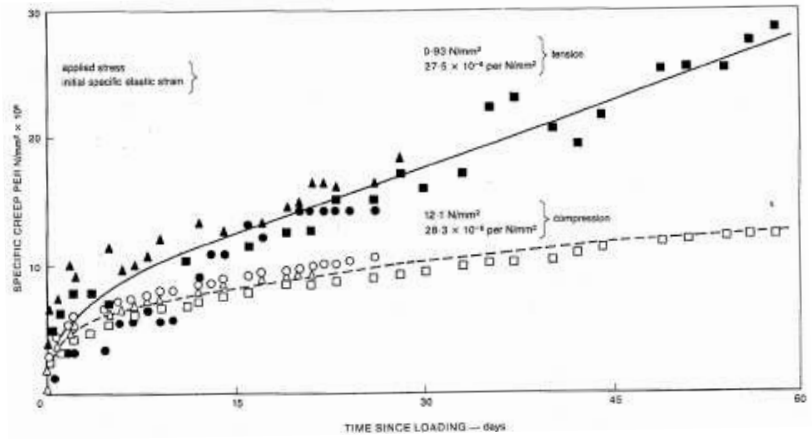

Figure (1.22): Basic creep in tension and in compression for concrete loaded at the age of 56 days (Brooks and Neville, 1977)

Comparing Figures (1.20) and (1.22) with Figures (1.21) and (1.23) respectively shows that the effect of increasing age at loading reduces basic creep in compression while basic creep in tension is not really reduced. The studies of Illston (Illston, 1965) and Bissonnette et al. (Bissonnette et al., 2007) on tensile creep revealed that increasing the age of loading results in decreasing total tensile creep. Figure (1.23) indicates also that for specimens which have been allowed to dry before loading, total creep under both type of loads is reduced and that total creep in tension is lower than that in compression (Brooks and Neville, 1977).

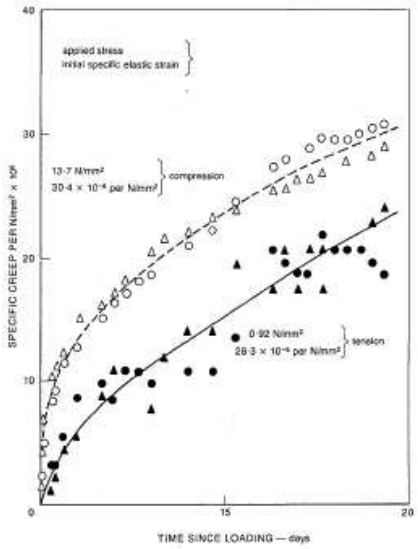

Figure (1.23): Total creep in tension and in compression for concrete loaded at the age of 56 days (Brooks and Neville, 1977**)**

To specify the effect of loading age, Atrushi (Atrushi, 2003) studied both tensile and compressive creep for different ages of loading. The study was carried out on basic creep of high performance concrete at early ages of loading in tension and in compression. As presenting in Figure (1-24), for the same stress/strength ratio of 40%, the magnitude of creep in tension as in compression increases with decreasing the age of loading. Right after the load application the creep in compression is high and then decreases to a progressively lower rate. In contrast, creep in tension is initially lower than in compression, but an almost linear rate is soon established which is much higher than in compression. Consequently, creep magnitude and creep coefficient are larger in tension than in compression.

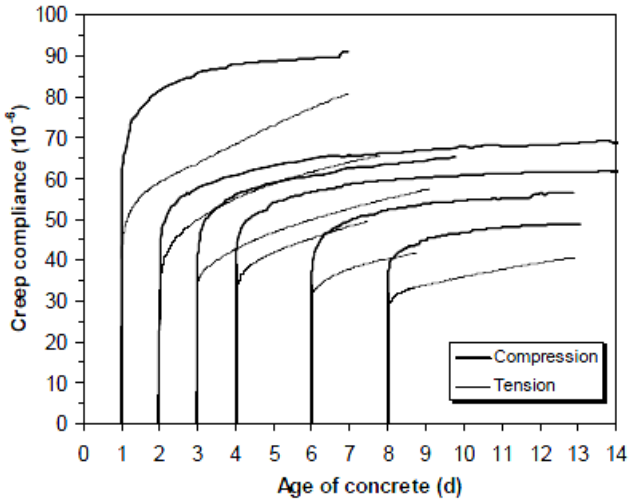

Figure (1-24): Comparison between creep in tension and compression of high performance concrete (Atrushi, 2003)

Another study that concerns the age effect is achieved by Briffaut et al. (Briffaut et al., 2012). The study concerns basic creep of concrete at different early ages of loading (24h – 120h). Compressive creep tests were achieved under a stress level equals to 30% of the compressive strength while tensile creep tests were accomplished under a stress level equals to 30% of the tensile strength (calculated from splitting test) at the time of loading.

A similarity between compressive and tensile creep strains is observed. For the results with the same loading age (120 h) it seems that the initial rate for the compressive test is slightly lower although this difference is not significant (see Figure (1.25)). So, it could be concluded that at early age, compressive and tensile creep strains are similar.

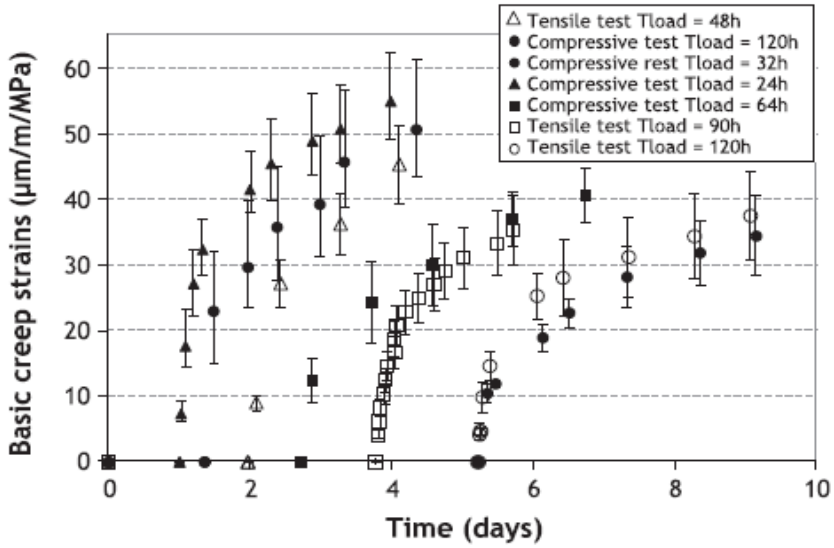

Figure (1.25): Compressive and tensile basic creep strains: loading direction and age effect (Tload= loading) (Briffaut et al., 2012)

These results of similarity between the rate of basic creep in tension and in compression are conformed to the results of Brooks and Neville (Brooks and Neville, 1977) that concerns the first period of basic creep for the concrete loaded at age of 28 days. Even though, in the work of this the last, the rate of basic creep in compression, unlike creep in tension, does not decrease with time. It could be mentioned here that in the work of Brooks and Neville (Brooks and Neville, 1977) the loading level in tension and compression (with reference to their ultimate strength) wasn't the same conversily to the work of Briffaut et al (Briffaut et al, 2012),

Hilaire (Hilaire, 2014) collected several results about the ratio of specific basic creep in compression to that in tension [Figure (1.26)]. The author indicated that it is difficult to compare these results due to the difference between their parameters (concretes used, size and geometry of specimens, environmental conditions and loading age). The author added that for

concretes which are loaded at a time when the hydration process is almost completed, the results appear to depend heavily on environmental conditions. For the autogenous conditions, compressive creep is much higher than tensile one [(Rossi et al., 2012) (Ranaivomanana et al., 2013) and (Reviron, 2009)] while in submerged conditions, creep compliances do not seem to depend on the direction of loading (Brooks and Neville, 1977).

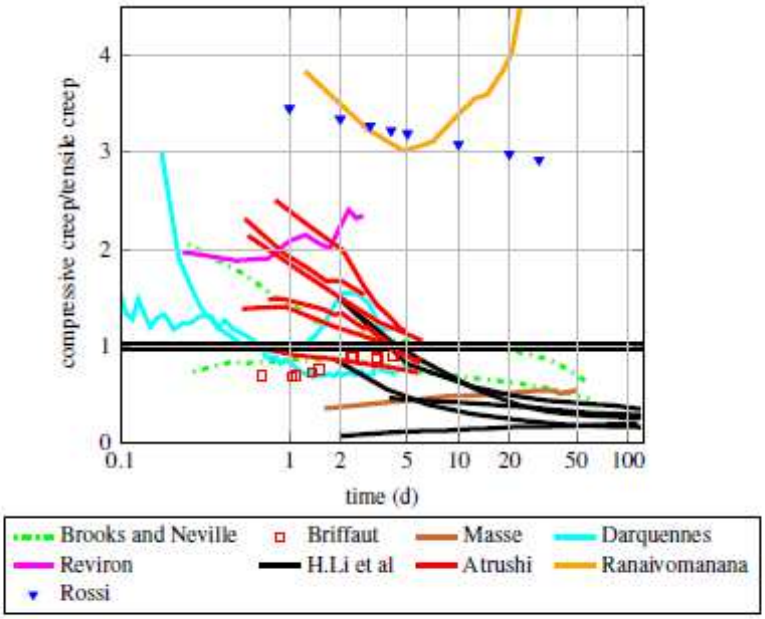

Figure (1.26): Comparison between specific basic creep in tension and in compression (Hilaire, 2014)

The effect of relative humidity on the tensile creep strain was studied by different researchers. Ward et al. (Ward et al., 1969) proposed that it is not correct to assume, according to the seepage theory, that the mechanism of creep in tension is similar to that in compression. These authors studied experimentally tensile creep in different relative humidity conditions.

Three humidity levels (100%, 50% and 30% RH) were studied and the results are shown in Figure (1.27). The series stored in water exhibited the highest creep, as it is expected by seepage theory. However, the magnitude of creep for the remaining two series was in the reverse order.

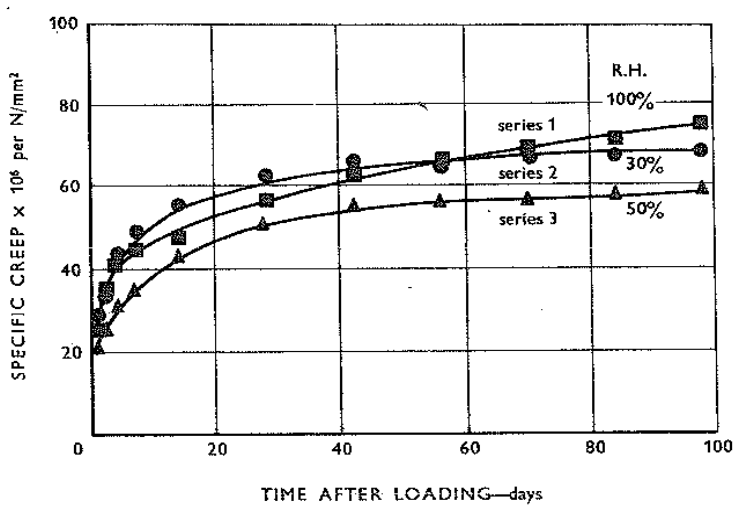

Figure (1.27): Specific tensile creep of concrete stored at different humidity. Age at loading=7 days; stress/strength=0.50 (Ward et al, 1969)

The initial microcracking and hence the rate of creep for the specimens stored in water is lower than that for the specimens stored dry. However, microcracks will exist in specimens of 100% and will propagate via adsorption. For a relative humidity lower than 100%, the proportion of tensile creep due to mechanisms of the adsorption will decrease and the creep will result from microcrack propagation. It can be seen that it is possible for the magnitude of microcracking creep of 30% RH to approach the magnitude of creep due to adsorption and microcracking (100% RH).

To prove their proposition, the authors studied the effect of the cycle humidity on the tensile creep. As it is shown in Figure (1.28), according to the authors, the increase in creep rate when the humidity is changed from 100% RH to 30% RH can probably be attributed to crack propagation resulting from the differential shrinkage. During re-saturation, the induced stress state would be dissipated and the propagation of cracks stopped. As the period of re-saturation was relatively short, microcracking creep due to adsorption was small.

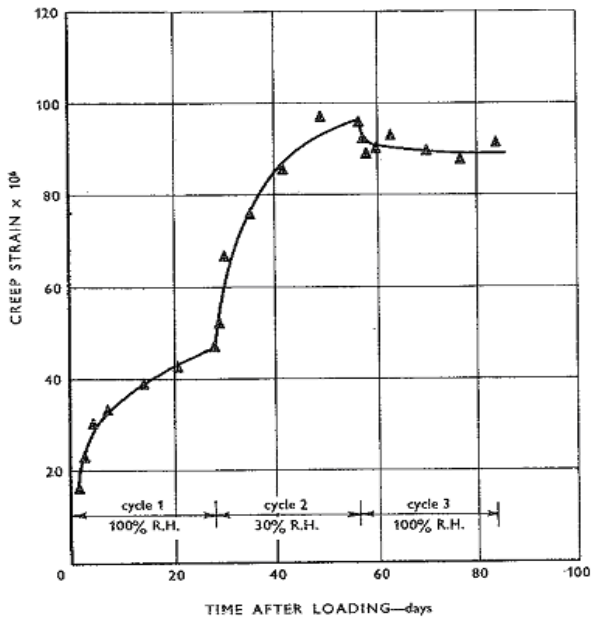

Figure (1.28): Tensile creep of concrete stored at varying humidity-stored wet before loading. Age at loading=28 days; stress/strength=0.30 (Ward et al, 1969)

These results are confirmed with the results of Domone (Domone, 1974). The author studied the effect of curing the concrete specimens either by immersing them in water or by sealing them till the time of loading (at age of 28 days and under stress of 35% of ultimate). Thereafter, the specimens were kept under constant relative humidity. It can be seen from Figure (1.29.a) and (1.29.b), for both cases (immersed and sealed), the creep is increased in the presence of drying. This result is similar to that of compressive creep i.e. the compressive creep strains under water or relative humidity equals 100% are lower than those under drying conditions (see section 1.2.1.6 – Figure (1.10)).

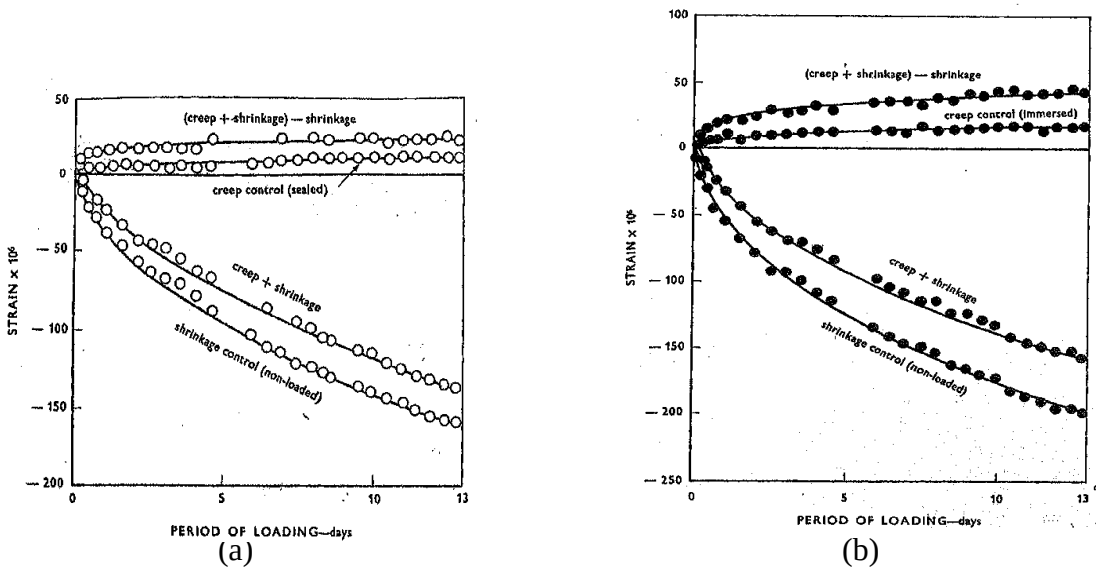

Figure (1.29): Combined creep and shrinkage of specimens: (a) cured sealed, (b) cured immersed (Domone, 1974)

The author also measured the creep of previously immersed concrete subjected to cycles of 4 days' air drying, 3 days' immersion, 4 days' air drying and 3 days' immersion while under load. It had been concluded that creep increases for both gain and loss of moisture (Domone, 1974).

The experimental work of Bissonnette et al. (Bissonnette et al., 2007) was about studying the tensile creep of concrete loaded at age of 7 days, under 50% relative humidity and sealed, for two loading levels. Unlike the results of Ward et al. (Ward et al, 1969) in which the creep strains under 50% RH are lower than those of sealed, the results of Bissonnette et al. (Bissonnette et al., 2007) revealed that creep strains of sealed concrete are much lower than those under 50% RH (see Figure (1.30)).

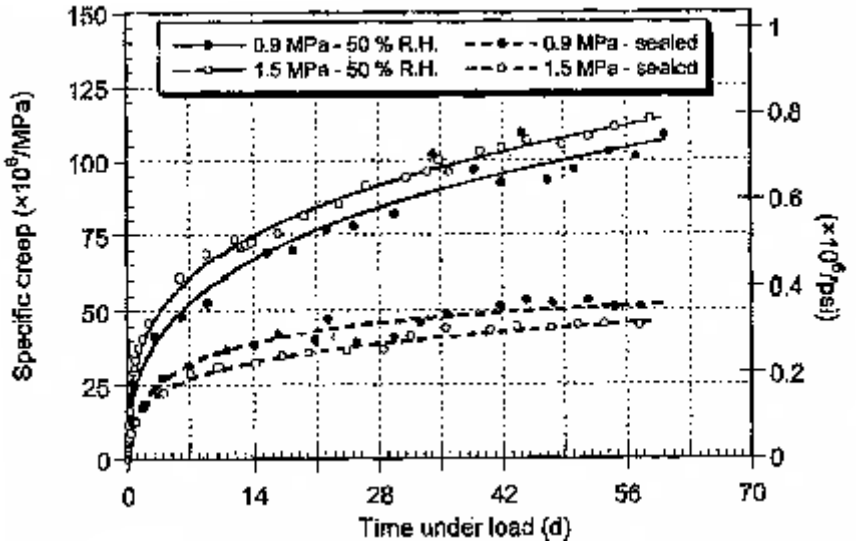

Figure (1.30): Specific creep strain vs. time for concrete loaded at age of 28 days (Bissonnette et al., 2007)

Bissonnette et al. (Bissonnette et al., 2007) also evaluated the effect of cement paste volume on creep value. An experimental test with paste volume of 22%, 27% and 32%, named C22, C27 and C23 respectively, was performed. The results which are presented in Figure (1.31) reveal that tensile creep increases with a reduction in paste content. This result is confirmed with the previous work of Ward et al. (Ward et al., 1969) which was carried on two different volume paste contents. This relation between the volume of cement paste and creep in tension is the opposite of the one that was observed with compressive creep behavior (see section 1.2.1.2).

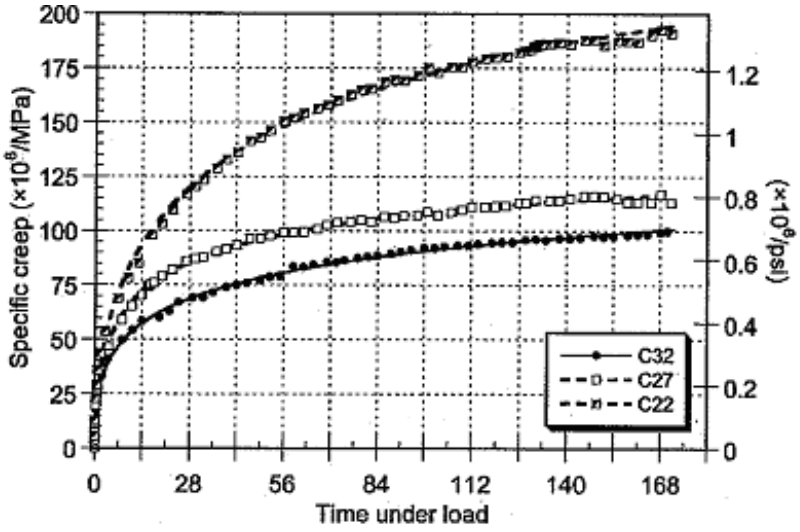

Figure (1.31): Tensile test creep results for mixtures C32, C27 and C22 at 50% RH (test starting at t_0=7 days) (Bissonnette et al., 2007)

This result is related to the microcracking initiation at the aggregate-matrix interface, and propagates preferentially via this interface. The volumetric aggregate content must then exert considerable influence upon the crack propagation. If this is the case, the aggregate content must also influence the magnitude of tensile creep [(Ward et al., 1969) and (Bissonnette et al., 2007)].

The effect of aggregate volume was studied as well by (Domone, 1974). The author studied the uniaxial tensile creep for three aggregate-cement ratios (4.5, 6 and 7.5) for two water-cement ratios (0.55 and 0.6). The specimens were loaded with stress-strength ratio of 35% at age of 28 days, kept under the same curing condition (either immersed in water or sealed) for all the time of loading (14 days). The results revealed that the specific tensile creep decrease with increasing aggregate-cement ratio (see Figure (1.32)).

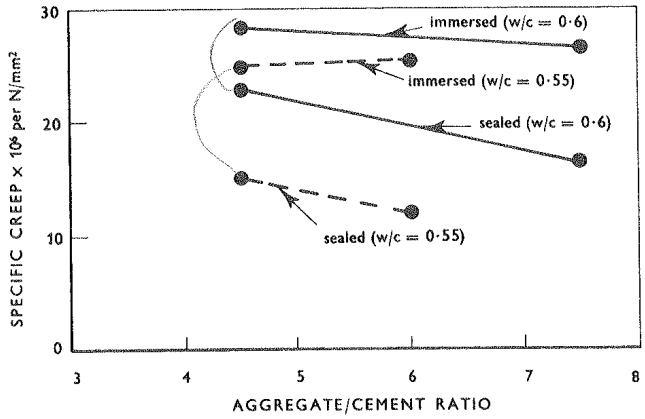

Figure (1.32): Influence of aggregate–cement ratio upon specific tensile creep (specimens loaded at 28 days) (Domone, 1974)

This result is opposite to the ones of the previous mentioned studies, where it indicates that increasing the aggregate quantity results in increasing the tensile creep due to the cracking at interface between aggregate and cement paste. However, the author did not give any explanation to this result. It could also be remarked from the same figure that the creep of sealed concrete is lower than that of immersed concrete.

Domone (Domone, 1974) also studied the effect of loading level on basic creep (sealed and immersed) in tension. Specimens were loaded at different stress levels, up to 90%. The results revealed that creep strain increases with the increasing of loading (see Figure (1.33) and (1.34)). These results are similar to those obtained from compressive creep (see section 1.2.1.3).

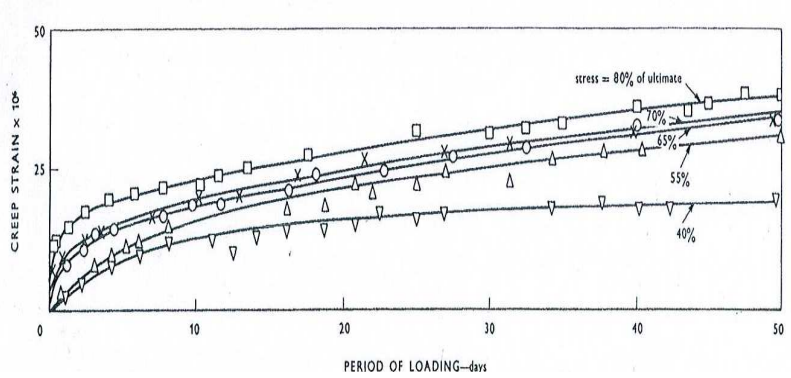

Figure (1.33): Creep strain vs. time, for sealed specimens loaded at age of 28 days (Domone, 1974)

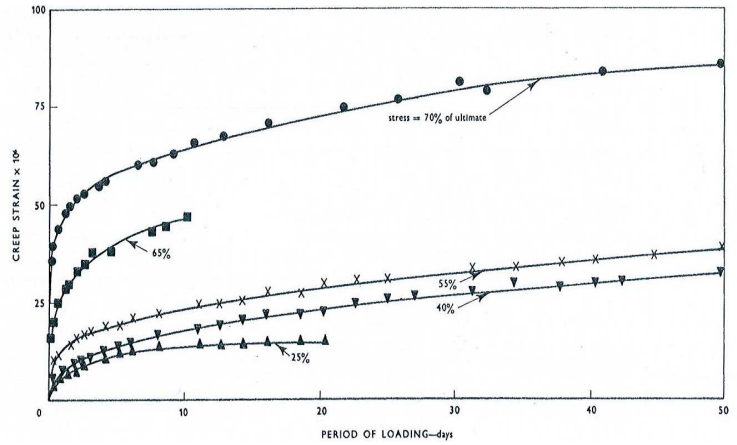

Figure (1.34): Creep strain vs. time, for immersed specimens loaded at age of 28 days (Domone, 1974)

From the previous studies, it could be concluded that tensile creep behavior is look like that of compressive creep. The compressive creep of concrete is related to the movement of water within cement gel and/ or moving the gel itself. As concrete is a brittle material, when a

tensile loading is applied, creep in tension is also related to cracking in addition to the previous causes.

1.1.3 Apparent Poisson's Ratio

The ratio of the lateral strain to the longitudinal strain under sustained load is called "creep Poisson's ratio". At low stresses, creep Poisson's ratio is unaffected by the level of stress, indicating that the longitudinal and lateral deformations due to creep have the same ratio corresponding to elastic deformations (Neville, 2011). Giaccio et al. (Giaccio et al., 1992) revealed that above a stress-strength ratio of 0.5, creep Poisson's ratio increases significantly and progressively with the increase of sustained stress. As well, it is presented by Neville (Neville, 2011) that Loo and Base (Loo and Base, 1990) found that when the applied stress level exceeds 0.8 to 0.9, the creep Poisson's ratio exceeds 0.5.

The study about the creep Poisson's ratio was expanded for multiple loading like in the study of Kim, et al (Kim et al., 2005) which includes the evaluation of basic creep in uniaxial, biaxial and triaxial direction. Tests were carried out on cubic specimens (200mm×200 mm×200 mm) for three different strengths of concrete, namely 26 MPa, 44 MPa and 54 MPa. The creep strains were measured in three principal directions. From the measured strains, Poisson's ratio at initial loading, Poisson's ratio resulting from creep strain and Poisson's ratio resulting from the combined creep strain and elastic strain were obtained. These two last are named "creep Poisson's ratio" and "effective Poisson's ratio", respectively. From analyzing the test results, it was found that the Poisson's ratio at initial loading, the creep Poisson's ratio and the effective Poisson's ratio are approximately equal for each concrete mix. Likewise, the Poisson's ratio at initial loading and the Poisson's ratio due to the combined strain slightly increase as the strength of the concrete increases (see Table (1.3)).

Table (1.3) Poisson's ratio at initial loading, creep Poisson's ratio and effective Poisson's ratio (Kim et al., 2005)

Concrete	Poisson's ratio at initial loading	Creep Poisson's ratio	Effective Poisson's ratio
CI	0.168	0.168	0.169
CII	0.188	0.187	0.188
CIII	0.190	0.179	0.189
The symbols CI, CII and CIII are related to the concrete strength of 26 MPa, 44 MPa and 54 MPa, respectively.			

The creep Poisson's ratio for the three concrete mixes does not depend on the stress states: namely the uniaxial, biaxial and triaxial stress states. Concerning to the creep Poisson's

ratio, the results which are shown in Figure (1.35) revealed the difficulty to determine whether the Poisson's ratio changes with time or remains constant due to the fluctuation.

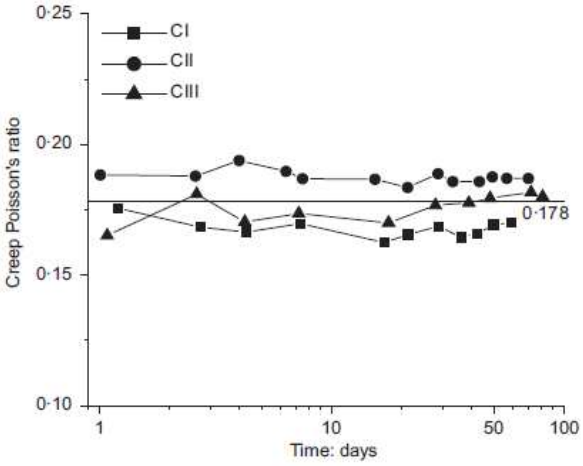

Figure (1.35): Creep Poisson ratio with time (Kim et al., 2005)

Regarding to Figure (1.36), it seems that the effective Poisson's ratio is constant with time.

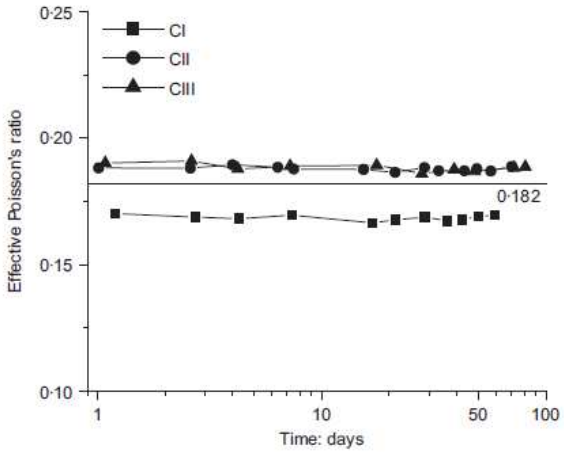

Figure (1.36): Effective Poisson's ratio with time (Kim et al., 2005)

Another work for studying the behavior of the creep Poisson's ratio under three dimensional loading was accomplished by Grasley and Lange (Grasley and Lange, 2007). The experimental work includes four types of cement past with different water-cement ratios and three of these mixes include Type C fly ash (mix 1, mix 2 and mix 4). The procedure involves placing a specimen in a confining cylinder and applying an axial compressive load. The sealed specimens were loaded at the age of one day. The findings from the confined compression experiment suggested that under multiaxial loading, the creep Poisson's ratio of Portland cement paste is relatively constant with age for a period of time, and then generally increases as dilatational compliance comes to a halt (see Figure (1.37)). It should also be

noted that the large volume fraction of elastic aggregates in concrete could damp the time-dependency of creep Poisson's ratio contributed by the paste fraction. Therefore, the potential error introduced by approximating creep Poisson's ratio as constant for typical structural concrete problems would be significantly less than if cement paste alone was considered (Grasley and Lange, 2007).

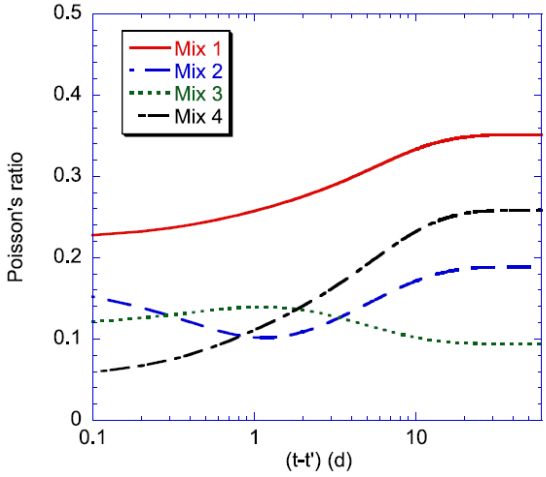

Figure (1.37): Creep Poisson's ratio as a function of time after loading (Grasley and Lange, 2007)

Like the previous result of Kim et al., 2005 (Kim et al., 2005), it could be seen from Figure (1.37) that the creep Poisson's ratio of mix 3 (where there is no fly ash in it) is almost constant.

To fix a value for the creep Poisson's ratio, Torrenti and Benboudjema (Torrenti and Benboudjema, 2014) analyzed several uniaxial, biaxial and triaxial creep tests. Figure (1.38) shows the results of this analysis in the case of biaxial tests of basic creep. The results showed that the creep Poisson's ratio tends to a value between 0.15 and 0.35. Note that the most recent test (Galenne, 2013), that was achieved on concrete nuclear power plant, led to a significantly larger Poisson's ratio (Torrenti and Benboudjema, 2014).

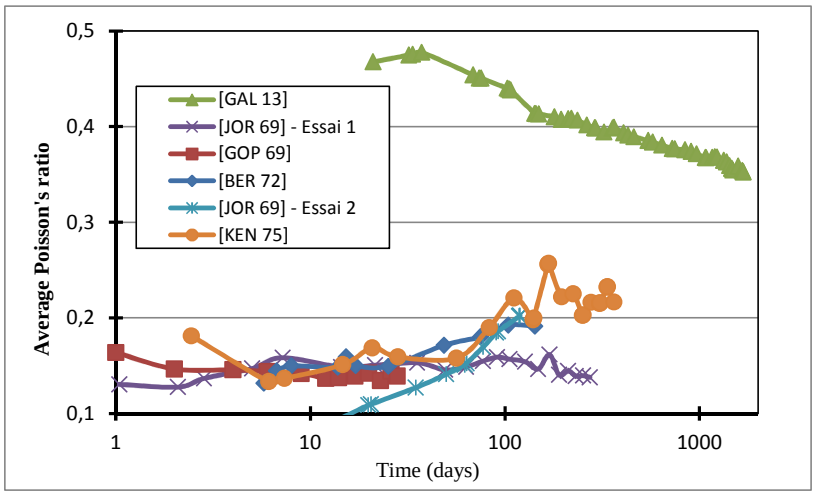

Figure (1.38): Experimental evolution of creep Poisson's ratio (Torrenti and Benboudjema 2014)

From Figure (1.38), it could be remarked that, from the time of loading until about the time of 100 days (except the results of Galenne (Galenne, 2013)), the values of creep Poisson's ratio are between 0.1 and 0.2, which are very close to those obtained by Kim et al., 2005 (Kim et al., 2005) that were between 0.15 and 0.2.

The study of Hilaire (Hilaire, 2014) presents the Poisson's ratio obtained from the total deformation (elastic + basic creep). The evolution of Poisson's ratio decreases sharply during the first 10 days and then it stabilized (see Figure (1.39)). As the previous mentioned results, the apparent Poisson's ratio stabilise after a while, however, the value obtained by Hilaire (Hilaire, 2014), is much lower (see Figure (1.39)).

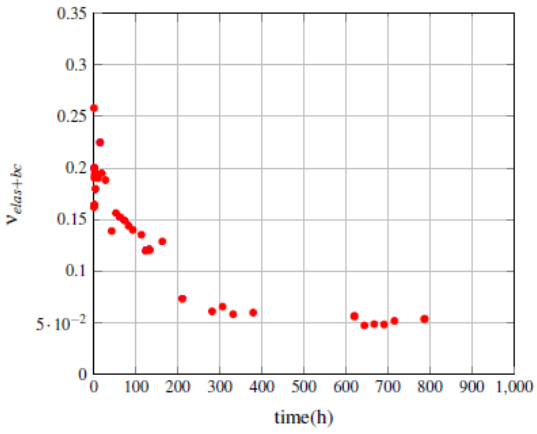

Figure (1.39): Poison's ratio vs. time (Hilaire, 2014)

The most recent work to study the evolution of Poisson's ratio of total strain due to loading, in one and two directions of loading for sealed and unsealed specimens, was done by Charpin (Charpin, 2015). Biaxial tests were carried out on rectangular prisms while uniaxial

tests were carried on cylindrical specimens. For basic creep tests, it was found that the creep Poisson's ratio decreases from 0.35 to 0.25 over the 10 years for the two dimension case while decreases much faster in the one dimension case and stabilized around zero after about 1 year of loading (see Figure (1.40)). For the drying creep, it was observed that the creep Poisson's ratio is again slightly decreasing, from its elastic value, through 11 years of loading. At this time, the results were close for one direction and for two directions. The authors mentioned that the main conclusion of their research is that at least for two directions sealed creep test, the creep Poisson's ratio is moderately decreasing. Nevertheless, and as the previous studies, the authors also concluded that assuming the creep Poisson's ratio as a constant value, is correct.

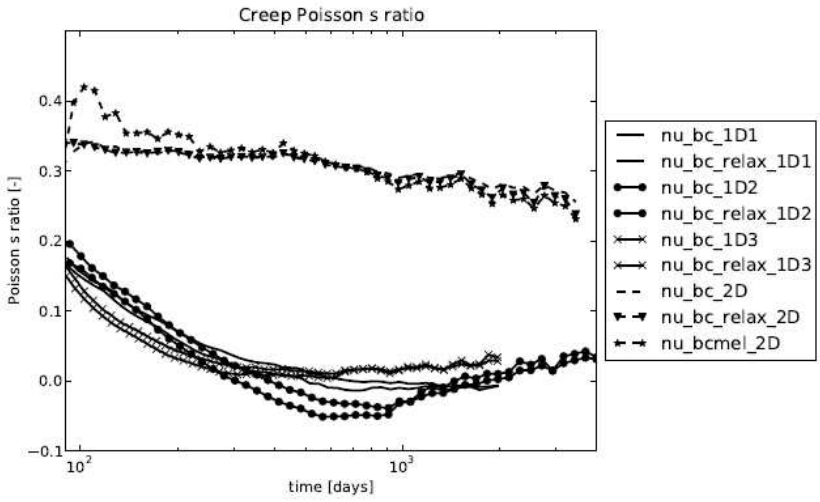

(a)

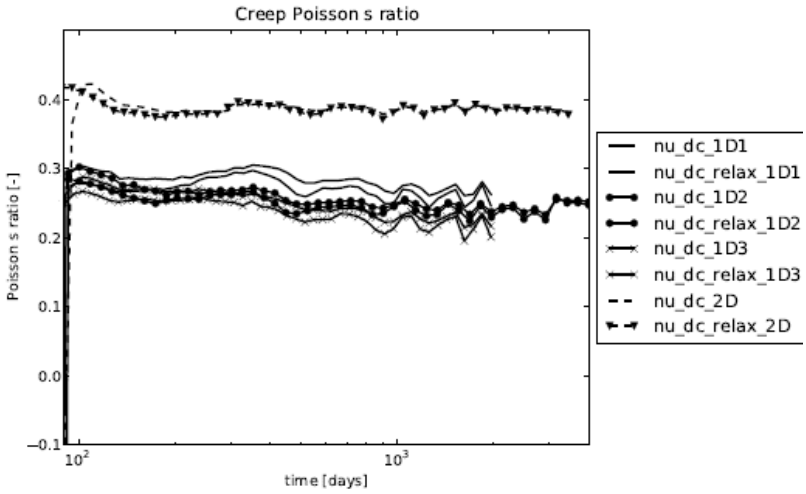

(b)

Figure (1.40): Development of creep Poisson's ratio with time in one direction (1D) and two directions (2D): (a) for basic creep, (b) for drying creep (Charpin, 2015)

Factors that affect creep were studied but it is also necessary to understand how the creep strain affects the structure under sustained load, positively and negatively.

1.1.4 Creep Effects

This section presents the creep effect on the serviceability, durability and concrete performance. The objection is to give a general idea about the advantages and disadvantages of creep strain.

When creep strain occurs, it will cause a relaxation in the existing stresses. For studying this creep effect, the work of Al-Rawi and Al-Qassab (Al-Rawi and Al-Qassab, 1986) was carried on reinforced concrete beams which were casted in I-shape molds having a channel section and subjected to drying shrinkage. For enhancing drying shrinkage, after curing the beams for 3 days, they were transferred to be exposed to a temperature of 35ºC and a relative humidity of 35% and they were saved there until a crack occurred and reached a fairly stable state. The flange of the mold acted as end restraint resulting in a tensile force and a cracking across the length of the beam. Prior to cracking, the tensile force which was very high (the stress/strength ratio closes to unity) and the drying condition promoted creep of concrete which in turn, leaded to a relaxation of the tensile stresses in concrete. They observed that this phenomenon increases the tensile strain capacity of concrete and consequently reduce the possibility of cracking (see Figure (1.41)). In addition, after cracking occurrence, the tensile stresses in concrete increase linearly from zero at the crack location to a maximum at its end. So, tensile creep took place at this zone, and resulting in a decreasing cracking width.

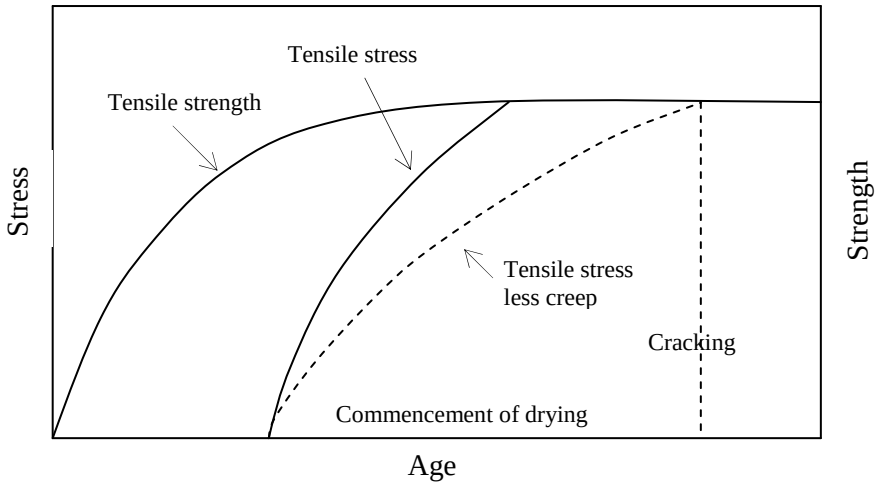

Figure (1.41): Sketch of cracking development (stress wise) (Al-Rawi and Al-Qassab, 1986)

To study the relaxation effect, prestress beams were studied by Mortensen et al. (Mortensen et al., 2003). The study includes the monitoring of post-tensioned concrete members (a single-cell box girder and a solid beam). They measured the losses of prestress due to shrinkage and creep strain throughout the time of loading. They found that the prestress loss increases when the relative humidity decreases, as shrinkage and creep strains are inversely proportional with the relative humidity. In addition, from the measured prestress losses, it was found that the box girders were more susceptible to the effect of moisture than the solid beams due to the higher surface to volume ratios.

The work of Asamoto et al., 2014 (Asamoto et al., 2014) was also on the relaxation effect on prestress beams. The authors measured the prestress loss, deformation and cracking development with various prestress levels. The prestress force was applied at early age of 1 day then at age of 7 days the second prestressing force was applied.

The result showed that the intentional creep induction by a higher first prestressing (creep promotion) at early ages reduces the prestress loss after another prestressing at the age of 7 days. As well, the flexural behavior of prestress beam (there where creep promotion), is not different from the beam which has the same dimensions but it was not exposed to the prestress (there where no creep promotion). Although, the maximum flexural crack width is slightly increased by the creep promotion. This last result is in contrast with that of Al-Rawi and Al-Qassab (Al-Rawi and Al-Qassab, 1986) which revealed that tensile creep leads to decreasing cracking width (as it was explained previously).

Concerning the creep effect on the mechanical properties of concrete, Roll (Roll, 1964) studied the compressive creep effect on the compressive strength of 1 mix of concrete and 3 mixes of mortar. The stress/strength ratios at age of loading (28 days) were 25%, 35%, 50% and 65%, for the mixtures of both concrete and mortars. The results revealed that for all the mixes, there was a slight increase in the strength due to sustained load (creep load). The strength's ratio of concrete creep specimens to those which were unloaded at the end of the test (1141 days) were 1.06, 1.08, 1.12 and 1.19 for stress/strength ratios of 25%, 35%, 50% and 65%, respectively.

Liu et al. (Liu et al., 2002) also studied the basic creep effect on the compressive strength of concrete. The work included two kinds of loading; in biaxial direction on specimens of 100mm×100mm×10mm with age of loading ranging between 14 days and 60 days, and in uniaxial direction on cube of 100mm with age of loading ranging between 60

days and 90 days. The result revealed that creep specimens which were subjected to a sustained load in two directions at an early age (30 days) have higher strengths than those specimens with no sustained loading at the same age. The same result was obtained for specimens loaded in one direction at age of 60 days while this phenomenon weakened the concrete at the age of loading of 90 days (see Table (1.4)). However, it must be mentioned here that for the last case, the applied loading level (60%) was higher than that in the previous cases (30%). In addition, and by using an optical with variable focus, it has been observed that the cracks tend to disappear under biaxial compression load. The authors indicated that the load helps the cement-based material at an early age to compact the whole cement gel framework and to promote the hydration. Besides, the hydration product may come close more easily under a moderate load and the hydrated grains around the cracks probably come closer with time if the humidity is appropriate which could resulting in closing the cracks.

Table (1.4): Creep specimen strength results (Liu et al., 2002)

No.	Creep type	Loading age (days)	Loading duration (days)	Strength of creep specimens (MPa)	Strength of noncreep specimens (MPa)
A-1	Biaxial	14	45	-	8.2
A-2	Biaxial	60	90	14.4	11.3
B-1	Biaxial	30	28	10.8	5.5
B-2	Biaxial	60	30	10.7	7.0
C-1	Uniaxial	60	12	19.7	18.3
C-2	High stress uniaxial	90	18	19.8	20.9

Although the work of Roll (Roll, 1964) was carried on total creep (basic and drying) while that of Liu et al. (Liu et al., 2002) was on basic creep, both of the researchers illustrated that the compressive strength increases due to creep loading.

The work of Asamoto et al. (Asamoto et al., 2014) was carried out to examine the effect of the creep on the mechanical properties of the concrete at early ages. A sustained compressive load was applied at an age of 1 day, and a second load was applied at an age of 7 days. The results revealed that if creep induced within the elastic range, both the compressive strength and Young's modulus of the cylindrical specimens were higher than those of the unloaded specimen (without creep). This finding confirms the results of Roll (Roll 1964) and

Liu et al., 2002 (Liu et al., 2002). Asamoto et al. (Asamoto et al., 2014) explained the increase in the strength with the seepage of the moisture in the fine pores, resulting in denser pore structure. However, when the direct tensile test was carried out, the tensile strength and Young's modulus were almost the same for the both type of specimens. On another hand, the creep promotion under a high stress beyond the elastic range has no effect on the compressive strength and may reduce the tensile strength (see Table (1.5)).

Table (1.5): Mechanical characteristics of concrete (Asamoto et al., 2014)

Specimen *	Compressive strength (MPa)	Compressive Young's Modulus (GPa)	Tensile strength (MPa)	Tensile Young's Modulus (GPa)
Non-loaded	37.70	27.22	3.04	25.60
$0.2f_c$_1d - 0.2 f_c_7d	40.62	29.38	3.01	25.01
0.3 f_c_1d - 0.2 f_c_7d	44.07	30.77	3.10	26.83
$0.4f_c$_1d - 0.4f_c_7d	39.51	29.19	2.57	25.42
* The names of specimens defined: stress level at age of 1day – stress level at age of 7days.				

Another study the residual to evaluate capacity of concrete after loading was done by Saliba et al. (Saliba et al., 2012). Here, the test of basic creep in bending was carried out on concrete beams (100mm×200mm×800mm). After curing in water for 28 days, three-point bending creep tests were performed on the specimens by loading them with 85% of their maximum strength. After 4 months, these creep specimens with the control specimens were all subjected to three-point bending test up to failure. The acoustic emission technique was used to evaluate the influence of creep on the cracking development. The results indicated that when concrete is submitted to a sustained load (quite high), two opposite effects appear: consolidation and consequently strengthening in the compression zone, and cracking and consequently weakening in the tension zone. It was also reported, that the fracture energy is higher for creep specimens than those of control. In general, the fracture energy increases as strength increases. This increase in fracture energy may be explained by the strengthening effect due to basic creep (Saliba et al., 2012).

1.2 Numerical Models

Creep could be modeled using different ways like standard codes, analytical models or rheological models. Some of these models take into account the effect of temperature and relative humidity on the creep strains. This study concerns with the effect of applied stress

and the nonlinearity between this applied stress and the creep deformation. Since, neither the effect of temperature nor the relative humidity is taken into account.

1.2.1 Models Used in Standard Code

The regulation models are the models that calculate the creep strain in a simple way like the ACI Committee (ACI Committee 209R-921, 1992) model and the CEB-FIP (CEB-FIP, 1998) model. These models do not take into account all the factors that affect creep, like temperature or relative humidity. So, creep strains obtained by using these models are not accurate. Even though, it is practical to use them to give a primary estimation of creep strains.

1.2.2 An Example of Analytical Model (Bazant and Prasannan, 1989)

The model that was proposed by Bazant and Prasannan (Bazant and Prasannan, 1989) is the most famous and the most used. This model is based on the solidification theory which uses a micromechanical analysis to express aging, through a suitable model, as a growth of the volume fraction of load-bearing solidified matter i.e. the cement hydrated. The microscopic component itself is proposed as non-aging viscoelastic material due to its physic-chemical nature.

The author adopted the rheological model which is illustrated in Figure (1.42), to reflect the concrete strains. This model represents aging as a consequence of the growth of the volume fraction of the solidified matter associated with the viscoelastic and viscous strains.

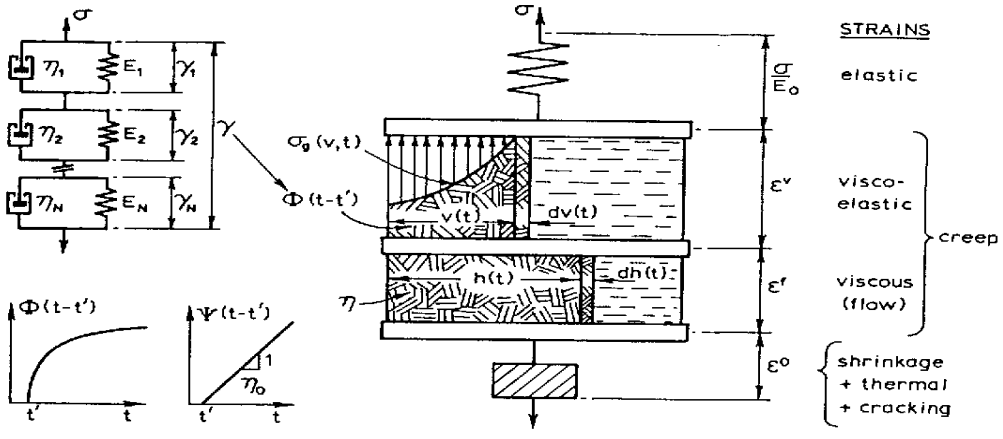

Figure (1.42): Model for role of solidification in creep (Bazant and Prasannan, 1989)

As it is illustrative in Figure (1.42), total strain ε and creep strain ε^c could be expressed as follows:

$$\varepsilon = \frac{\sigma}{E_o} + \varepsilon^c + \varepsilon^o \tag{1.2}$$

$$\varepsilon^c = \varepsilon^v + \varepsilon^f \tag{1.3}$$

where σ is the stress, E_0 is the Modulus of Elasticity, σ / E_0 is the elastic strain, ε^0 is the strain which is independent on stress like shrinkage and thermal dilatation, ε^v is the viscoelastic strain, and ε^f is the viscous strain (flow).

The basic hypothesis illustrated by this model is that the volume elements $dv(t)$ solidified at various times are all subjected to the same strain, which is equal to the overall (macroscopic) creep strain. This hypothesis implies the coupling of all these volume elements to be in parallel.

The micro-stress $\sigma_g(v,t)$ introduced in the solidified matter at time t, is defined as the stress at the location where solidification has occurred and when the volume of all the solidified matter was v. A layer of thickness $dv(\tau)$ is assumed to solidify and bind with the previously solidified matter at time τ, at which the volume of all the solidified matter is v. The solidifying material at microscale is considered to be non-aging and linearly viscoelastic.

Since, on the one hand, the creep curve continues to change for long ages, and on the other hand, the growth of volume fraction of hydrated cement terminates earlier, the latter cannot be related to the effect of aging on creep. The solidification theory of Bazant and Prasannan (Bazant and Prasannan, 1989) solved this contradiction by introducing the effective load-bearing fraction as a moderate interpretation of $v(t)$. This fraction can continue to grow up to long ages as a result of progressive formation of bonds between hydrated cement particles, e.g., the phenomenon of polymerization of tricalcium silicate hydrate in cement gel.

The solidification theory gives a good indication about the creep rate at low loading levels but not at high levels at which the creep rate becomes to increase rapidly. The increasing in creep rate leads to nonlinearity between creep strain and stress. This nonlinearity is physically related to the damage that occurs in concrete due to creep effect. This phenomenon gave the motivation to develop creep-damage models.

1.2.3 Rheological Models Based on Spring and Dashpot Units

This paragraph presents some rheological models that are based on spring and dashpot units of Maxwell and/ or Kelvin-Voigt arranged in parallel or in series.

1.2.3.1 Nonlinear Creep-Damage Model under Uniaxial Compressive Load (Mazzotti and Savoia, 2003)

A rheological nonlinear creep-damage model was developed by Mazzotti and Savoia (Mazzotti and Savoia, 2003). The model takes into account both creep nonlinearity and damage propagation growth at high stress levels. The creep strain is modeled by extending the solidification theory of Bazant (Bazant, 1977) in a nonlinear range which is evaluated as a function of a damage index, using a law calibrated from experimental results. It is also assumed that most of the creep strain does not produce damage and that only a fraction of it contributes to damage evolution with time.

The general time step, the pseudo-elastic incremental equations governing the creep nonlinearity and damage growth with time are integrated in a closed form by considering mean values of damage index and of nonlinear creep variables. So, an effective strain ε_{eff} is defined for the creep-damage instead of the equivalent strain ε_{eq} defined by Mazars and Pijaudier-Cabot (Mazars and Pijaudier-Cabot, 1989).

$$\varepsilon_{eq} = \sqrt{\sum_{i=1}^{n} \left\langle \varepsilon_i^{el,d} \right\rangle_+^2} \tag{1.4}$$

where $\left\langle \varepsilon_i^{el,d} \right\rangle_+$ is the positive principal component of the damage elastic strain and is defined in the following equation:

$$\varepsilon^{el,d} = \varepsilon^{el} + \varepsilon^{d} \tag{1.5}$$

where ε^{el} represents the instantaneous elastic strain while ε^{d} represents the damage strain. The effective strain is defined as the summation of instantaneous damaged elastic strain and a fraction of creep strain, as it is presented in Equation (1.6).

$$\varepsilon_{eff} = \varepsilon^{el} + \beta \varepsilon^{v} \tag{1.6}$$

The coefficient β represents a fraction of creep strain (ε^{v}) contributing to damage evaluation and is considered, for simplicity, independent of loading level.

The model is able to capture the creep-damage interaction mechanism of concrete under uniaxial compression, covering the whole range of stress levels, from low stress where the behavior is substantially viscoelastic, to nonlinear creep for medium-level stresses (not accompanied by significant concrete damage), to very high stresses where failure may occur by tertiary creep.

Later on, the damage coefficient (β) was also used in the models of Reviron et al. (Reviron et al. 2007), Benboudjema and Torrenti (Benboudjema and Torrenti 2008), Omar et al. (Omar et al. 2009) and Briffaut et al. (Briffaut et al. 2011).

1.2.3.2 Nonlinear Chemo-Thermo-Viscoelastic Damage Model (Benboudjema and Torrenti 2008)

This model which was developed by Benboudjema and Torrenti (Benboudjema and Torrenti 2008) is simple and robust. The mechanical behavior of concrete is modeled by coupling the elastic damage model of Mazars (Mazars, 1986) with creep represented by a rheological model. The assumptions that were adopted to develop this model are as follows:

- Chemo-thermal model

The evolution of hydration is achieved by using the chemical affinity.

$$\dot{\xi} = \tilde{A}(\xi)\ \exp\left(-\frac{E_a}{RT}\right) \tag{1.7}$$

where E_a is the activation energy (J mol^{-1}), R is the ideal gas constant 8.3145 (J K^{-1} mol^{-1}), T is the temperature (K), ξ is the hydration degree and $\tilde{A}(\xi)$ is the chemical affinity (s^{-1}) given by the following equation:

$$\tilde{A}(\xi) = a + b\xi + c\xi^2 + d\xi^3 + e\xi^4 + f\xi^5 + g\xi^6 \tag{1.8}$$

where a, b, c, d, e, f, g are constant parameters of a material which can be identified from a semi-adiabatic test.

- Elastic damage model

The relationship between apparent stresses σ, effective stresses $\tilde{\sigma}$, damage D, elastic stiffness tensor E, total strain ε, elastic strains ε_e, basic creep strains ε_{bc}, thermal strain ε_{th}, autogenous shrinkage ε_{au} and total strain ε are represented by Equations (1.9) and (1.10).

$$\sigma = (1 - D)\,\tilde{\sigma} \tag{1.9}$$

$$\dot{\tilde{\sigma}} = (1 - D)\,E(\xi)\,\dot{\varepsilon}_{el} \text{ and } \dot{\tilde{\sigma}} = (1 - D)\,E(\xi)\left(\dot{\varepsilon} - \dot{\varepsilon}_{bc} - \dot{\varepsilon}_{au} - \dot{\varepsilon}_{th}\right) \tag{1.10}$$

The damage criterion defined by Mazars (Mazars, 1986) is:

$$f_t(\xi) = \varepsilon_{eq} - k_0(\xi) \tag{1.11}$$

where ε_{eq} is the equivalent tensile elastic strain, and $k_0(\xi)$ is the tensile strain threshold and it is equal to $\frac{f_t(\xi)}{E(\xi)}$

$$\text{If } \varepsilon_{eq} \le k_0(\xi), \quad D = 0 \tag{1.12}$$

$$\text{Otherwise,} \quad D = 1 - \frac{k_0}{\varepsilon_{eq}}\left[(1+A_t)\exp(-B_t.\varepsilon_{eq}) - A_t\exp(-2B_t.\varepsilon_{eq})\right] \tag{1.13}$$

where A_t and B_t are constant material parameters which controls the softening branch in the stress-strain curve in tension.

In the finite element analysis, strain softening can lead to a mesh dependency which produces a failure without any control of energy dissipation (Pijaudier-Cabot and Bazant, 1987). To overcome this shortcomings, a characteristic length which is related to the mesh size [(Rots, 1988) and (Cervera and Chiumenti, 2006)], is introduced.

For this model, damage considered coming only from tensile stress and the density of the dissipation energy is given by Equation (1.13).

$$g_{ft}(\xi) = \frac{f_t(\xi)\ (1 + A_t / 2)}{B_t} \tag{1.14}$$

While the characteristic length l_c is calculated from the fracture energy $G_f(\xi)$, and density of the dissipation energy $g_{ft}(\xi)$.

$$l_c = \frac{G_{ft}(\xi)}{g_{ft}(\xi)} \tag{1.15}$$

- Basic creep model

To represent the basic creep model, several rheological elements of Kelvin-Voigt combined in a series are used (see Figure (1.43)).

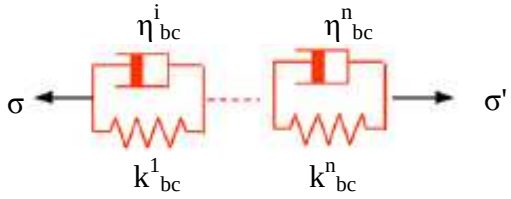

Figure (1.43): Kelvin-Voigt elements for predicting creep strain (Benboudjema and Torrenti 2008)

The incremental equilibrium equation for the Kelvin-Voigt unit named *i* is:

$$\dot{\tilde{\sigma}} = \dot{\tilde{\sigma}}_{sp} + \dot{\tilde{\sigma}}_{dp} \tag{1.16}$$

where $\dot{\tilde{\sigma}}_{sp}$ and $\dot{\tilde{\sigma}}_{dp}$ are the effective stresses acting on the spring and on the dashpot, respectively.

The behavior law of the spring is:

$$\dot{\tilde{\sigma}}_{sp} = k_{bc}^{i}(\xi)\dot{\varepsilon}_{bc}^{i} \tag{1.17}$$

The behavior law of the dashpot is:

$$\dot{\tilde{\sigma}}_{dp} = \eta_{bc}^{i}(\xi)\dot{\varepsilon}_{bc}^{i} \tag{1.18}$$

where k_{bc}^{i} and η_{bc}^{i} are the stiffness of spring and viscosity of the dashpot, respectively, of Kelvin-Voigh unit. The effect of age on basic creep of concrete is taken into account by the dependency between the material parameters and the degree of hydration. The stiffness parameters for each Kelvin-Voigh unit are calculated from the following equations (De Schutter, 1999):

$$k_{bc}^{i}(\xi) = k_{bc\_\infty}^{i} \frac{0.473}{2.081 - 1.608\bar{\xi}} \bar{\xi}^{0.62} \tag{1.19}$$

$$\eta_{bc}^{j}(\xi) = \eta_{bc\_\infty}^{j} \frac{0.473}{2.081 - 1.608\bar{\xi}} \bar{\xi}^{0.62} \tag{1.20}$$

By combining the Equations (1.16) - (1.20), a non-linear second-order differential equation is obtained represented by Equation (1.21).

$$\tau_{bc}^{i}\ddot{\varepsilon}_{bc}^{i} + \left(\tau_{bc}^{i}\frac{\dot{k}_{bc}^{i}(\xi)}{k_{bc}^{i}(\xi)} + 1\right)\dot{\varepsilon}_{bc}^{i} = \frac{\dot{\tilde{\sigma}}}{k_{bc}^{i}(\xi)} \tag{1.21}$$

where τ_{bc}^{i} is the characteristic time which is considered constant. In solving this last equation, the deformation of each Kelvin-Voigt element chain can be calculated.

This model allows predicting the damage of material in tension if the compressive stresses are small compared to the compressive strength. On the contrary, it is not suitable for describing dilatancy and behavior of high biaxial or high triaxial compressive stresses.

- Coupling between creep and damage

To represent the nonlinearity of creep at a high stress level, the proposal of Mazzotti and Savoia (Mazzotti and Savoia, 2003) was adopted. As it was mentioned previously (section 1.2.3.1), the authors proposed to include a part of creep strains into the expression of the equivalent strain (ε_{bc}) defined by Mazars (Mazars, 1986):

$$\varepsilon_{eq} = \sqrt{(\varepsilon_{el} + \beta \varepsilon_{bc})_+ : (\varepsilon_{el} + \beta \varepsilon_{bc})_+} \tag{1.22}$$

where ε_{bc} is the creep strain, ε_{el} is the elastic strain and β is a fraction of creep strain contributing to damage evolution.

1.2.3.3 Nonlinear and Viscoelastic Model (Sellier, 2009)

Another nonlinear and viscoelastic rheological model was developed by Sellier (Sellier, 2009) this model proposes for non saturated concrete that the applied stress changes the effect of the capillary pressure. In addition, the damage state (microcracks) that exists around the unsaturated capillary pores is also supposed to be depend on the applied stress. So, the applied stress may lead to either close or open these microcracks. As a result, that will decrease to either increase or decline the transmission of capillary effects to the solid skeleton.

This theory is supported by using a numerical model of a composite material including an elastic matrix, elastic inclusions (more rigid to the matrix) and capillary pores with lower pressure (in an unsaturated case), (see Figure (1.44)). The nonlinearity of capillary effect, which depends on the applied stress, provides the capability to simulate shrinkage and drying creep. The model consider the difference in creep mechanism under deviant stress of a dominate part for slipping without volume variation, and of a hydrostatic part which is tangle with the slipping. As a result, a volume variation happens due to the reduction in the space of the pores.

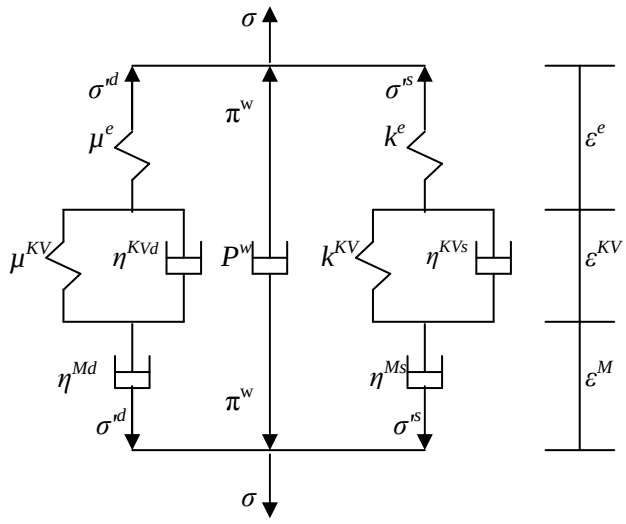

σ : total stress
σ^{rs} : spherical part on solid skeleton
σ^{rd} : deviator part
π^w : hydraulic stress due to the capillary depression P^w.
s : represent the spherical model
d: represent the deviator model

Figure (1.44): Stresses partition partially spherical, deviator and hydraulic stress (Sellier, 2009)

1.2.3.4 Linear Creep-Damage Model (Thai et al. 2014)

This model which was presented by Thai et al. 2014 (Thai et al. 2014) describes the creep of cement-based materials with the effects of damage. The model represents the cement-based materials behavior based on the pseudo-strain approach of Schapery (Schapery, 1984) coupled with the isotropic damage model of Mazars (Mazars, 1986). This procedure relies on the material represented as a composite consisting of spherical elastic inclusions (aggregates) and voids (pores), embedded in a linear viscoelastic matrix (cement paste) whose behavior is assumed to be ruled by 3-chain generalized Maxwell model (see Figure (1.45)).

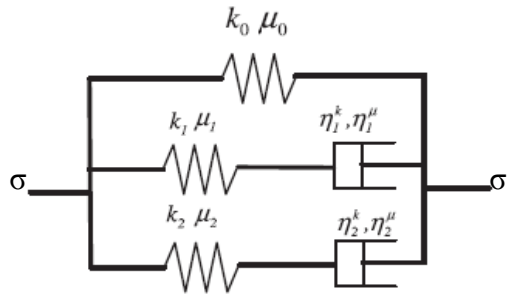

k_0, k_i : moduli of generalized Maxwell model describing the effective bulk modulus of the material
μ_0, μ_i : moduli of generalized Maxwell model describing the effective bulk modulus of the material
$\eta_i^{m,k}$, $\eta_i^{m,\mu}$: viscosities

Figure (1.45): Generalized Maxwell model with 3 chains used to describe the behavior of the matrix (Thai et al. 2014)

1.2.3.5 Basic Creep Model (Hilaire, 2014)

The rheological diagram chosen by Hilaire (Hilaire, 2014) to model the basic creep consists of two aging elements: a Kelvin-Voigt unit placed in series with a dashpot. The basic

creep observed at young age is modeled mainly by the Kelvin-Voigt element while the long-term basic creep is modeled by using a second dashpot η_{am} (see Figure (1.46)).

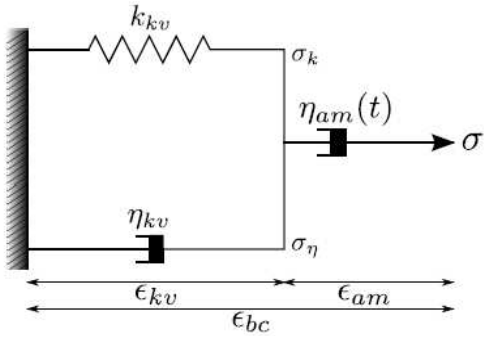

Figure (1.46): Rheological model of basic creep (Hilaire, 2014)

This model take into account the non-linear character of basic creep and delayed fracture of concrete under high mechanical loading, by adding the coefficient of Mazzotti and Savoia (Mazzotti and Savoia, 2003) in equivalent strain equation of Mazars (Mazars, 1986). It is worth to be mentioned that the model is capable to compute basic creep in tension and compression. This model is able to take into account the complacency difference between the tensile basic creep and the compressive basic creep.

As was seen, there are no sufficient experimental results about the creep effects on the residual mechanical properties of concrete to be concluded. So, the effects of creep on the development of mechanical properties of concrete (Young's modulus, compressive strength and tensile strength) was adopted in this study and presented in chapter two.

The previous presented models didn't take into account the effect of the difference in stiffness between aggregate and cement paste. This effect is represented by the resistance of aggregate to the creep of cement paste under the applied loading. This resistance produces tensile stresses which generate microcracks at the aggregate-cement paste interface. Recently, mesoscopic mesh has been used to study the failure of concrete beam under flexural load which highlight the presence of microcracking due to the sustained load (Saliba et al., 12).

So, in our study, mesoscopic model was adopted for simulating the concrete as a material which is composed from aggregate and cement paste, as it is presented in chapter three of this study.

CHAPTER II: EXPERIMENTAL INVESTIGATION OF MECHANICAL CHARACTERISTICS OF CONCRETE

The objective of this work is to study the effect of creep and quasi instantaneous loading on the concrete mechanical behavior. This chapter includes a description of the materials that have been used and the laboratory experimental tests that were carried out. Creep tests were realized on cylindrical concrete specimens for different concrete loading ages and loading levels.

Summary of Chapter II

2.1 Fabrication of concrete and system used for measuring its mechanical properties

This paragraph includes the steps of casting, curing and preparing the concrete specimens to be suitable for the tests that were decided to be achieved. It also includes the description of the devices and the apparatus used throughout performing the tests.

2.2 Effect of preloading in compression on the concrete tensile strength

The section of a prestressed structure is subjected firstly to compressive stress followed, for part of it, by a tensile stress due to external load or creep strain. Before finding out the creep effect on the tensile resistance, it was decided to verify the effect of quasi-instantaneous loading. So, specimens were loaded in compression until a determined loading level and then indirect tensile test was performed on these preloaded specimens.

2.3 Compressive creep

The work presented in this paragraph was carried out to overcome the lack in studying the compressive creep effects on the residual mechanical properties of concrete. Therefore, compressive creep tests were carried out on concrete specimens at different loading levels. Thereafter, either the compressive strength test was carried out for evaluating the elastic modulus and the compressive strength or the indirect tensile strength was achieved for evaluating the tensile strength. In addition, as the Poisson's ratio is important in two directions prestressed structures, the apparent Poisson's ratio was studied here.

2.4 Creep in tension (Brazilian creep)

Concrete beams subjected to flexural loading and concrete under restrained shrinkage are subjected to tensile stresses that lead to tensile creep. To verify the effect of tensile creep on residual tensile strength, indirect tensile creep tests were carried out followed by the indirect tensile strength test.

2.1 Fabrication of Concrete and Experimental Devices

2.1.1 Concrete Composition

It was important to cast concrete with high-performance to obtain reliable results. So, cement, sand and gravel of high-quality were used. The objective was to cast concrete that creeps under the load that could be applied by the equipped creep apparatus in the laboratory. To achieve this purpose, it was necessary to cast concrete with rather high quantity of cement paste. The slump was decided to be 10 ± 1cm (which is quite high), the water/ cement ratio was decided to be equal to 0.5 and that of sand/ gravel equal to 1.2 (the sand/gravel ratio is same as the standard concrete used in the 3SR laboratory). Therefore, the Abraham test was carried out several times until the decided slump was obtained. Thereafter, the quantity of cement, sand and gravel were calculated according to that (see Table (2.1)).

Table (2.1): Type and quantities also of concrete compositions used

Concrete compositions and properties	Quantities and values
Water	174 kg/m^3
Cement (CEM I B 52.5)	348 kg/m^3
Sand (1.8 mm)	826 kg/m^3
Gravel (0.5/8 mm)	991 kg/m^3
Concrete compressive strength at age of 30 days	42.1 MPa

2.1.2 Casting of Specimens

Mixing of the concrete ingredients was achieved by using a mixer of 25 liters capacity. The mixer was damped then charged with the ingredients as follows: half amount of the gravel, half amount of the sand, all the cement, and then the residual half of the sand followed by the gravel. The mixer was operated for mixing the ingredients until a homogeneous colour was remarked which took about 2 minutes. Then, while the mixer was operating, the water was added for about 30 seconds thereafter the mixer was left working for 3.5 minutes. After that, the mixer was stopped and the ingredients were wiped out of it. The slump test was achieved for each batch of concrete immediately at the end of mixing.

For all the tests, PVC cylindrical molds, of 70mm inner diameter and 140mm high, were used. A needle vibrator of 18mm diameter was used for compaction the concrete layers after casting it inside the molds. The concrete was poured in 2 layers; the first one which was about third of the mold height, was vibrated for about 5 seconds then after the second layer

was cast which took the rest of the height, both of the two layers were vibrated for about 15 seconds.

2.1.3 Curing Conditions

After molding, the fill molds were covered with polyethylene sheets to prevent the water evaporation. After 24 hrs, the concrete specimens were carefully unmolded and placed in a water tank until the age of creep loading which was decided to be 30, 60 or 90 days. All the specimens that were kept for the creep test were wrapped by aluminium scotch to prevent the water evaporation. Afterword, these specimens were transferred to be stored in air under controlled conditions of $(20 \pm 1)^{o}$C and (50 ± 5)% RH throughout the time of creep test which persisted for 30 days for all the creep series.

2.1.4 Preparing the Surfaces of Specimens

To allow the load to be distributed uniformly over the area of loading, the parallel top and bottom surfaces of the specimens had been smoothen. A grinding machine mark Tour Colchester which is presented in Figure (2.1), was used for smoothing the circular surfaces of all cylindrical specimens that were used in this work.

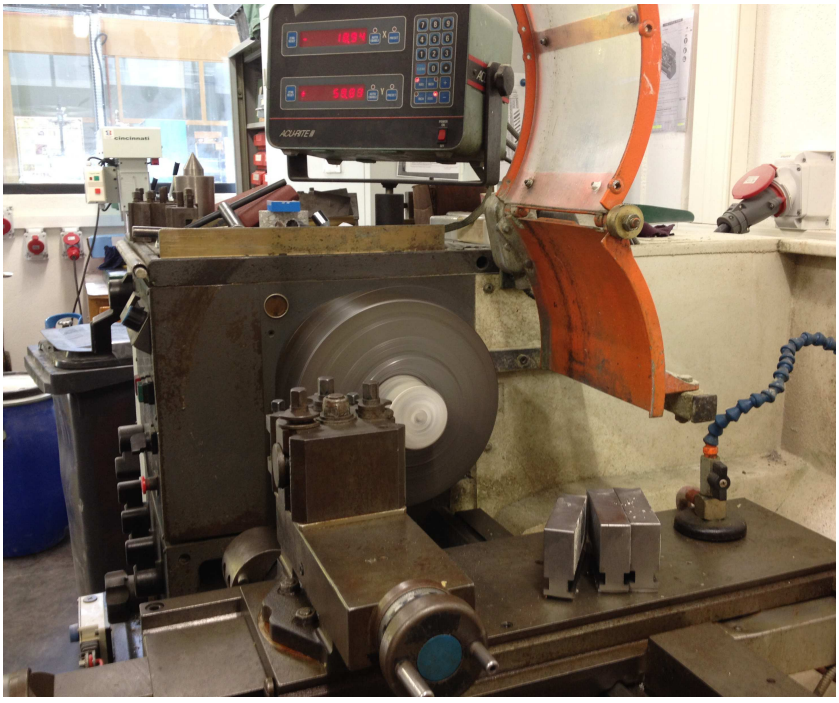

Figure (2.1): grading machine (Tour Colchester)

Figure (2.2.a) and Figure (2.2.b) reveal the surface level variation (0.1mm/70mm) of random samples that had been certificated by grading machine (Tour Colchester).

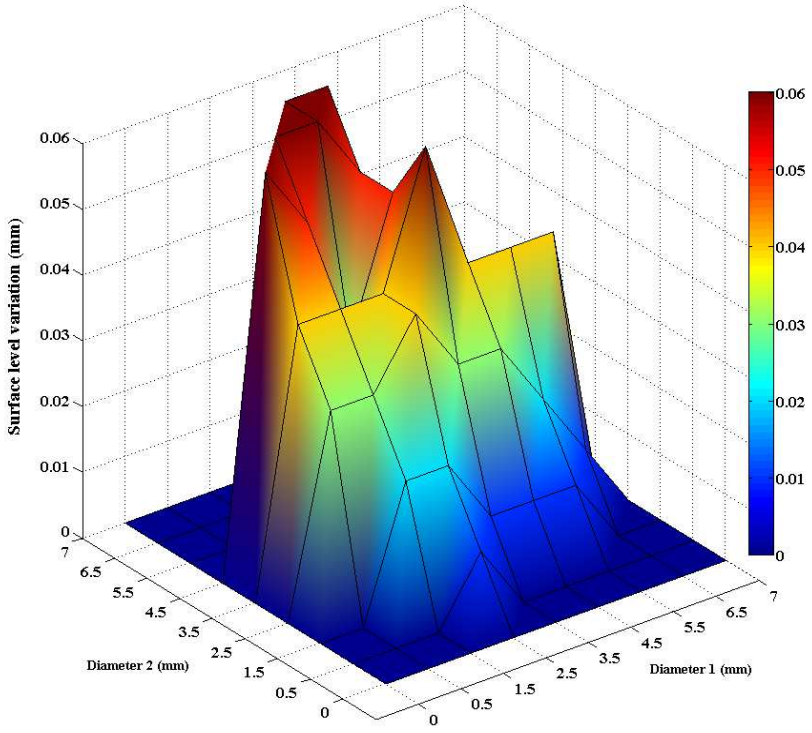

(a)

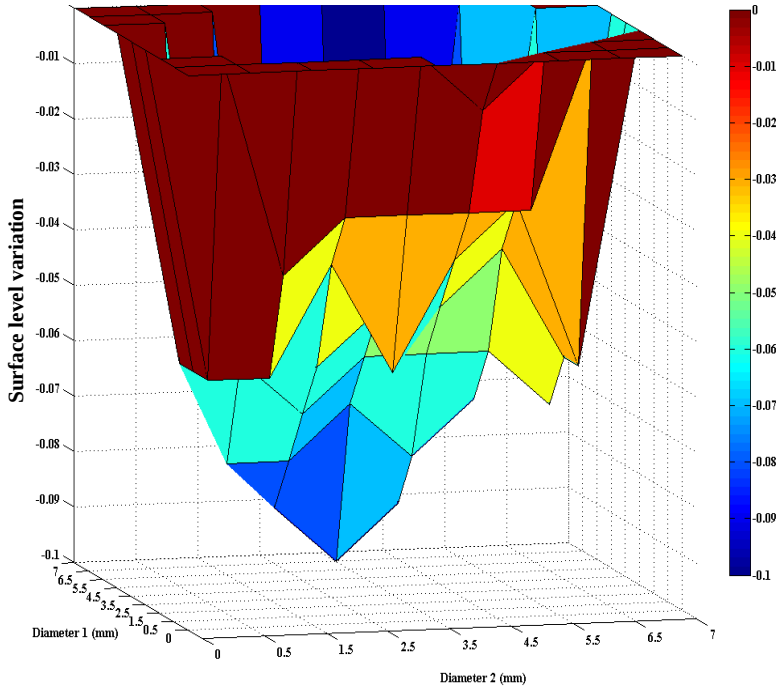

(b)

Figure (2.2): (a) Surface level of sample AB7, (b) Surface level of sample AB8

2.1.5 General Description Of The Schenck Press

To measure the elastic modulus and to perform compressive strength tests, the Schenck press device was the best choice for its capacity and its ability to record the strain during compressive tests.

The Schenck device (Schenck Hydropuls) is a servohydraulic press of 1 MN capacity fully controlled hydraulically. It is capable of developing the displacement of the axial jack with a speed ranged from 10µm/min to 25mm/s, (see Figure (2.3)). This machine has a very precise force sensor positioned in the lower plate. This force sensor of a wide range (1 MN) is able to cover all the tests. It is also equipped with a displacement sensor of range ± 125mm that is installed in the axial jack to control the displacement during the test. The system of the Schenck device is able to register the data of the force sensor, strain gauge sensor and displacement sensor.

To permit the applied load to be distributed uniformly over the specimen bearing surfaces even if they are not perfectly parallel, a hinge is placed and centered on the upper bearing surface of the specimen before initiating the test. In addition, 2 apparatus were fabricated in the 3SR laboratory for preventing the eccentricity of the load to be applied on sample surfaces. One of them is composed of 2 parts that could be joined together by screws to form a square plate with a circular hole to surround the circumference of the upper part of the cylindrical specimen (diameter equal to 70mm). The size of the square plate is 20cm to permit the plate which is placed on the upper face of the loaded specimen to be fitted inside it, see Figure (2.4).

Figure (2.3): Schenck device

The other one is a ring with inner diameter just fit the circumference of cylindrical specimens of 70mm diameter while the outer diameter of this ring is designed to be of the same size as one of the circles that are drawn on the lower plate of the Schenck device. The ring is composed of 2 parts that could be joined by screws to be placed at the bottom of the loaded specimen, see Figure (2.4). It must be mentioned that both of the square plate and the ring are removed as soon as the jack of Schenck device touch the upper loading surface of a specimen for preventing any lateral confinement.

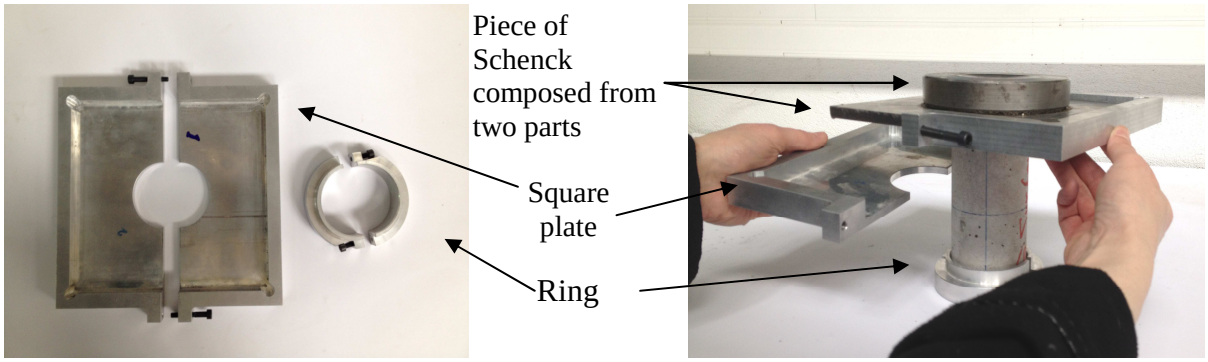

Figure (2.4): Centering system of Schenck press: Ring and square plate both of them omposed from 2 parts

To fix the cylindrical specimen which is prepared for the Brazilian test, an apparatus* which is presented in Figure (2.5) was designed and fabricated in the 3SR laboratory. This device is supplied with screws for positioning the specimen laterally at the center of the device. These screws are released as soon as the jack of Schenck device touches the upper lateral side of the specimens to prevent any lateral confinement.

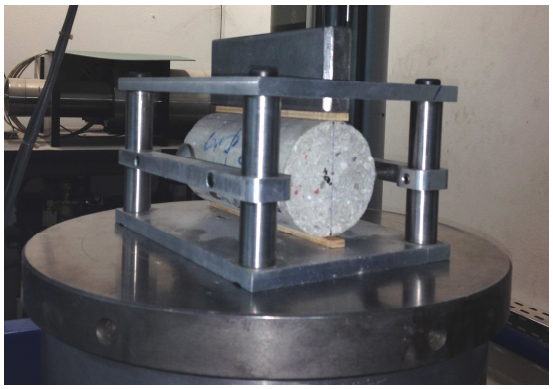

Figure (2.5): Apparatus used to hold the tested specimen throughout the Brazilian test

* The device is explained in details in section 2.4.1

2.1.6 Extensometer Used for Measuring the Specimen Strains

An extensometer is assembled around the specimen as a belt which is called diametrical belt, see Figure (2.6.a). This equipment also includes 3 LVDT (named Ex1, Ex2 and Ex3) arranged in a parallel way to the axial loading of specimen for measuring the longitudinal strain throughout the test. Another LVDT (named Ex4) is placed parallel to the tangent of a specimen to acquire the diametrical strains during the test.

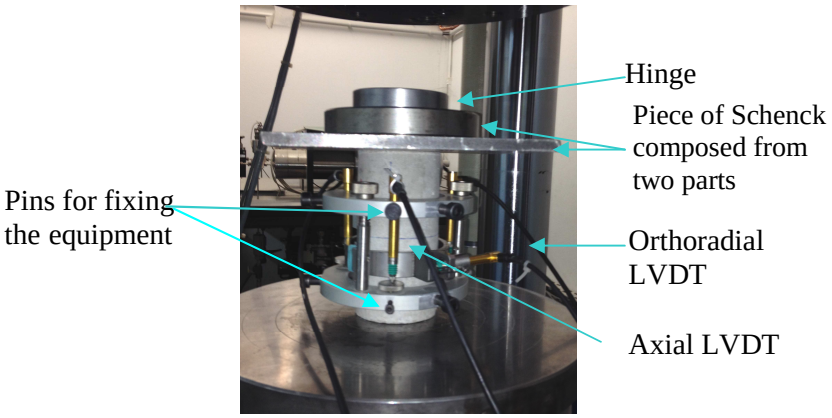

(a)

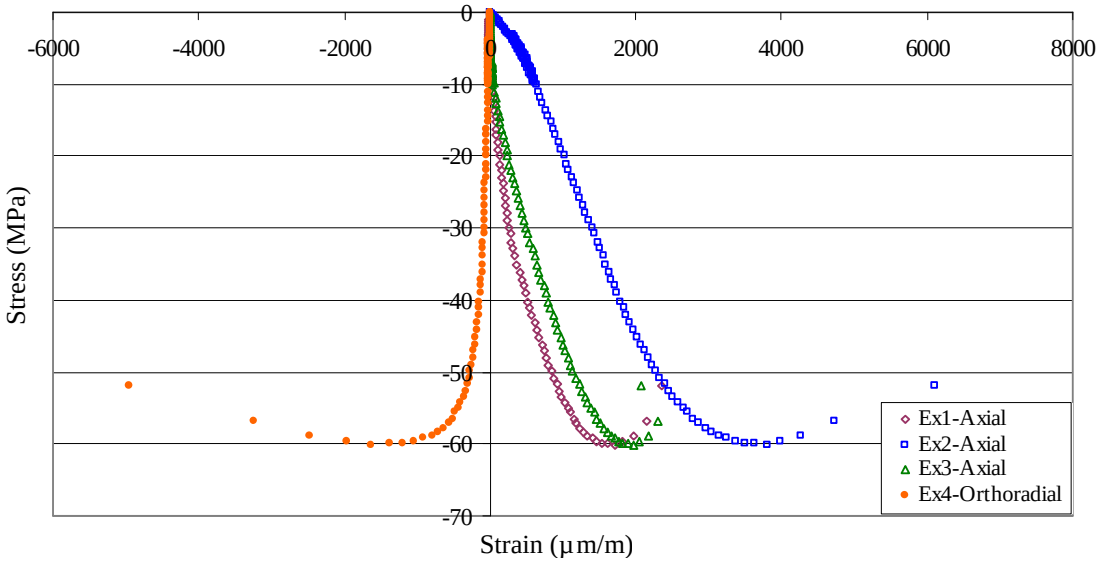

(b)

Figure (2.6): (a) Specimen equipped for achieving the compressive test, (b) Stress vs. strain results obtained throughout the test

The acquired data of the displacement with that of axial stress are useful for drawing stress–strain diagrams and for computing the elastic modulus, see Figure (2.6.b). For obtaining the strain for each step of the applied stress, the different between the actual and the

initial displacements is divided by the distance between the pins that are fixing the extensometer, see Figure (2.6.a).

2.1.7 Compressive Strength and Elastic Modulus Development with Time

The results obtained from compressive strength tests which were carried out on the sound specimens, i.e. specimens had not subjected to a previous loading, throughout the experimental work (different casting but the same compositions ratios), are presented in Figure (2.7) and (2.8). The development of compressive strength with time is represented in Figure (2.7). A modified Eurocode formula is also presented in the same figure and fitted with the experimental results to have a standard deviation equals to 4.1. The formula of this equation is as follows:

$$f_c = exp[\, s(1-\sqrt{\frac{28}{t}}\,)] \times f_{28} \qquad (2.1)$$

where f_c is the compressive strength in MPa at the present time (t) in days, f_{28} is the compressive strength at age of 30 days (= 42.1 MPa) and s is the factor that was found to be equal to 0.6.

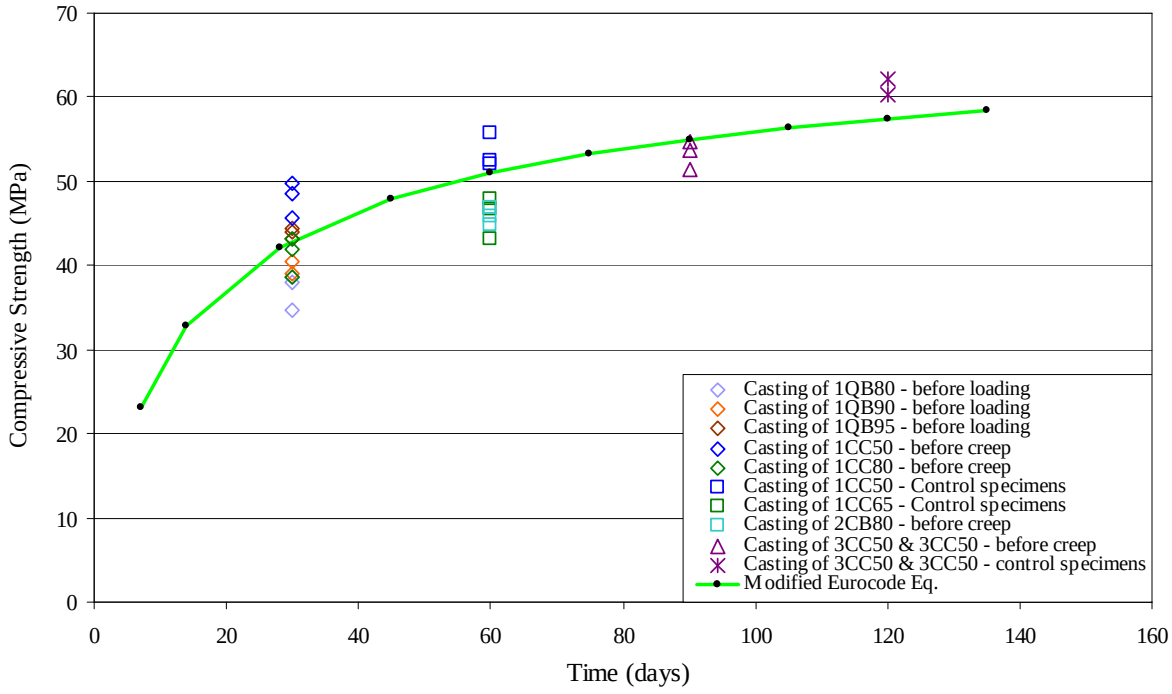

Figure (2-7): Compressive strength development vs. time for sound concrete

The formula of f_c (Eq. 1) was submitted in the Eurocode equation of calculating the elastic modulus (instead of f_c value) to be modified with the experimental results that varies with time. The standard deviation equals to 6.1 and the formula of this equation is as follows:

$$E = 22 \times \left(\frac{fc}{9} \right)^{0.3} \tag{2.2}$$

where, E is the elastic modulus in GPa which evaluates with time in days.

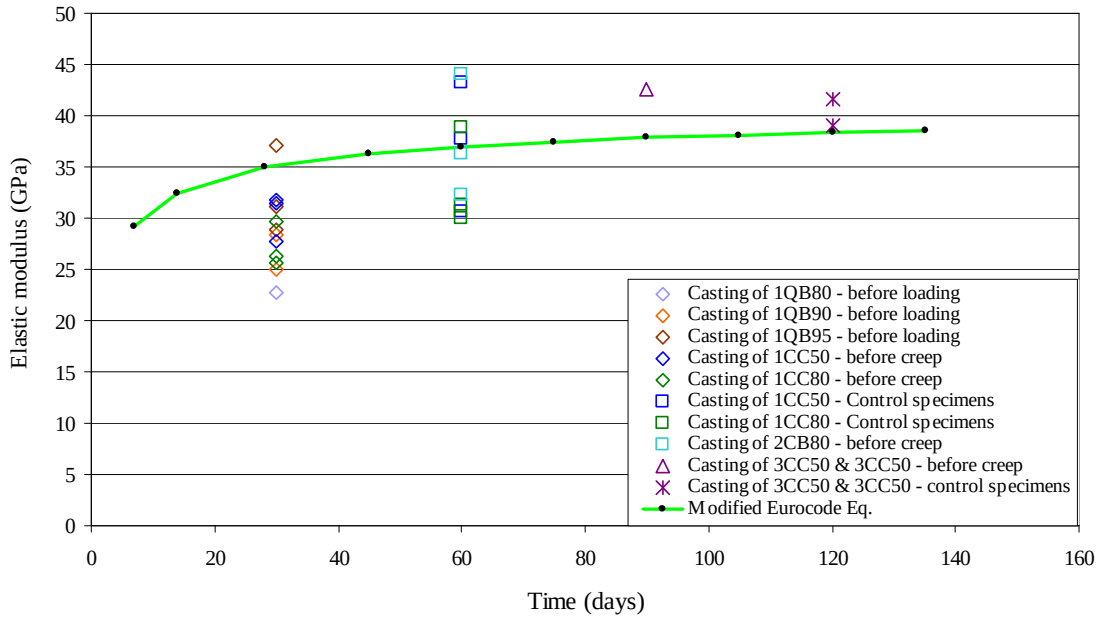

Figure (2.8): Elastic modulus development vs. time for the sound concrete

2.2 Effect of Quasi-Instantaneous Preloading in Compression on the Concrete Tensile Strength

For structures that are loaded in compression, the designer takes all the necessary precautions to make its compressive strength adequate to support the load. Prestressed structures are first subjected to compressive stresses during the prestress process and then can be submitted to tensile stresses. In these structures, the section is subjected firstly to compressive stresses followed for part of them by tensile stresses due to external load or creep strain which lead to relaxation of stresses. So, before finding out the compressive creep effect on the tensile resistance, it is important to verify the compressive preloading effect. If the tensile strength of concrete decreases after subjecting it to compressive creep loading, the negative effect could occur due to creep or as soon as a compressive load is applied.

2.2.1 Steps Followed for Achieving the Study of the Compressive Preloading Effect

This test consists of loading a concrete specimen until a specific level and then doing a Brazilian test on it. To determine the preloading for different compression stress/strength levels, the compressive strength must be evaluated before. This was done on 3 specimens at age of 1 month for each casting (2 castings were made as it will be explained in this section). After finding the maximum compressive strength of concrete, 3 levels of compressive preloading were achieved at the levels of 80%, 90% and 95% of the strength of concrete for the series 1QB80, 1QB90 and 1QB95, respectively, see Table (2.2). In fact, 3 concrete casting were made; the first and the second for achieving the loading level of 80% and 90%, respectively. The third casting was prepared to accomplish the loading level test of 95% in addition to the level of 90%. The specimens were preloaded in compressive for about 15 minutes and test stopped at a specified level (80%, 90% or 95%, depending on the series). At the end of preloading test, an indirect tensile test (Brazilian test) was done on the preloaded specimens. The number of the specimens used for each test is indicated in Table (2.3).

Table (2.2): Definition of series name

Series name	Definition of series				
	Type of 1st test	Age of 1st loading	Loading level of 1st test	Type of 2nd test	Age at failure test
1CC50	Comp. creep	1 month	50%	Comp. strength	2 months
1CC65	Comp. creep	1 month	65%	Comp. strength	2 months
1BB50	Brazilian creep	1 month	50%	Brazilian strength	2 months
1BB80	Brazilian creep	1 month	80%	Brazilian strength	2 months
1BB90	Brazilian creep	1 month	90%	Brazilian strength	2 months
2CB80	Comp. creep	2 months	80%	Brazilian strength	3 months
3CC50	Comp. creep	3 months	50%	Comp. strength	4 months
3CC80	Comp. creep	3 months	80%	Comp. strength	4 months
1QB80	Comp. quasi-instantaneous	1 month	80%	Brazilian strength	1 month
1QB90	Comp. quasi-instantaneous	1 month	90%	Brazilian strength	1 month
1QB95	Comp. quasi-instantaneous	1 month	95%	Brazilian strength	1 month
Note: The number situated in the beginning of the series name represents the age of loading. This number is followed by two letters to represent the name of first and second test while the last number represents the loading level.					

Table (2.3): Number of specimens prepared for each loading test

Casting order	Series name	Specimens No		
		Compressive test on sound specimens	Brazilian test on sound specimens	Comp. preloading-Brazilian test
First	1QB80	3	3	3
Second	1QB90	3	3	3
Third	1QB90	3	6	4
	1QB95			4

2.2.2 Results Obtained from the Compressive Quasi-Instantaneous Preloaded Preloading

The indirect tensile strength values obtained from the Brazilian tests that were accomplished on sound specimens and on those of quasi-instantaneous preloaded specimens in compression are presented in Figure (2.9) and in Table (2.4). The values in this figure represent the average of 12 specimens for unloaded (3 for each one of casting 1 and 2, and 6 for casting 3), 7 specimens for preloading level of 90% (3 for the first casting and 4 for the second) while for preloaded until the level of 95%, 3 specimens of the second casting was realized, see Table (2.3).

It could be seen from Figure (3.9) that the compressive preloading level of 80% has no significant effect on the concrete tensile strength. However, the compressive preloading has negative effect for preloading levels higher than 80%. It could be seen from Table (2.4) that the decreasing in the tensile strength is 16% for preloading level of 90% and 20% for preloading level of 95% i.e. the negative effect increases with increasing the preloading level. As concrete is a quasi brittle material, the extension that occurs in the transverse direction, due to the Poisson ratio effect, generates microcracks in the direction parallel to the applied load. These microcracks increase as the applied loading level is increasing until it reaches the level of failure (loading level equal to 100%). Hence, when the compressive preloaded concrete specimen is subjected to the Brazilian test, it fails with a loading value lower than that applied on sound specimens. However, as the Brazilian test gives scattered results, more tests will need to be carried out to better qualify these results.

Table (2.4): Effect of quasi-instantaneous preloading in compression on tensile strength

Compressive preloading level	0%	80%	90%	95%
Indirect tensile strength (MPa)	3.91	3.90	3.27	3.13
Decreasing in tensile strength *	-	0.26%	16%	20%
* Decreasing in tensile resistance= 100×(Resistance before preloading - Resistance after preloading) / Resistance before preloading				

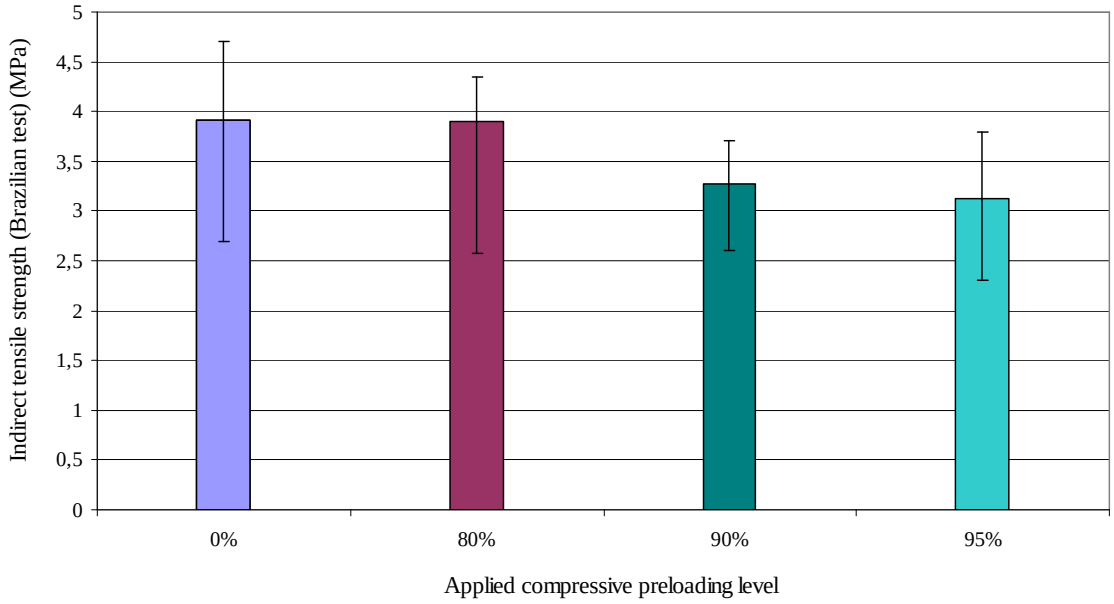

Figure (2.9): Effect of compressive preloading of different levels on the tensile strength

2.3 Compressive Creep

As it was seen in chapter one section 1.1.4 [the work of Roll (Roll, 1964), Liu et al. (Liu et al., 2002), Asamoto et al., (Asamoto et al., 2014) and Saliba et al. (Saliba et al., 2012)] that very few studied were done to evaluate effect of creep on the mechanical properties of concrete. For covering the lack on this subject and to verify creep effect, the creep test was carried in tension and in compression.

The compressive creep effects on the compressive strength, tensile strength and elastic modulus were studied and presented in this section.

2.3.1 Creep Device

The creep device used was designed and fabricated at 3SR laboratory. This device which is seen in Figure (2.10) works by transforming a force into a moment then thanks to a multiplier system into a much larger force than the initial one to be applied on the specimens.

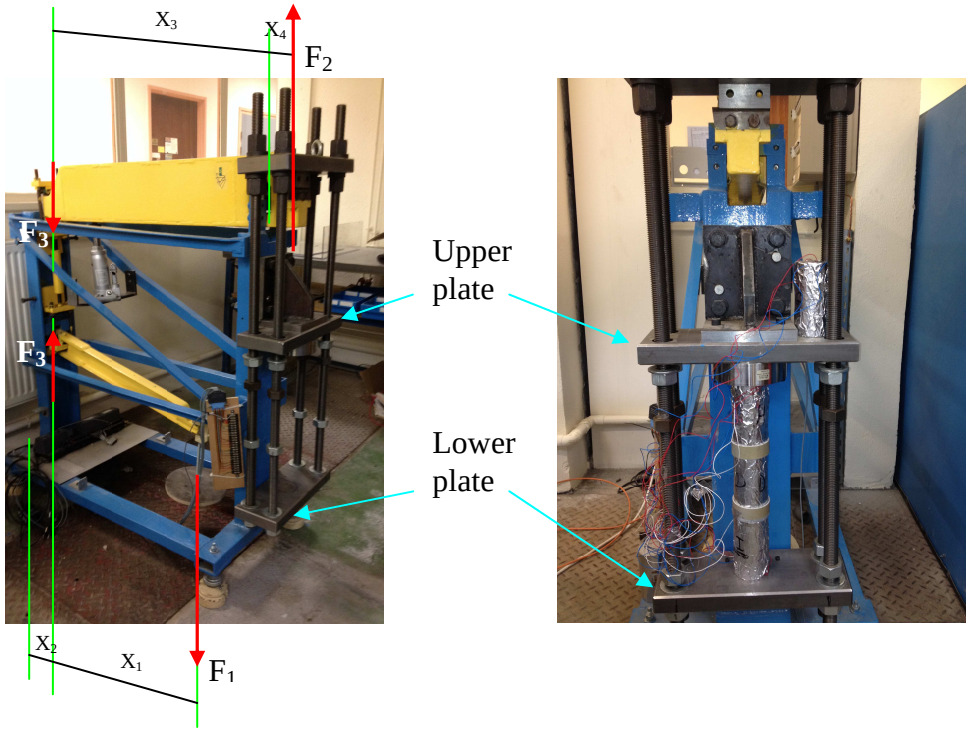

Figure (2.10): (a) Side view of the creep device, (b) Front view of the creep device after arranging the specimens inside it

As it is shown in the sketch of the force system which is represented in Figure (2.11), weights are placed at the end of beam 1 to apply the force F_1. The moment which is composed from F_1 on beam 1 is transmitted to beam 2 by the force F_3 that is applied at joint 1 (J_1) and then its reaction at joint 2 (J_2). The moment which is due to F_3 on beam 2 is balanced by F_2. In fact, F_2 has a direction inverse to F_1, lifts the lower plate on which the creep samples are placed. As the upper plate which is over the column of the creep specimens is fixed, the distance between these two plates will decrease holding the creep specimens to be in touch with the upper plate. So, the compressive force (F_2) that is applied on the specimens is given by the following equation:

$$F_2 = F_1 \left[\frac{(X_1 + X_2)}{X_2} \cdot \frac{X_3}{X_4} \right] \tag{2.3}$$

where $X_1 = 75\,cm$, $X_2 = 5\,cm$, $X_3 = 99.5\,cm$ and $X_4 = 10\,cm$. So, if 1kg is being placed at the free end of beam1, the applied load on the upper side of the loaded specimens (support 2) will be equal to 159 kg.

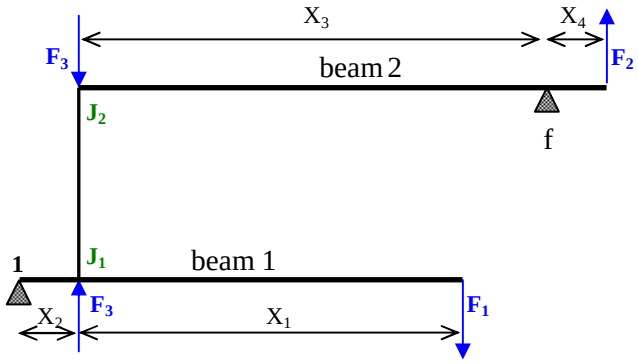

Figure (2.11): Sketch of the force system of the creep device

The cylindrical concrete (high=140mm) specimens were inserted in the creep frame tester to form a 3-cylinder column of height 420mm which is adequate considering the space between the upper and the lower plates. Then strain gauges were connected to a digital strain meter for measuring strains. These measured strains represent the total strain due both to the loading (initial and creep strains) and to the eventual thermal and/or shrinkage strain.

2.3.2 Specimen Preparation and Instrumentation

For each creep test, 6 specimens were prepared, 3 of them were loaded while the 3 others named control specimens remain unloaded. The control specimens were stored under the same conditions of those loaded to measure the strain taken place without external load i.e. eventual thermal expansion or drying. The number of channels of strain measurements was limited so only 2 of the loaded specimens and 1 of the control specimens were equipped with strain gauges. After taking all the specimens out of water, 2 of the chosen specimens to be loaded were instrumented with 3 strain gauges. After leaving the specimens in air for 1 day, 2 of the strain gauges were glued vertically at 2 opposite sides while the 3rd one was glued circumferentially, adjusting their centres at the middle of the specimen height. The same arrangement was used for the control specimen however for this specimen the circumference strain gauge had not been used and the lateral strain was proposed to be equal to the axial strain. The gauges adapted were of N2A-06-10CBE-350 type and of length equal to 28mm, and the glue used for sticking them was of GA-2 type. Both the gauges and the glue were fabricated by Vishay Micro-measurements Company. The specimens were left for 1 day

in the air so that the glue takes its hardness. After joining the wires with the strain gauges, paste of CAF4 type was applied on the gauges and on the parts of wires joined with them, to protect them from the humidity. When the paste became dry, within 6 hours, all the specimens were immerged again into the water tank. At the age of loading, all the specimens were taken out of water. As only the basic creep was decided to be measured, the creep and the control specimens were covered with aluminum scotch for preventing the evaporation of water out of the specimen. It should be mentioned that at each step, the conductivity of the wires was verified by the multimeter device, see Figure 2.12.

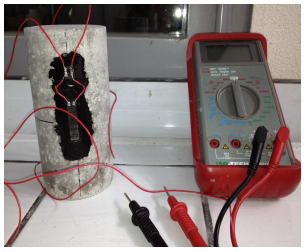

(a)

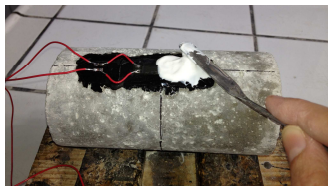

(b)

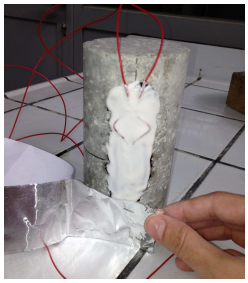

(c)

Figure (2.12): (a) Fixing the wires and verifying the conductivity by a multimeter, (b) Applying CAF4 paste, (c) Covering the specimen with an aluminum scotch

2.3.3 Compressive Creep Effect on Residual Compressive Strength and Elastic Modulus

As it was mentioned previously, the principal aim of this study was to find out the creep effect on the residual mechanical properties of concrete. Here, for studying the effect of compressive creep on the development of compressive strength and of elastic modulus, two different ages of loading were used, 1 month and 2 months.

2.3.3.1 Steps Followed for Achieving the Study of the Compressive Creep Effect

At the age of loading, the compressive strength test was carried out for determining the ultimate compressive strength and consequently deciding the load that should be applied to attain the chosen loading level for the creep test. The compressive creep test was then carried out on series named 1CC50 and 1CC65 at age of 1 month while series 3CC50 and 3CC80 at age of 3 months, see Table (2.1). At age of loading, the compressive strength test was carried out on 3 specimens for each one of the series 1CC50 and 1CC65 while for the series 3CC50 and 3CC80, the test was achieved on only 3 specimens for representing the two series because both of them were made from the same casting. As it was mentioned previously, for each test,

3 specimens were loaded in the creep device named creep specimens and 3 were unloaded named control specimens.

After measuring the maximum compressive strength, the compressive loading level (stress/strength ratio) was decided for each creep series. The chosen loading levels were 50% for series 1CC50 and 3CC50, 65% for series 1CC65, and 80% for the rest series, see Table (2.1). The conditions of storage during the creep test were the same for all the series. So at the end of water curing duration (1 month or 3 months), the creep and the control specimens were covered with aluminum scotch and stored in air at (20±1)^{o}C and (50±5)% RH

At the end of creep loading which persisted for 1 month for all the series, Young's modulus and the compressive strength test were evaluated on the creep and on the control specimens. After the compressive strength test, the modulus of elasticity was computed from the average of 3 strains measured by the axial LVDT with the corresponding applied stress. The modulus of elasticity was calculated within the range from 22 MPa to 28 MPa for which a plateau of the elastic modulus is observed as it is shown for an arbitrary chosen specimen in Figure (2.13). This range was determined according to the more stable results obtained from the relation between the derivation of elastic modulus verses the applied compressive stress throughout the compressive strength test for randomly chosen specimens, see Figure (2.14). The elastic modulus and the obtained maximum compressive strength from the compressive strength test for the creep and the control specimens were compared for each series.

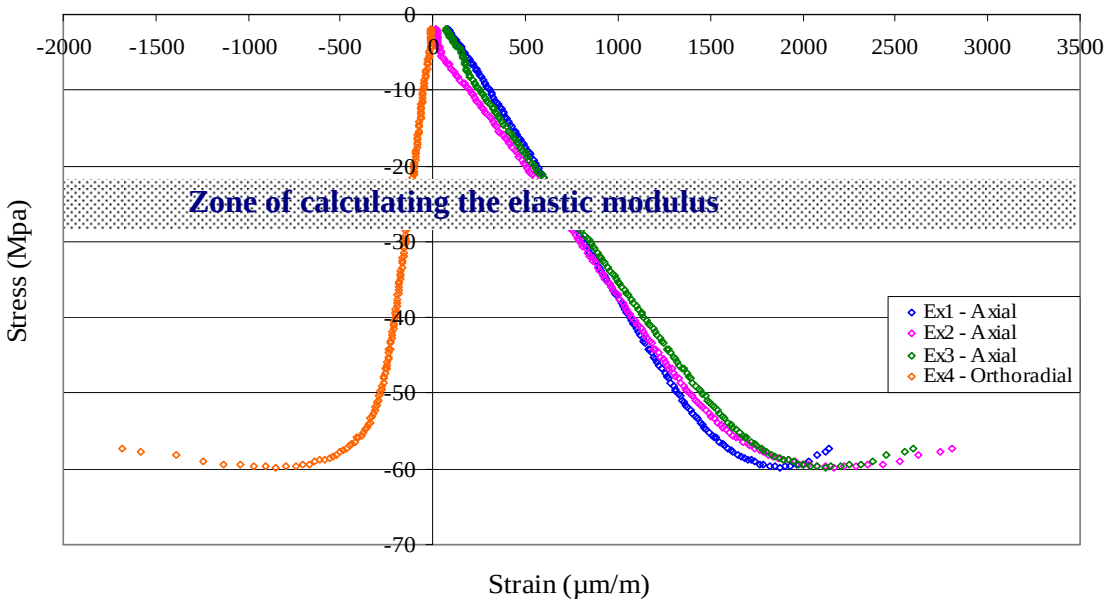

Figure (2.13): Stress vs. strain of compressive strength test of one specimen (named A)

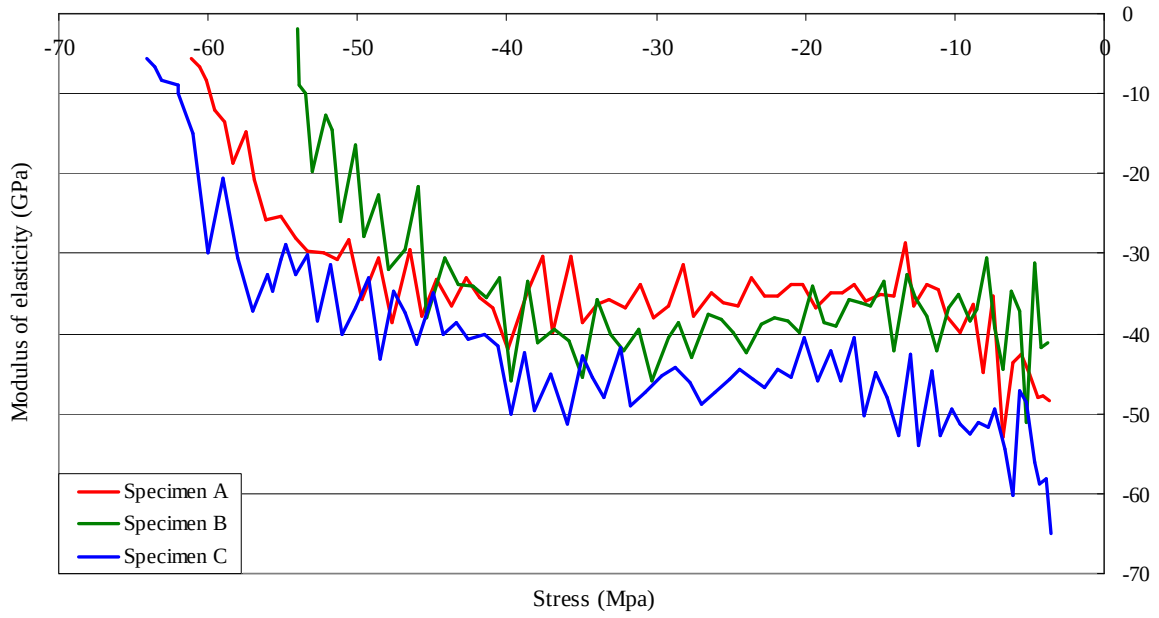

Figure (2.14): Derivation of the elastic modulus vs. stress of three specimens

2.3.3.2 Results Obtained from the Compressive Creep

To obtain the total strains due to the loading (initial and creep strains), the measurements obtained from the strain gauges fixed on control specimens are subtracted from those fixed on loaded specimens at each time of strain registration. The results of total axial strains due to loading are shown in Figure (2.15) while those of total circumferential strains are presented in Figure (2.18). Creep strains that obtained after subtracting the initial strain (strain occurs immediately after the applied force reaches to the required limit) from the total strain due to loading, are presenting in Figure (2.16) and Figure (2.19), for axial and circumferential creep, respectively. The specific creep strains i.e. creep strain divided by the corresponding applied stress are represented in Figure (2.17) for the axial strain and Figure (2.20) for the circumferential strain.

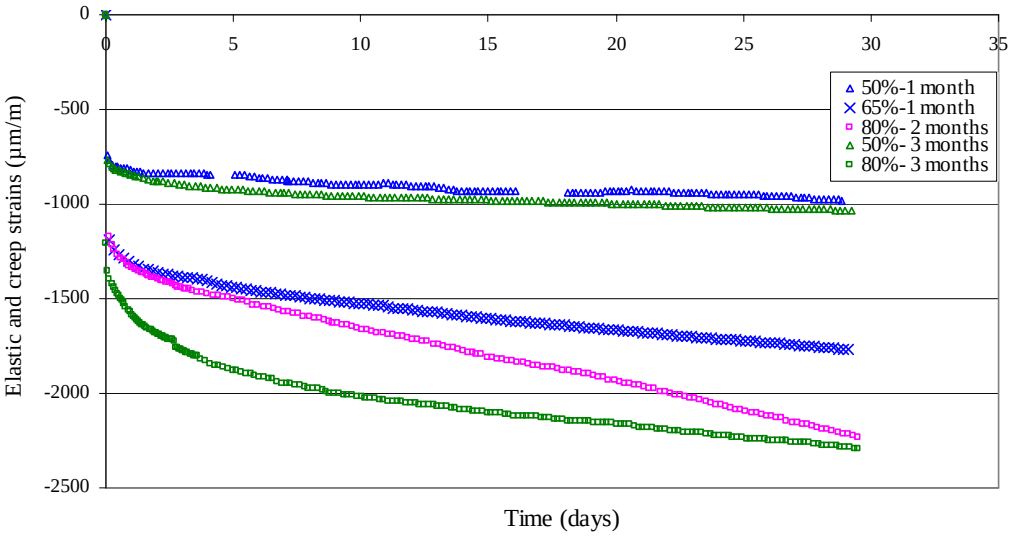

Figure (2.15): Total axial strains (elastic and creep) vs. time due to compressive load

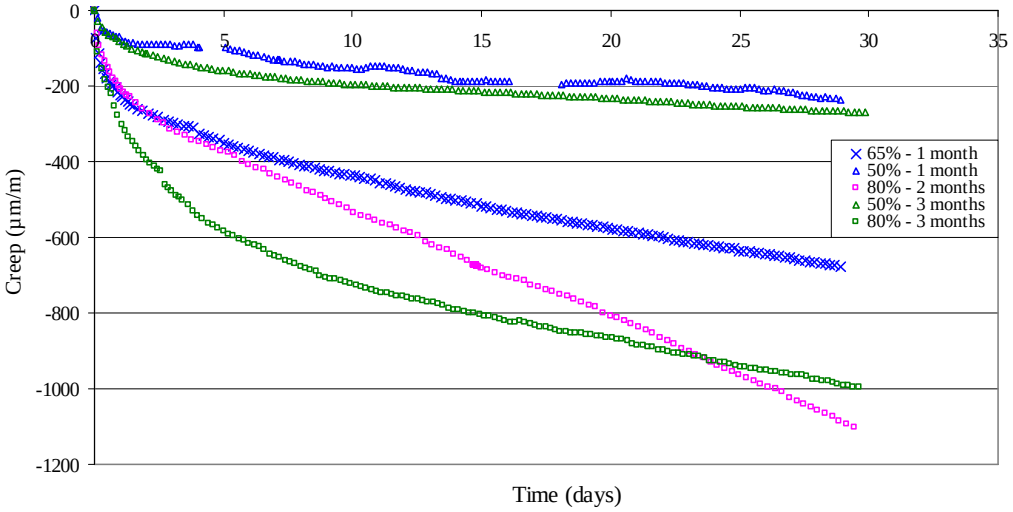

Figure (2.16): Axial creep strain vs. time due to compressive load

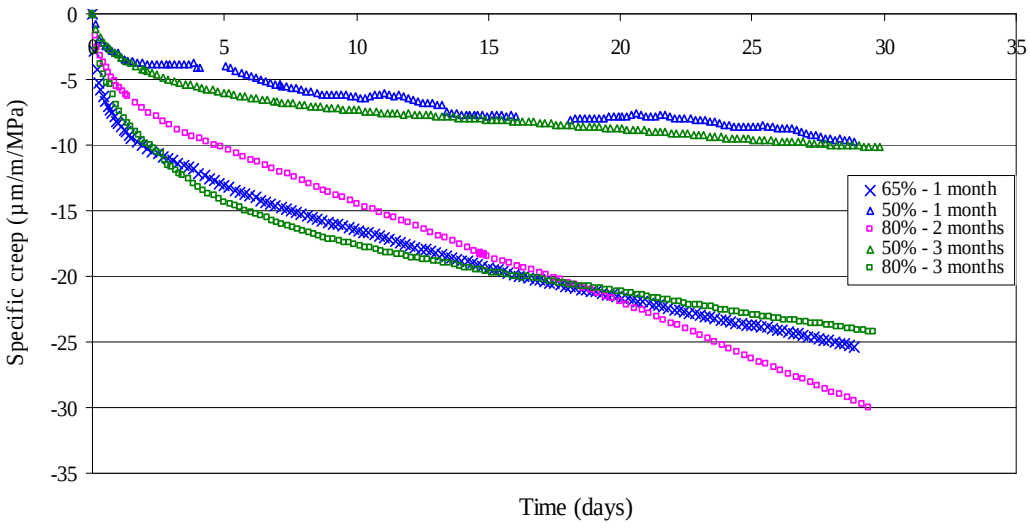

Figure (2-17): Axial specific creep vs. time due to compressive load

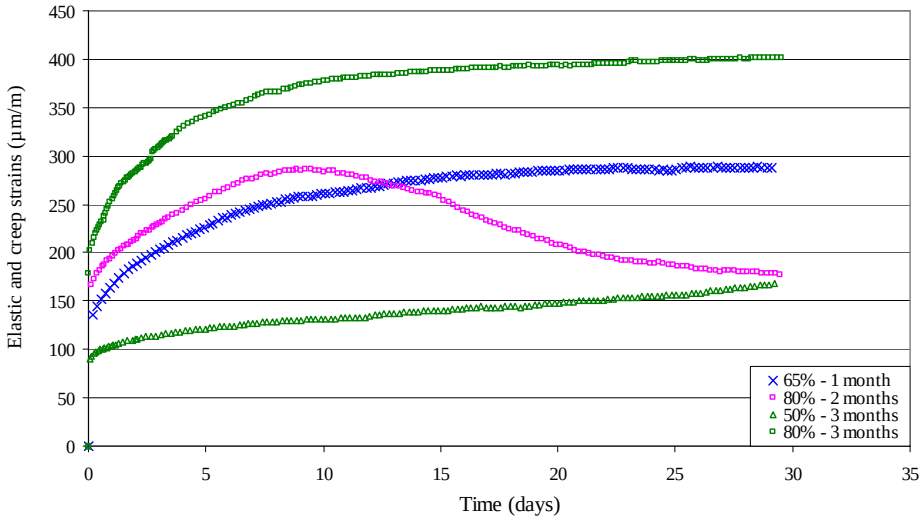

Figure (2.18): Total radial strains (elastic and creep) vs. time due to compressive load

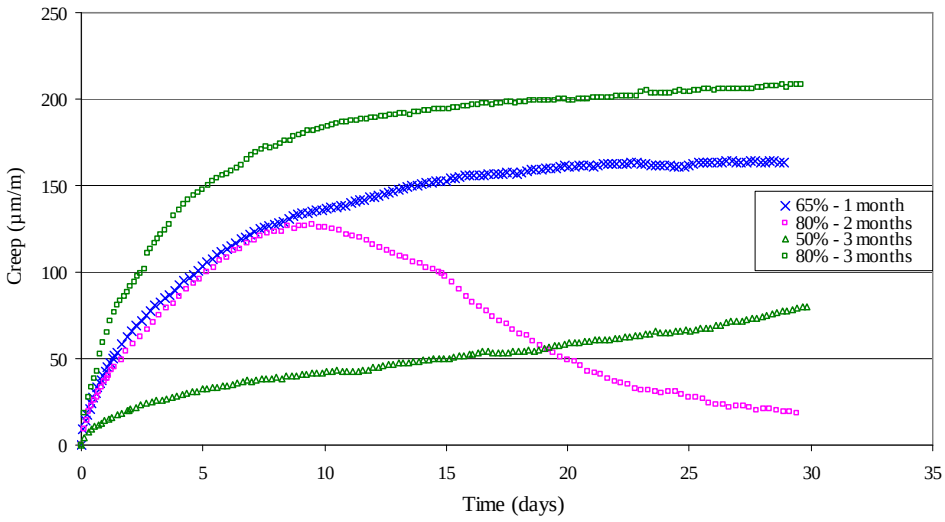

Figure (2-19): Radial creep strains vs. time due to compressive load

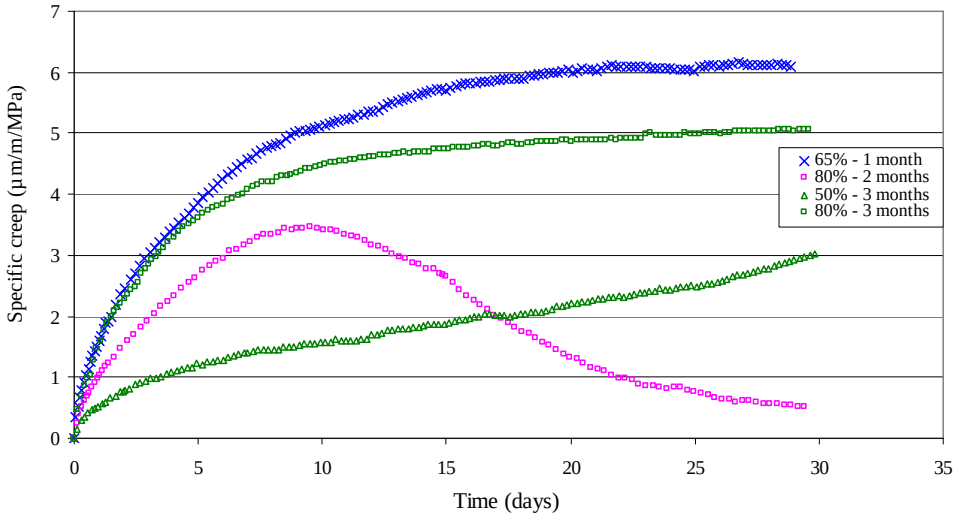

Figure (2.20): Radial specific creep strains vs. time due to compressive loading

As it was expected for the same age of loading, the total strain due to loading (elastic and creep), creep and specific creep strains increase as the stress/strength level is increased, and that for both axial and circumference directions. That is related to the nature of creep phenomena which occurs when an external load is applied resulting in water seepage and gel flow and slide one over the other inside the loaded concrete. So, it is well known that the creep strains increase as the applied stress is increased for the same concrete characteristics (see section 1.1.1.3 and 1.1.1.4).

It could also be remarked from Figures (2.15), (2.16), (2.17), (2.18), (2.19) and (2.20) that for the same stress/strength level, as the age of loading is increased, creep and specific creep strains increase too. These results are in accordance with to the results of Polivka et al. (Polivka et al., 1964) as it is presented by Neville and Dilger (Neville and Dilger, 1970). The results of their work revealed that, for concrete subjected to the same stress/strength ratio, a creep of 130×10^{-6} when loaded at 3 days and of 110×10^{-6} when loaded at 1 day, for creep measured after 25 to 28 days. Neville (Neville and Dilger, 1970) related this finding to the growth in strength under loading. For concrete loaded at earlier ages, the gain in the strength is higher than that at later ages. Therefore, for the same initial applied stress, the stress/strength ratio decrease faster with time, resulting in smaller creep.

Another justification that could be given here for this result is that when concrete is aging and with available of free water, the hydration process continues. Progressively, the pores inside the concrete will be filled up with cement products. So, when concrete is loaded at later ages, the water and gel particles will not find enough spaces to flow inside the concrete skeleton. Consequently, the energy provoked by these particles on the hardened cement paste will lead to microcracks occurrence. As a result and due to these microcracks, there will be an increase in the amount of creep strain in addition to the relatively small flow of water and gel particles.

Moreover, an additional creep strain could arise due to microcracks at cement paste-aggregate interface. These microcracks occur due to the tensile stresses as under the applied loading level of concrete, only the cement paste undergoes creep while the aggregate act as an obstacle to this creep. Even though, at mesoscopic scale, as the flow of cement gel and water is more accessible at young age than that at late age, the concentration of stresses at the aggregate-cement paste interface for new concrete may be relaxed faster than those for old concrete. Therefore, the microcracks at the aggregate-cement paste interface for new concrete are expected to be less than those for old concrete.

The results obtained from the compressive strength tests which were done on creep and control specimens at the end of creep test, are presented in Table (2.5), Figure (2.21) and (2.22). It could be seen that when concrete had been loaded at age of 1 month, after 1 month of loading i.e. at age of 2 months, the compressive strength and the modulus of elasticity of creep specimens is greater than that of control specimens, for the both loading levels (50% and 65%). On the contrary, when concrete had been loaded at age of 3 months, after 1 month of loading i.e. at age of 4 months, the creep specimens have lower compressive strength than those of control specimens, for 50% and 80% loading levels.

These results are in accordance with the results of Roll (Roll, 1964), Liu et al. (Liu et al., 2002), Asamoto et al. (Asamoto et al., 2014) and Saliba et al. (Saliba et al., 2012). All the findings of these studies agree that concrete subjected to compressive sustained load at early or young ages reveal higher compressive strength [and higher elastic modulus according to the work of Roll (Roll, 1964) and Asamoto (Asamoto et al., 2014)] than unloaded concrete. Even though, the work of Liu et al. (Liu et al., 2002) gave conflicting findings for uniaxial loaded concrete at late age (90 days) with high level (60%) i.e. the creep specimens revealed lower compressive strength than the control specimens, see section 1.1.4 for more details.

The explanation that could be given is that when concrete is being loaded at young ages, the applied load pushes the cement gel to be moved from their places to a wider place, to fill the pores inside the cement paste. With time and under the sustained load, the size of concrete specimen becomes smaller and denser than that which was not loaded. As a result, the dense specimens (creep specimens) reveal higher resistance than those which are less dense (control specimens). While in the case of loading concrete at later ages, most of the pores had already been filled with the rehydration products. Therefore, when the load is applied at these late ages, there will be not sufficient place available for the water and the cement gel particles to move easily. So, these moving particles become to apply a pushing force on the hardened cement resulting in microcracking occurrence. In addition, as it was mentioned previously, tensile stresses take place at aggregate-cement paste interface due to the incompatible strains between the cement paste and the aggregate. Therefore at mesoscopic scale, unlike the case of loading at young age in which the cement gel and the water can flow easily and may result in relaxation of these stresses, these tensile stresses lead to microcracking at the cement paste-aggregates interface. Consequently, the old concrete loaded specimens which become weaker due to these microcracks, give lower resistance than the unloaded specimens.

Table (2.5): Compressive strength and elastic modulus of concrete after compressive creep tests

Age at beginning of creep loading	1 month		3 months	
Time duration of creep loading	1 month		1 month	
Casting number	1	2	3	
Creep loading level (%)	65	50	80	50
fc before creep (MPa)	41.2	48.0	53.3	
E before creep (GPa)	27.3	30.4	42.7	
fc of control specimens (MPa)	45.9	53.4	61.2	
fc variation with the age *	+ 11.4(%)	+ 11.3(%)	15.3(%)	
fc of creep specimens (MPa)	48.5	59.7	57.3	57.6
fc variation due to creep **	+ 5.7(%)	+ 11.8(%)	- 6.4(%)	- 5.8(%)
E of control specimens (GPa)	33.3	37.2	40.4	
E variation with the age *	+ 21.9(%)	+ 22.4(%)	+ 5.4(%)	
E of creep specimens (GPa)	36.9	42.1	40.5	40.0
E variation due to creep **	+ 10.8(%)	+ 13.2(%)	+ 0.25(%)	- 1.2(%)

** Fc variation with the age %= 100 × (Fc (or E) of control Spec.– Fc (or E) before creep)/ Fc (or E) before creep*

*** Fc variation due to creep %= 100 x (Fc (or E) of creep Spec.– Fc (or E) of control Spec.)/ Fc (or E) of control Spec.*

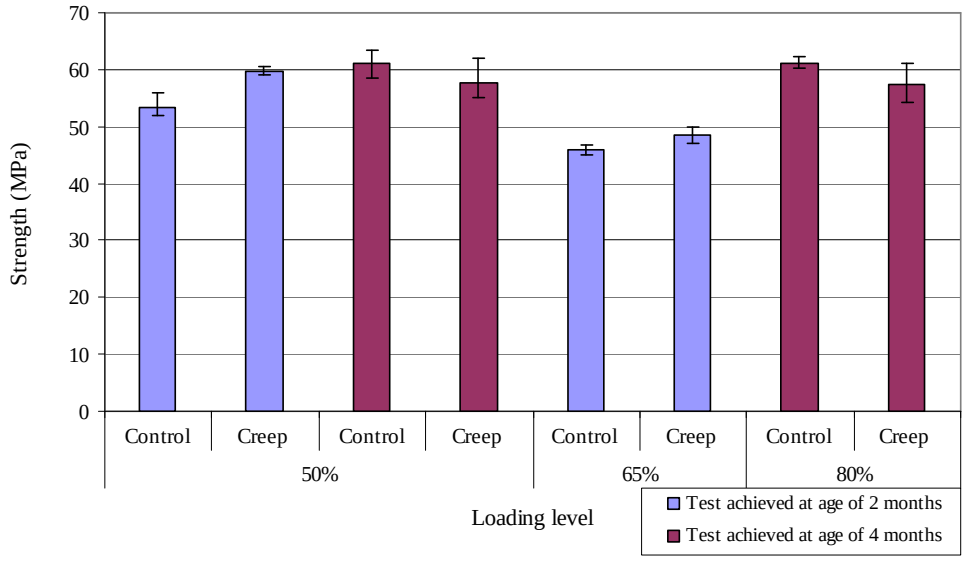

Figure (2.21): Compressive strength vs. time for creep and control specimens

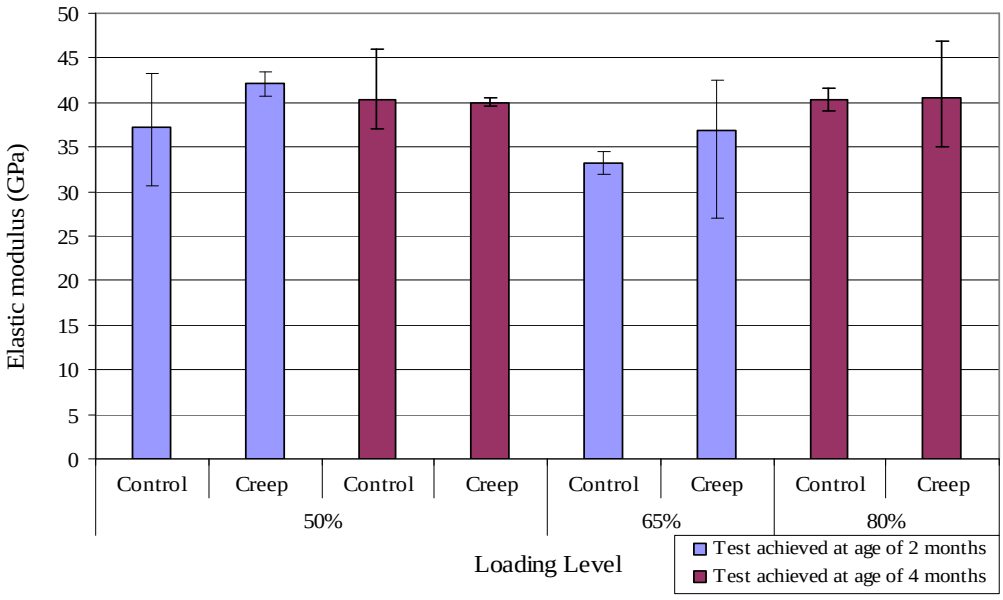

Figure (2.22): Elastic modulus vs. time for creep and control specimens

It could be seen that at loading age of 3 months, the modulus of elasticity is about the same for creep and control specimens and that for the both loading levels (50% and 80%). This means that there is no significant effect of creep loading on the elastic modulus when the creep loading is applied at age of 3 months.

2.3.3.3 Tomography Test for Verifying Creep Effect on Microcracks Development

To confirm that creep specimens at the highest loading level used (65%) at age of 1 month were sound and free from microcracks, a tomographic scan was done.

For creating radiographic images, X-Ray is applied on the concrete sample through which the ray passes to be dropped on a detector. This detector analyses this dropped ray which is an integration of the X-Ray attenuation of the object for developing an X-Ray radiograph. So, for an object of composite material, its X-Ray radiograph contains different shades from white to black colour, depending on the absorption degree of the X-Ray photons by the materials existing in the object. As this image of X-Ray radiograph is of 2 directions, the tomographic technique was evolved for composing a three direction field of X-Ray attenuation coefficient inside an object. For the Tomography of the laboratory 3SR, the object is rotated and different projections are collected by an image acquisition system.

2.3.3.4 Results of Tomographic Test

The tomographic images with a voxel (volumetric pixel) size of 25µm of the inner 45mm of the creep specimen that was loaded at age of 1 month with stress/strength ratio of 65%, revealed that there are no visible macrocracks at this scale (see Figure (2. 23)). Even though, may be that there are cracks at smaller scale.

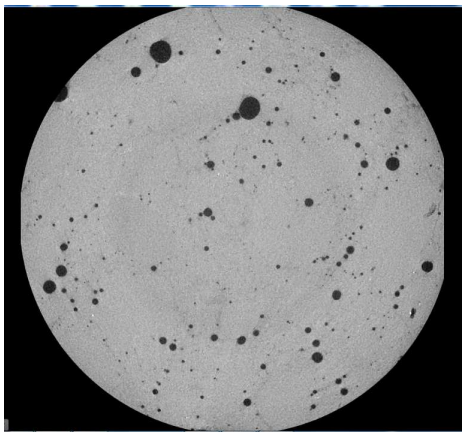

Figure (2.23): Tomographic slice of creep specimen of 65% loading level that applied at age of 1 month

This result confirms the justification given in section 2.3.3.2 that creep loading at relatively young ages (here 1 month), does not reduce the mechanical characteristic of concrete.

2.3.3.5 Permeability Test for Verifying Creep Effect on Microcracks Development

Another way to verify the occurrence of microcracks in creep specimens for the concrete loaded at age of 3 months with a loading level of 80% is to perform permeability test. The test was achieved by an instrument developed by laboratory 3SR which is shown in Figure (2.24).

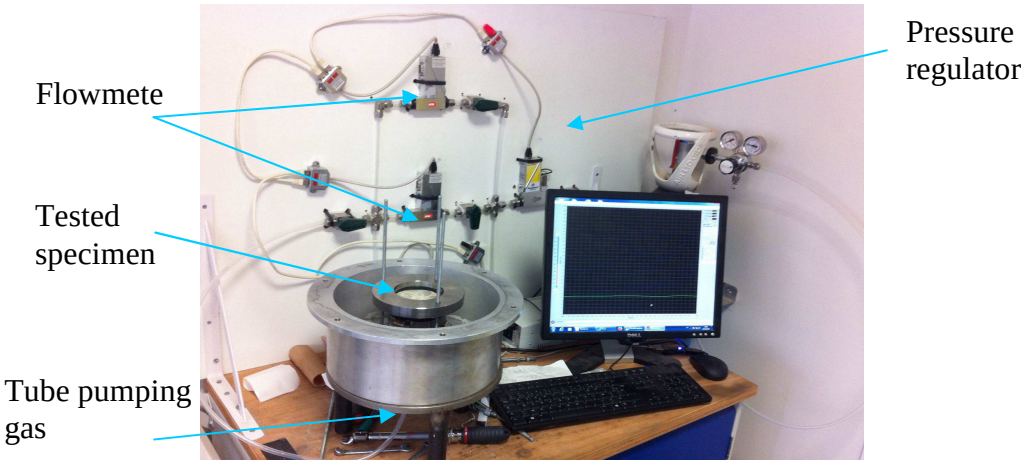

Figure (2.24): Permeability instrument developed by laboratory 3SR

Samples of 2 control specimens (of 70mm diameter and 41mm length) and of 1 creep specimen (of 70mm diameter and 34mm length) were chosen to achieve the permeability test.

Gas was used for measuring the longitudinal permeability of the gas. In this test, the gas is injected with a chosen pressure at the bottom of the specimen and the device measures the flux of gas at the output of this specimen. For preventing the gas to exit from the lateral direction (parallel to the axial axes) of the cylindrical specimens, all the specimens were covered with aluminium scotch, rubber plate then several necklaces .

For measuring the permeability by using gases, it is not sufficient to inject the gas with only one pressure. In fact, the permeability of an incompressible fluid can be directly obtained by applying the equation of Darcy which is as follows:

$$q = -\frac{k}{\eta} grad\ p \tag{2.4}$$

Darcy's law is only valid when the flow of fluid percolating through the medium is of laminar type, the physicochemical interactions between the medium and the fluid are neglected, and viscous forces of the fluid are dominant compared to inertial forces.

The volumetric rate Q (m^3/s) of unidirectional flow is:

$$Q = \frac{kS}{\eta}\frac{\Delta p}{L} \tag{2.5}$$

Where, L is the length of the material in the flow direction, and S is the percolation surface. As gases have a compressible character and their flow is not purely viscous throughout a porous medium, the Darcy's law could not be used directly for calculating its permeability. Thus, when gas flows, its speed varies at each point with the pressure. However, since the flow rate of the mass remains constant that makes possible to determine the apparent permeability. If the flow measurement is done at the output, the apparent permeability of the material can be given by the following equation:

$$k_a = \frac{2\eta\, p_i L Q_s}{S\left(p_i^2 - p_{atm}^2\right)} \tag{2.6}$$

where, Q_s is the total volume flow measured at the output, p_i is the applied pressure (initial), p_{atm} is the left pressure (atmospheric). Klinkenberg (Klinkenberg, 1941) proposed a linear relationship between the apparent permeability k_a and the intrinsic permeability k.

$$k_a = k\left(1 + \frac{\beta}{p_{av}}\right) \tag{2.7}$$

where, p_{av} is the average pressure of gas and β is the intrinsic coefficient (Klinkenberg, 1941). The idea of this equation is to translate the influence of the morphology of the pore space on the intensity of the sliding phenomenon. In equation (2.7), the apparent permeability evolves in a linear way versus the inverse of the average pressure, see Figure (2.25).

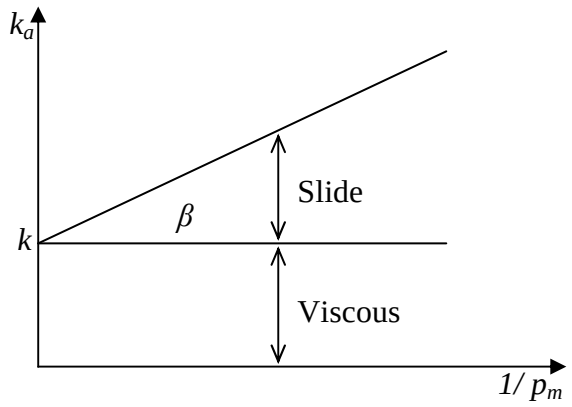

Figure (2.25): Method of Klinkenberg (Klinkenberg, 1941) for determining the intrinsic permeability

Thus, the intrinsic permeability k shown in Figure (2.25) corresponds to the value of the apparent permeability when $1/p_{av}$ tends to zero. As well, the coefficient β which depends on the geometry and morphology of the pore space is formulated by Klinkenberg, 1941 (Klinkenberg, 1941) as follows:

$$\beta = \frac{4c\lambda p_{av}}{r} \tag{2.8}$$

Where, c is a constant, r is the radius of the pore and λ the mean path of the gas molecules. Thus, the β coefficient increases as the pores are closer. In practice, the gas permeability k is not purely intrinsic in the material, because it depends on the degree of saturation. Namely, it decreases as the saturation of the medium increases.

2.3.3.6 Results of Permeability Test

After injecting the gas with 4 different pressure in each specimen (2 control specimens and 1 creep specimen), the apparent permeability (k_a) versus the inverse of average pressure of the gas ($1/p_{av}$) was drown. Three equations (1 for each specimen) were identified to find out the intrinsic permeability (k), see Figure (2.26).

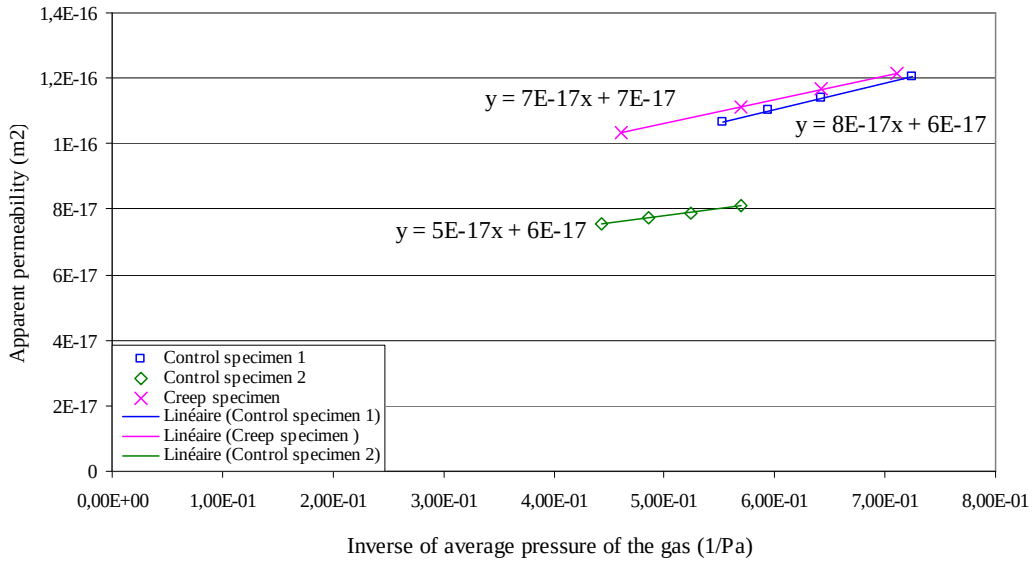

Figure (2.26): Apparent permeability vs. the inverse of average pressure of the gas

It can be seen from Figure (2.26) that the intrinsic permeability k of the creep specimen (7E-17 m^2) is very close to those of control (6E-17 m^2 for the both specimens). That means, and contrary to what was expected, this test is not adequate for revealing the existence of microcracks in creep specimen.

2.3.4 Compressive Creep Effect on the Tensile Strength

Structural beams that are subjected to prestress load are first completely under compressive stresses. Due to this compressive stress, the creep phenomenon takes place. Later on, due to stress relaxation or flexural loading, the tensile stress may take place in some zones of the beam. Hence, to know if cracks may appear in these tensile zones, it is important to study the effect of compressive creep on the concrete tensile strength.

2.3.4.1 Steps Followed for Achieving the Study

The compressive strength test was carried out on 3 specimens of series 2CB80 at age of 2 months, see Table (2.1).

After measuring the compressive strength, the compressive loading level (stress/strength ratio) was decided to be 80%. As for the other series, at the end of water curing duration which was for 2 months in this case, creep and control specimens (3 specimens for each one) were covered with aluminium scotch and stored in air at (20±2)^{o}C and (50±5)% RH.

At the end of compressive creep loading which endure for 1 month, a Brazilian strength test was carried out on all the specimens of 3 months age, and then a comparison between the maximum indirect tensile strength of creep specimens and control specimens was made.

2.3.4.2 Obtained Results

As it was mentioned previously, by subtracting the strains of control specimens from those of corresponding loaded ones, the total strains due to loading (initial and creep strain) is obtained. The results of total axial strains due to loading are shown in Figure (2.15) while those of total circumference strains are shown in Figure (2.18). Likewise, the compressive creep strains which are shown in Figure (2.16) for the axial and Figure (2.19) for the circumference are obtained by subtracting the initial strain from the total strains due to loading. The specific creep strains i.e. creep due to 1 MPa, are represented in Figures (2.17) and (2.20) for the axial and the circumference, respectively.

The results of the Brazilian test that was carried out at the end of compressive creep test, on the creep and control specimens are represented in Figure (2.27). The average indirect tensile strength is 4.51 MPa for creep specimens and 4.41 MPa for the control specimens. As the results are very close, that means that when concrete is subjected to compressive creep of loading level 80% at age of 2 month for 1 month, the tensile strength of concrete is not significantly affected.

Asamoto et al. (Asamoto et al., 2014) also studied the compressive creep effect on the tensile strength using a direct tensile strength test. The results revealed that the tensile strength was almost the same for creep and control specimens loaded with compressive creep levels of 20% and 30% while for higher level (40%) compressive creep may reduce the tensile strength, see Table (1.5). The last result is confirmed to the previous study of Liniers (Liniers, 1987) which was carried out to investigate the effect of compressive preloading (for up to 7 days) on the tensile strength by using the Brazilian test. The results revealed that very important tensile strength losses are obtained after compressive loading over 40% of the compressive strength as microcracks takes place under such loading. Likewise, tensile strength decrease and damage increases with increasing the time of preloading in compression.

Comparing the previous results with those of the actual study, it could be seen that the effect of compressive creep on the tensile strength of the actual study where the preloading level was 80% is similar to that of Asamoto et al. (Asamoto et al., 2014) for compressive creep levels of 20% and 30%.

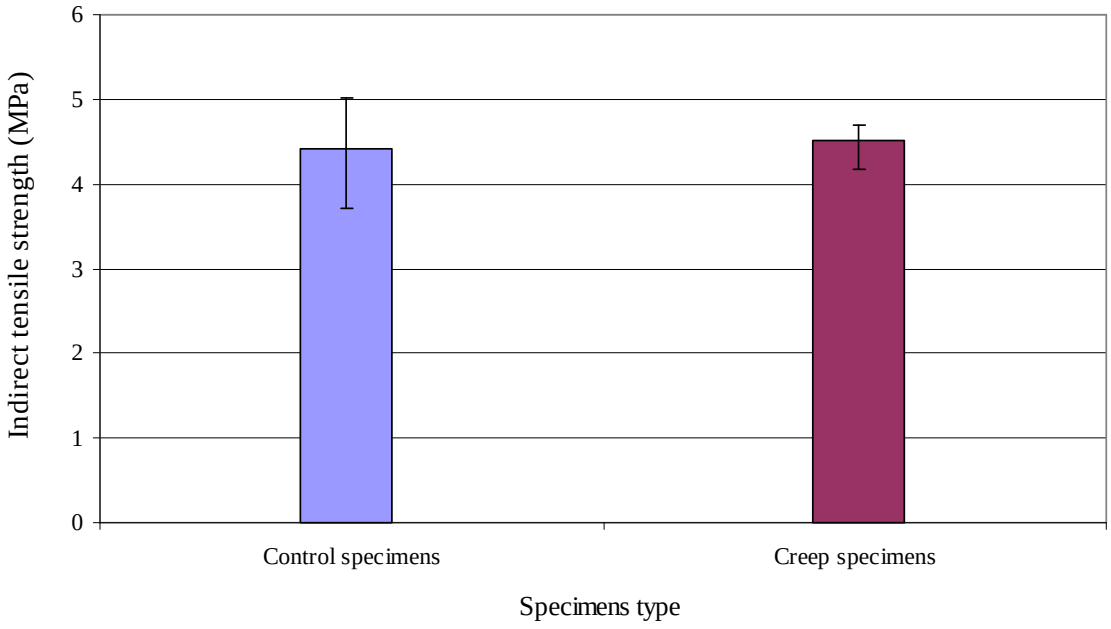

Figure (2.27): Effect of compressive creep of loading level 80% and loading age of 2 month on the concrete tensile strength

As it was seen previously, loading concrete at young age (1 month) has a positive effect on the compressive strength due to the flow of cement gel to fill out the larger provided spaces resulting in concrete more dense. Nonetheless, when concrete is going on age with the availability of water, the hydration process continues consequently. Progressively, the pores inside the concrete will be filled up with cement products. Hence, when concrete is loaded at rather later ages (here 2 months), there will not be sufficient spaces for all the water and the gel particles to diffuse inside the hardened cement past when the creep loading is applied. As a result, the force incited by these particles will create microcrakes in the hardened cement paste. So, the effect of these microcracks that weaken the concrete may be equivalent and compound the effect of the flowed gel that made the concrete denser.

2.3.5 Apparent Poisson's Ratio (Concept and Results)

The Poisson's ratio is the ratio of the lateral strain to the longitudinal strain and is usually calculated in the elastic zone. As concrete is a quasi brittle material the Poisson's ratio is an important parameter to know the effect of compressive loading on the lateral deformation.

In this work, the Poisson's ratio has been investigated at elastic limit that is between 22 MPa and 28 MPa which is the same investigation zone as that of the elastic modulus. The

Poisson's ratio is calculated by dividing the lateral strain by the average of the 3 longitudinal strains measured by the LVDT. Figure (2.28) shows the Poisson's ratio versus time of a random specimen, knowing that the time was computed from the stress level of 3 MPa until the end of the test. It could be seen that the Poisson's ratio is about 0.18, always measured, as mentioned before, between 22 MPa and 28 MPa. All the tested specimens had about the same Poisson's ratio which their values were situated within the range of 0.18 to 0.23.

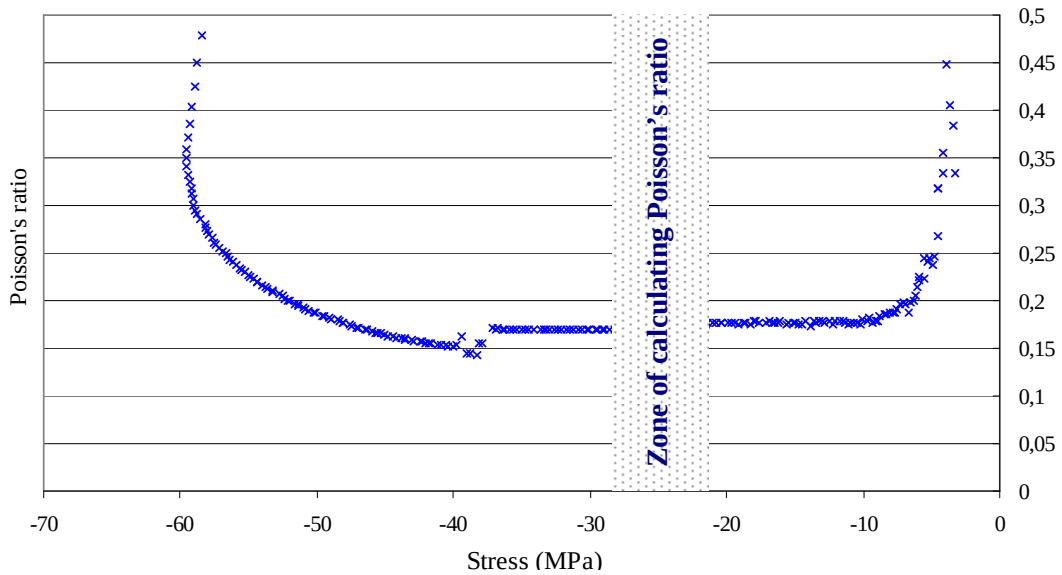

Figure (2.28): Poisson's ratio vs. time of compressive strength test (sample subjected to creep loading level of 50%)

The importance of the Poisson's ratio arises also for prestressed structures in two directions in which the cracking occur within a range higher than that for uniaxial compressive load. To understand the effect of compressive creep loading on the lateral strain, what is called creep Poisson's ratio was studied here. The creep Poisson's ratio is obtained by dividing the lateral creep strain on the longitudinal creep strain. As well, by dividing the combined creep and elastic lateral strain to that of longitudinal one, the effective Poisson's ratio is obtained. To compare the creep and the effective Poisson's ratio in one hand and the elastic Poisson's ratio (the one usually measured and used) in another hand, the Poisson's ratio at elastic zone throughout the compressive strength test was also studied.

Figure (2.29) represents the effective Poisson's ratio for different loading levels and at different ages of loading. It could be seen from the case of loading level of 65% in which the concrete was loaded at age of 1 month. After about 8 days of loading, the value of the effective Poisson's ratio is equal to 0.2. This value is similar to the Poisson's ratio of concrete

measured in the elastic zone. This result is similar to that of loading level of 80% at loading age of 3 months which is stabilized after 5 days at about 0.18. This result is similar to the result of Kim et al. (Kim et al., 2005) for the loading in 2 and 3 direction in which the Poisson's ratio was about 0.19 while in 1 direction it was little bit less and equal to about 0.17.

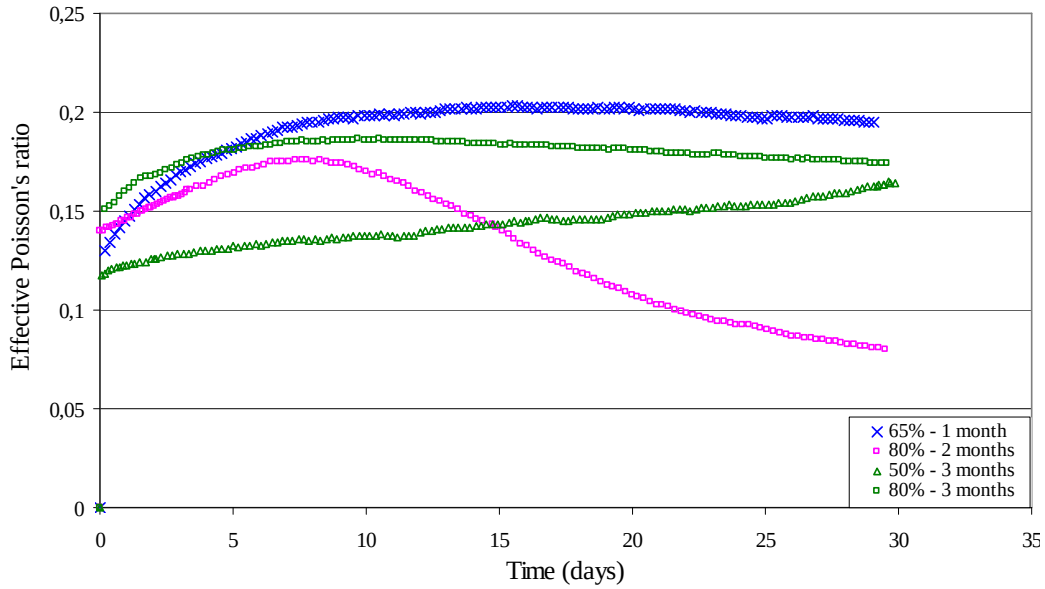

Figure (2.29): Effective Poisson ratio calculated from the combined elastic and creep strains vs. time due to compressive load

These results are not similar to those for the same loading level (80%) at age of 2 months. Here, after 5 days of loading, the effective Poisson's ratio reaches its maximum value which is equal to 0.17 then it begins to decrease until the end of loading. Figure (2.18) shows that the lateral strain gives the same shape of that of the Poisson's ratio i.e. the curve increases and then decreases.

For the loading level of 50% at age of 3 months, the curve is increasing continuously until the end of loading. This shape is similar to that of lateral deformation of the same specimens, see Figure (2.18). To understand this curve, the loading duration should probably be longer until the Poisson's ratio reaches a stable value.

The creep Poisson's ratio is represented in Figure (2.30) for different loading levels and at different age of loading.

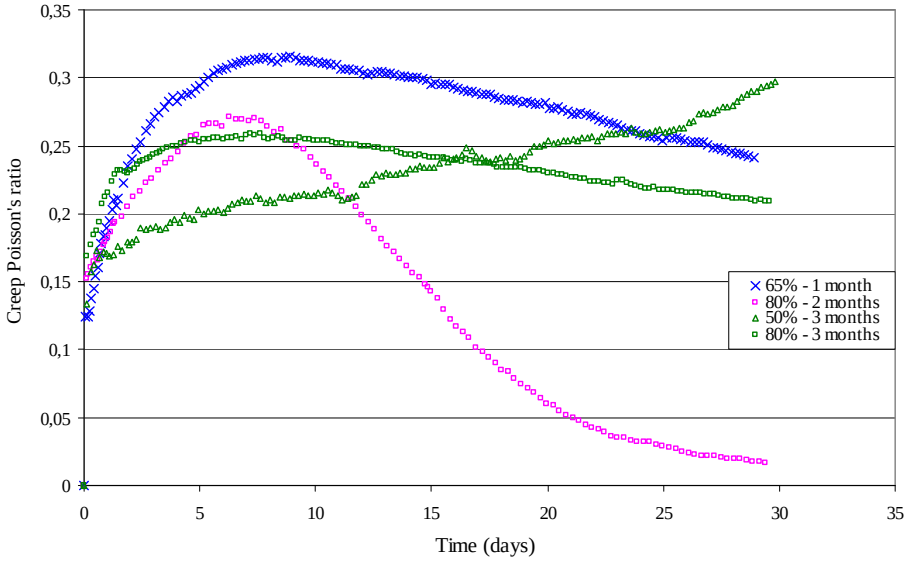

Figure (2.30): Creep Poisson's ratio vs. time due to compressive load

The behavior of the creep Poisson's ratio for the loading the level of 65% and loading age of 1 month is similar to that of the loading level of 80% and the loading age of 3 month. For the both cases, the curve increases then it slightly decreases, although the maximum values are different. It could be seen that for the loading level of 65% where the concrete loaded at age of 1 month, the curve of creep Poisson's ratio reaches its maximum value at the age of about 7 days which is equal to 0.31 while for the case of loading level of 80% where the load was applied at age of 3 month, it reaches its maximum value of 0.25 at the age of about 4 days. That means, as time progresses, the longitudinal strain becomes more important than that of lateral. These results are similar to those of Charpin (Charpin, 2015) for the basic creep in 2 direction in which the values of creep Poisson's ratio decrease from its maximum value of 0.35 to the value of 0.25.

The results of the creep Poisson's ratio for loading level of 50% at age of 3 month, give the same curve shape of that for the effective Poisson's ratio. Here, the values of the curve increase until they reach their maximum value at the end of loading. As it was explained for the effective Poisson's ratio, to understand the values of the creep Poisson's ratio, the loading duration should be longer at least to catch the maximum value and to see if this value becomes stable or decreases. Even though, this result is analogous to the results of Bergues and Habib (Bergues and Habib, 1972), and Jordaan and Illston (Jordaan and Illston, 1969), as presented by Benboudjema (Benboudjema, 2002). The finding of these works show that the curves of creep Poisson's ratio continue to increase until the end of loading, see Figure (1.38).

The curve of the creep Poisson's ratio for the loading level of 80% and at the age of loading of 2 months has a similar shape to that of the effective Poisson's ratio. Here, the curve increases to reach its maximum value at the age of 5 days to be equal to 0.26 then it decreases to reach a zero value at the end of the test. This finding is similar to that of Charpin (Charpin, 2015) for the basic creep of 1 direction loading test, where the value of the Poisson's ratio decreases (from about 0.15 - 0.2) to stabilize around zero.

2.4 Creep in Tension (Brazilian Creep)

In addition to determine the effect of compressive creep, it is important to study the effect of tensile creep on the residual tensile strength as the concrete beams subjected to flexural loading and the concrete under restrained shrinkage are subjected to tensile stresses.

2.4.1 Instrument Used for Fixing the Specimens throughout the Brazilian Creep Test

In order to perform the tensile creep test, it was proposed to do a Brazilian tensile test. Specimens laterally loaded into a frame device and measuring the lateral strains (the elongation in the diameter that is perpendicular to loading) throughout the application of sustained compressive force. In order to accomplish the Brazilian tensile strength test on the creep and control specimens at the end of creep test, it was necessary to apply the creep test on at least 3 cylindrical specimens. As it is already difficult to achieve the Brazilian test which is applied on only 1 cylindrical specimen, it was necessary to design a frame to maintain the 3 specimens to be arranged laterally (the axis of the specimens is horizontal and perpendicular to the applied load) one over the other throughout the creep test. So the apparatus which is illustrated in Figure (2.31) and (2.32) was designed and fabricated in the 3SR laboratory. This apparatus is composed from a rectangular base plate (14.5cm×20cm) over which the specimens are arranged laterally one over the other. At the corners of this plate, there are 4 columns joined to carry 6 beams (3 at each side) that slide vertically on these columns. Each beam is supplied with 2 screws (the distance from centre to centre between these screws is 11cm) to hold the specimens. To avoid restraining the specimens, these screws are released as soon as the specimens become in touch with the creep load (F_a). Another plate includes a rectangular hole is joined at the upper side of the columns. Inside this hole, a beam which has a base of 2cm×15cm and a height of 5cm is handled to transport the creep force (F_a) to the creep specimens. In addition, 2 plates are arranged at the outer sides perpendicularly to the axis of the specimens. These plates have slots to allow the plywood

strips of 1cm in width and 16cm in length, aligned between the cylinders, to slide inside them during the creep test.

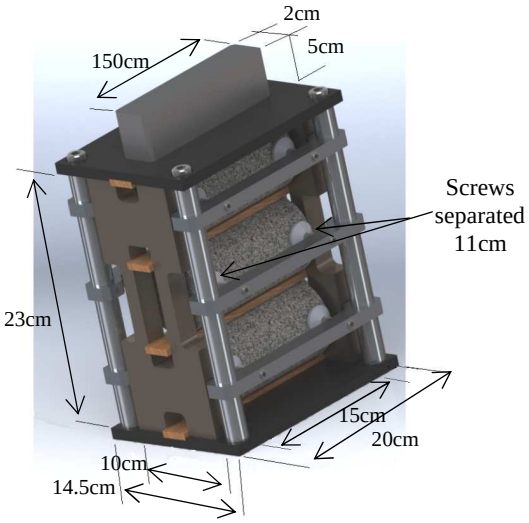

Figure (2.31): Apparatus for holding specimens throughout the Brazilian creep test

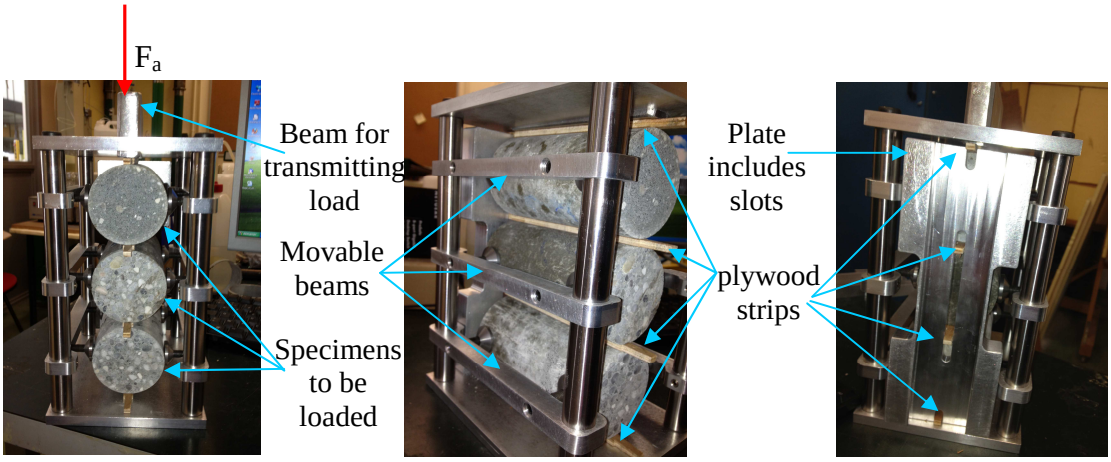

Figure (2.32): Arranging the specimens in the Brazilian apparatus

This apparatus is loaded in the same creep device that was used for achieving the compressive creep test, see Figure (2.33).

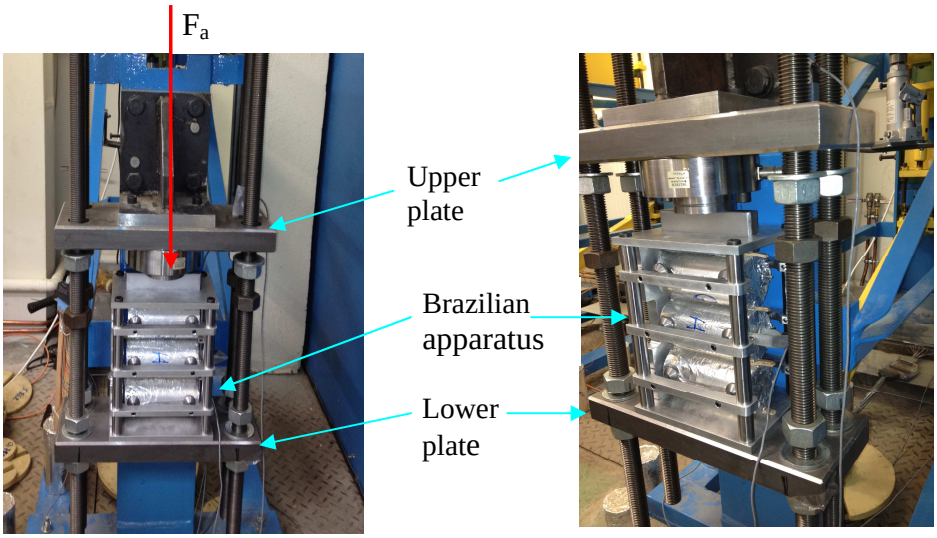

Figure (2.33): The Brazilian apparatus installed in the creep device

2.4.2 Instruments Used for Measuring the Tensile Creep Strains

Like the compressive creep, 3 specimens were prepared to be loaded (creep specimens) and the other 3 were unloaded (control specimens). All the specimens were taken out of water to be dried in air for one day in order to stick the screws with them a displacement transducer is joined at time of creep loading. Displacement transducers, type PI-2-50 equipped from Tokyo Sokki Kenkyujo Co., Ltd., where used for measuring the displacement during the creep test, see Figure (2.34). The displacement transducer used has a simple structure of strain gauge attached to the end of an arch-shape spring plate.

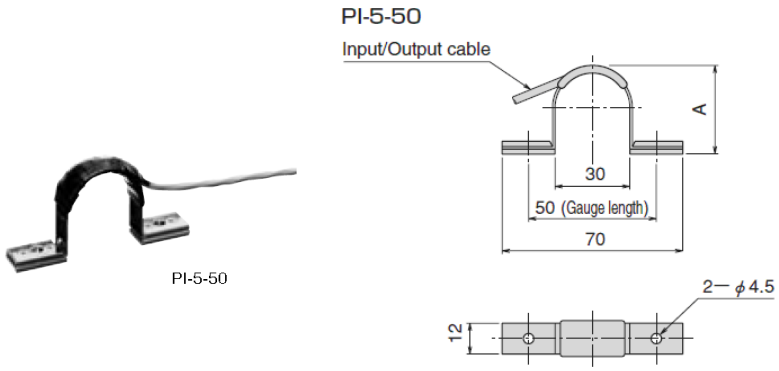

Figure (2.34): Displacement transducer type PI-2-50

For each test, 3 transducers were used; 2 were fixed on 2 creep specimens and another one was fixed on one of the control specimens. The product used for sticking the screws of displacement transducers was Sikadur-31 CF from Sika. After one day, the Sikadur becames

hard so all the specimens were immerged again into the water tank and take out again at the age of loading. To avoid drying and take only the basic creep into account, the creep and the control specimens were covered with aluminium scotch, see Figure (2.35).

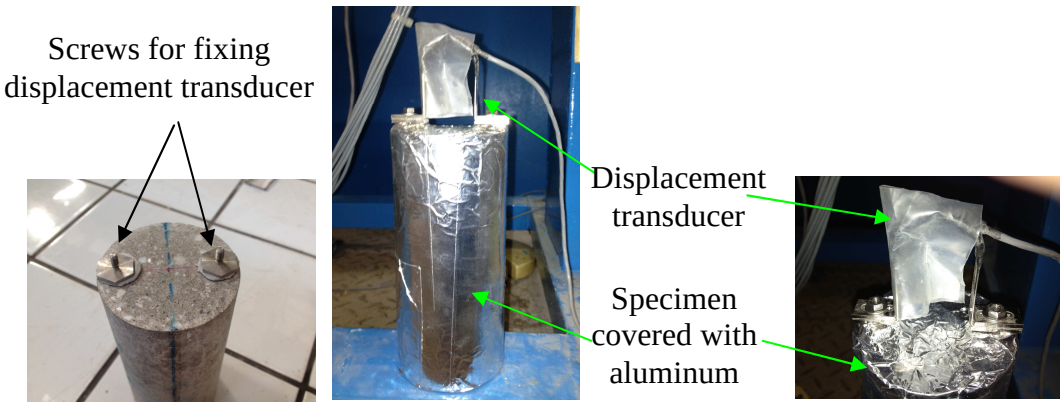

Figure (2.35): Fixing the displacement transducer on a specimen

2.4.3 Brazilian Creep Effect on the Concrete Tensile Strength

As it was mentioned before, the aim of achieving the tensile creep test was to determine its effect on the concrete tensile strength.

2.4.3.1 Steps Followed for Achieving the Study of the Brazilian Creep Effect

At the end of water curing (at age of 1 month) the Brazilian test was carried out on 3 specimens for each series named 1BB50 and 1BB80 while 4 specimens were tested for series 1BB90 to find the tensile strength, see Table (2.1). After achieving the indirect tensile strength test, 3 indirect tensile loading levels (stress/strength ratio) were chosen for carrying out two creep tests. The applied compressive load to impose the indirect tensile stress is computed from the following formula:

$$P = a(f_t \cdot d \cdot l \cdot \pi / 2) \qquad (2.9)$$

where, P is the applied compressive load, a is the percentage of loading level to be applied, f_t is the indirect tensile strength, d and l is the specimen diameter and length, respectively.

The adopted loading levels were 50% for creep series 1BB50, 80% for series 1BB80 and 90% for series 1BB90. The conditions of storage during the creep test were the same for all the series and they are identical to that of compressive creep. Hence, at the end of water curing duration, the creep and the control specimens were covered with aluminium scotch and stored in air under temperature of (20±1)^{o}C and relative humidity of (50±5)% throughout the

creep test. As it was already stated, for each test, 3 specimens were loaded in the creep device called creep specimens and 3 other were unloaded to be used as control specimens.

At the end of creep test which persisted for 1 month for all the series, the Brazilian test was carried out on the creep and control specimens. For applying the Brazilian test, the creep specimen is placed in the same position as that was for creep test. The maximum indirect tensile strength (f_t) was computed by using Equation (2.9) and a comparison between the creep and the control specimens was done.

2.4.3.2 Results Obtained from the Brazilian Creep Test

As explained previously, the total strain due to the loading is obtained by subtracting the strains of control specimens from those which were loaded. The creep strains are obtained by subtracting the initial strain from the strains due to the sustained load. So, it was difficult to obtain the creep strain. It could be seen from Figure (2.35) which represents the creep strain of 2 loading levels that, as expected the creep increases with increasing the loading level. It could also be remarked that the curves are not smooth. The disturbance is probably related to the temperature variation between the night and the day.

The results of the Brazilian test that was carried out at the end of Brazilian creep test, on the creep and control specimens, are presented in Table (2.6) and Figure (2.37).

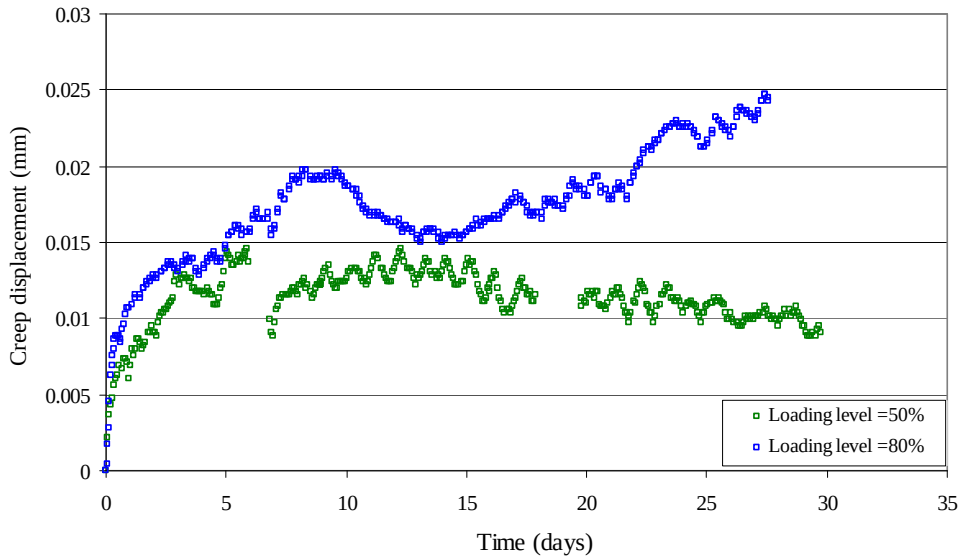

Figure (2.36): Lateral creep strains vs. time of Brazilian creep test

Table (2.6): Variation of concrete tensile strength after tensile creep

Age at beginning of creep loading	1 month		
Time duration of creep loading	1 month	1 month	1 month
Casting number	1	2	3
Creep loading level	90%	80%	50%
f_t before creep (MPa)	3.4	3.0	2.9
f_t of control Spec.	3.8	3.5	4.0
f_t variation with the age *	+12(%)	+17(%)	+38(%)
f_t of creep specimens	3.7	3.7	4.8
f_t variation due to creep **	-2.6(%)	+5.7(%)	+20(%)
** f_t development with the age %= 100 × (f_t of control Spec.– f_t before creep)/ f_t before creep*			
*** f_t development due to creep %= 100 x (f_t of creep Spec.– f_t of control Spec.)/ f_t of control Spec.*			

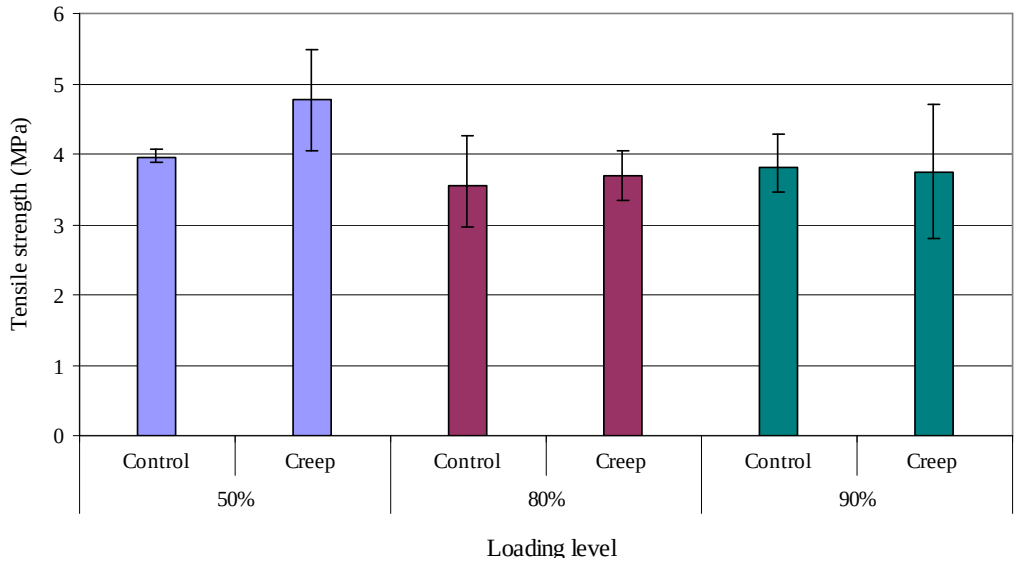

Figure (2.37): Experimental results of tensile strength vs. loading level for creep and control specimens

After creep loading level of 50%, the creep specimens have higher tensile strength than those of control specimens while when the creep level was 80% and 90%, the tensile strength is about the same for the creep and control specimens.

The justification that could be given here is that, for the lowest tensile creep loading (50%), the applied compressive load works on moving the cement gel to the larger provided spaces resulting in concrete more dense in the direction of loading and the direction perpendicular to loading (due to Poisson's ratio). However, as concrete is a quasi brittle material, the microcracks develop quickly in the direction of tensile stresses i.e. the lateral direction. So, when concrete is being loaded at level of 80%, the negative effect of microcracks become to exceed the useful effect of gel flow inside the pores. When the applied load is increased to reach the level of 90%, the microcracks amount becomes greater and more detrimental that lead to weaken the concrete. As well, as the Brazilian test results are more scatters than those of compressive strength test, more experiments must be achieved to validate these results.

In this chapter, creep tests in compressive as well as in tension were realized for different ages of loading and for different loading levels. In addition, quasi-instantaneous preloading tests (loading until a certain level) were achieved. The objective was to study the creep and the preloading effect on the development of the residual mechanical properties of concrete. From the performed tests, the following points were concluded:

1- The compressive preloading level of 80% has no significant effect on the concrete tensile strength. Even though, higher loading levels have negative effect on the tensile strength of concrete. This negative effect increases with increasing the preloading level. The decreasing in the tensile resistance was 16% for preloading level of 90% and 20% for preloading level of 95%. That could be related to concrete properties, which is considered as a quasi brittle material. So, when a compressive load is applied to a high loading level, microcracks will occur in the direction parallel to the applied load and these microcracks increase with the applied loading up to failure (loading level equals to 100%). Hence, when the concrete specimen is subjected to the Brazilian test, it reveals a lower resistance than that of unloaded specimen. However, as the Brazilian test gives scattered results, more tests would be needed to confirm this result.

2- For the same compressive loading level, when the age of loading increases, creep and specific creep strains increase too. When concrete is aging and because of the presence of free water, the hydration process continues and the pores of cement past are filled up with cement product. So, when concrete is loaded at later ages, the flow of water and gel particles will not find enough spaces for diffusing inside the concrete skeleton. As a result, the energy provoked by these moving particles on the hardened cement paste will lead to microcracks occurrence.

Due to these microcracks, there will be an increasing in creep strains in addition to creep strains due to the relatively small movement of water and gel particles.

3- When concrete is subjected to compressive creep at age of 1 month and for 1 month, the compressive strength and the modulus of elasticity of creep specimens are greater than those of control specimens, for the loading levels that dealt with this study (50% and 65%). On the contrary, when concrete had been loaded at age of 3 months, after 1 month of loading the creep specimens have lower compressive strength than those of control specimens, for 50% and 80% loading levels.

This difference in the results is related to the age of loading, i.e. when concrete is being loaded at young ages, the applied load promotes the cement gel to be moved from their places to a wider place to fill up the pores inside the cement paste. As a result, the size of concrete specimen becomes smaller and denser than that which was not subjected to creep. So, the dense specimens (creep specimens) reveal higher resistance than those which are less dense (control specimens). On the contrary, the concrete that had been preserved under water, is loaded at later ages, most of the pores had already been filled with the hydration products. Hence, when load is applied at these late ages, there will be not sufficient place available for the water and the cement gel particles to move easily. So, these particles apply a pushing force on the hardened cement resulting in microcracks occurrence. As a result and due to these microcracks, the creep specimens give lower resistance than those of control. Nevertheless, it could be seen that at loading age of 3 months, the modulus of elasticity is about the same for creep and control specimens and for both loading levels (50% and 80%). This means that there is no effect of creep loading on the elastic modulus when the concrete is loaded at age of 3 months.

4- Tomographic images with a voxel (volumetric pixel) size of 25µm of the inner 45mm gave evidence that creep specimens that were loaded at age of 1 month with loading level of 65% are sound and free from macrocracks at this scale.

. The permeability test did not confirm the proposal given here about the microckracs occurrence when concrete is loaded at 3 month with loading level of 80%.

5- The results of the Brazilian test that carried out at the end of compressive creep test revealed that tensile strength of creep and control specimens are very close. It remains to be said that compressive creep test was carried out at age of 2 month with loading level of 80% and persisted for 1 month.

Creep loading concrete at 1 month has a positive effect on the compressive strength due to the flow of cement gel inside the pores resulting in concrete more dense. However, for

aging concrete, the pores inside the concrete will be filled up with cement products. Therefore, when concrete is loaded at rather later ages (here 2 months), there will not be enough spaces for all the water and the gel particles to diffuse inside the hardened cement paste when the creep loading is applied. As a result, the force promoting by these particles will create microcrakes in the hardened cement paste. As a result, the negative effect of these microcracks may be equivalent the useful effect of the flowed gel that made the concrete denser.

6- The results obtained for the effective Poisson's ratio and for the creep Poisson's ratio, for different creep loading levels and ages of loading, are not homogeneous. The results of loading level 65% at age of 1 month have about the same shape and maximum value of that of loading level 80% at age of 3months. Moreover, the results of creep Poisson's ratio of those both cases become stable after several days of loading and reach about the same value (0.2 for loading level 65% at age of 1 month and 0.18 for loading level 80% at age of 3 months). These results are also similar to that for Poisson's ratio calculated within the elastic range (between 0.18 and 0.23).

7- The tensile creep specimens of loading level 50%, have higher tensile strength than those of control specimens while for loading level of 80% and 90%, the tensile strength was about the same for the creep and control specimens. That could be related to the useful effect of creep process at the rather low tensile loading level (50%) where the applied sustained load works on moving the cement gel particles to the larger provided spaces resulting in concrete more dense. However, as concrete is a quasi brittle material, the microcracks develop quickly in the direction of tensile stresses i.e. the lateral direction (due to Poisson's ratio). So, when concrete is being loaded at higher level of 80% or 90%, the negative effect of microcracks is compensated by the effect of gel flow inside the pores. For very high loading level (90%), the microcracks amount becomes greater and more destructive which leads to weaken the concrete. Even though, as the Brazilian test results are more scatters than those of compressive strength test, more tests must be done to confirm these results.

CHAPTER III: MESOSCOPIC SIMULATION FOR PREDICTING CONCRETE CREEP AND FOR EVALUATING RESIDUAL MECHANICAL PROPERTIES

The existing models for estimating creep strains of concrete generally assume that concrete is a homogeneous material. The coupling between creep and damage (microcracking) was done by adding a coefficient (Mazotti and Savoia, 2003) which is difficult to calibrate (De Larrard, 2010). As concrete is a composite material, these models could not take into account the incompatible strains between cement paste and aggregate during creep loading. So, mesoscopic model was adopted in this study for simulating concrete as a composite material and thus creep is computed according to the parameters of concrete composite materials (aggregate and cement paste). Therefore and due to sustained load, the cement paste creeps while the aggregate act as an obstacle to this creep resulting in microcracking at the aggregate-cement paste interface. These microcracks in turn may lead to the deterioration of mechanical properties of concrete and increasing creep rate and thus nonlinearity relation between the creep strain and the applied load. Thus, creep strain is coupled with damage (microcracking) in an adequate manner.

The effects of creep strains on the residual mechanical properties of concrete mainly: Young modulus, compressive strength and tensile strength were not clearly mentioned in previous creep studies (see for instance, Saliba et al. 2012). As it was presented in chapter two, the experimental results of this study revealed that, the compressive creep has two different effects on the development of residual mechanical properties of concrete depending on the age of loading. In other words, when concrete is loaded at young age (1 month), creep strain improves the residual mechanical properties. But, when the load is applied at late age (3 months), creep strain leads to the deterioration of these properties for each loading level. However, concerning the indirect tensile creep, the creep effect on the tensile strength depends on the loading level. Namely, the tensile creep loading level (50%) increases the tensile strength while the high loading level (90%), decrease the tensile strength of concrete. So, a mesoscopic simulation was used because it has been thought that, the mesoscopic scale may manifest the results that had been obtained experimentally due to microcracking at the aggregate-cement paste interface, as it was mentioned above.

Therefore, the first objective of this chapter is to show the effect of microcracks on the decrease of the elastic modulus and the strength of concrete. The second aim is to show the role of microcracks at the aggregate-cement paste interface on the increase of the creep strain

level and on the apparent nonlinearity behavior of creep strain with respect to the loading level.

This chapter is inspired from an article that was written by Zainab Kammouna, Matthieu Briffaut and Yann Malecot, with the same title of this chapter. This article includes the presentation of a viscoelastic model which was adopted for computing creep strains of a mesostructure composed of aggregate and cement paste under variant loading levels, in tension and in compression.

After a short presentation of the model and the meshing technique used in this study, the creep of concrete in compression and in tension were studied in the first part of this chapter. This part allows verifying the ability of the model in estimating the creep of concrete under different loading levels and mainly for studying the nonlinearity of creep strain with respect to stress level. The experimental results of Roll (Roll, 1964) for the compressive creep and of Illston (Illston, 1965) for the tensile creep were adopted and used to verify the effect of microcracks generated by incompatible strains in developing the creep strains under different stress/strength ratios.

These results from literatures were adopted because the experiments done in this study took a long time especially the one concerning loading concrete at late age (3 months curing + 1 month loading). In addition, the apparatus of holding creep specimens throughout the Brazilian creep test was long to be designed and manufactured.

As the existing models for estimating the creep of concrete do not take into account the changes in the mechanical properties of concrete throughout the time of loading, the creep calculations may be under or over estimated. Therefore the second part of this chapter presents the evolution of the concrete behavior law due to incompatible strains and damage generated throughout long term loading.

In addition, simulations of Brazilian creep strain and its effect on the tensile strength that were not included in the mentioned article were developed and prestressed at the end of this chapter. It must be mentioned that this study is mainly dedicate to massive structures in the first modelling step and thus only basic creep is taken into account, but drying creep could also been considered.

Summery of Chapter III

3.1 Creep–Damage Coupling Models

The paragraph presents the existing models that assume concrete as a homogeneous material for estimating creep. In addition, the mesoscopic models that assume concrete as a material composed from aggregate and cement paste was presented.

3.2 Creep Simulation

This paragraph includes, the adopted model and mesoscopic mesh generation used for representing concrete as composite material. Here, the damage occurs at the aggregate-cement paste interface as the cement paste creeps while the aggregate acts as an obstacle.

3.3 Simulation of Stress-Strain Evolution

To evaluate the creep effect on the residual mechanical properties, stress-strain relation was simulated by using the mesoscopic model before creep and after creep in tension and in compression.

3.4 Simulation of Indirect Tensile Creep (Brazilian Creep)

To evaluate the magnitude of indirect tensile creep stains that were experimentally measured, the Brazilian creep strain was simulated and then the results were compared with the experimental ones.

3.1 Creep-Damage Coupling Models

3.1.1 Macroscopic Scale Models

The existing models for estimating creep of concrete, based on a reheological model generally assume that concrete is a homogeneous material, as it is the case for instance in the models of Sellier (Sellier, 2009), Benboudjema and Torrenti (Benboudjema and Torrenti, 2008) and Bazant (Bazant, 1978). Therefore the incompatible strains between cement paste and aggregate throughout creep loading could not be taken into account.

It is well known that the relation between the stress level and creep strains is not linear. This nonlinearity could be attributed to the microcracks at aggregate-cement paste interface which is directly related to the stress level. Indeed, creep of concrete is mainly related to the creep of cement paste rather than that of aggregate, and this the lasts act as an obstacle to the global creep. Consequently, tensile stresses arise close to the interface between cement paste and aggregate which could lead to microcracks in this zone. Therefore, a decrease in the

elastic modulus and in the concrete strength, and an increase in the amount of creep strain under the same loading level is expected. This increase in the creep strain is seen as nonlinearity of the strain with respect to the stress level. To reproduce this nonlinearity at macroscopic scale, a coupling between damage and creep was proposed by Mazotti and Savoia (Mazotti and Savoia, 2003) and used by Reviron et al. (Reviron et al., 2007), Benboudjema and Torrenti (Benboudjema and Torrenti, 2008), Omar et al. (Omar et al., 2009) and Briffaut et al. (Briffaut et al., 2011). However, this coupling coefficient which was introduced in the equation of equivalent strain by Mazars (Mazars, 1986) remains difficult to calibrate (De Larrard, 2010). Another work carried out to find another solution was to use a rheological law which depends on the stress level. Nevertheless, with this last method the tertiary creep could not be achieved because the concrete is considered to be a homogenous material without coupling with damage.

3.1.2 Mesoscopic Scale Models

Mesoscopic approaches were already used for modelling drying shrinkage incompatibilities at ambient temperature (Grassl et al., 2010 and Lagier et al., 2011), at elevated temperatures (Grondin et al., 2011, and Grassl and Pearce, 2010) and for modelling the autogenous and thermal shrinkage (Briffaut et al., 2013 and Schlangen et al., 2006). Another mesoscopic model developed by Saliba et al. (Saliba et al., 2012) has also been used to study the failure of concrete beam under flexural load and highlight the presence of microcracking during the sustained load. Recently Thai et al. (Thai et al., 2014), represent concrete as a composite material which consist of spherical elastic inclusions (aggregate and/ or voids) imbedded in a linear viscoelastic matrix. Nevertheless, the model does not take into account microcracks at cement-aggregate interface level which occurs due to incompatible deformations between these two materials.

As it was mentioned previously, the aim of this chapter is to study the influence of microcracks, due to incompatible strain between cement paste and aggregate, on the creep strains amplitudes. Hence, a viscoelastic damage model developed by Benboudjema and Torrenti (Benboudjema and Torrenti, 2008) was adopted for computing creep of cement paste using a mesoscopic mesh technique for representing the greatest size of aggregate (more than 1mm) in the cement paste (Nguyen et al., 2010).

3.2 Creep Simulation

3.2.1 Mesoscopic Mesh

The algorithm of mesh generation used in this study was developed by Nguyen et al. (Nguyen et al., 2010). Numerical simulations are performed in two dimensions (plane strain) on a Representative Elementary Volume (REV) of concrete of 100×100 mm² (see Figure (3.1)). In this mesoscopic approach, two phases are considered; cement paste and aggregate. It is essential in this mesh generation to represent the fine aggregate when simple behavior law is considered. Even though, using an aligned mesh for representing aggregate, strongly increase the number of the element to perform correctly the fine aggregate. So, the mesh is not adapted to the exact shape of aggregate, but the properties of the material are projected on a finite element mesh square grid. The model used for aggregate is an elastic damage model whereas the cement paste is described with a viscoelastic damage model. The advantage of using a mesoscopic approach arises in the possibility of using simplified behavior laws. The macroscopic damage occurs due to the geometric representation of cement and aggregate which have different material properties. The source of complex behavior observed at the macroscopic scale is assumed to be due to geometric representation of the constituents and the contrast between material properties. At the mesoscale, the rupture is assumed to be only due to extension. Therefore, the damage due to compressive stress is not considered.

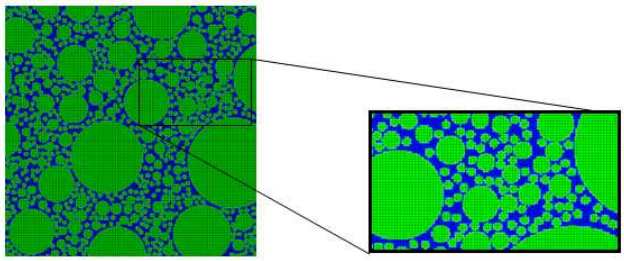

Figure (3.1): Mesh of the REV

3.2.2 The Adopted Model

The chemo-thermo-viscoelastic damage model used is described in Benboudjema and Torrenti 2008, and Briffaut et al. 2011 (Benboudjema and Torrenti 2008, and Briffaut et al. 2011). This model allows predicting correctly the degradation of material in tension. However it is not suitable for describing the behavior of high biaxial/ triaxial compressive stresses.

The relationship between apparent stresses σ, effective stresses $\tilde{\sigma}$, damage D, elastic stiffness tensor E, total strain ε, elastic strains ε_e, basic creep strains ε_{bc}, thermal strain ε_{th}, autogenous shrinkage ε_{au}, total strain ε, is given by:

$$\sigma = (1-D)\tilde{\sigma} = (1-D)E(\xi)\dot{\varepsilon}_e = (1-D)E(\xi)(\dot{\varepsilon} - \dot{\varepsilon}_{bc} - \dot{\varepsilon}_{au} - \dot{\varepsilon}_{th}) \tag{3.1}$$

The damage criterion defined by Mazars (Mazars, 1986) reads:

$$f = \varepsilon_{eq} - k(D) \qquad \text{and} \qquad k(D) = \varepsilon_{do} \quad \text{if} \quad D = 0 \tag{3.2}$$

where ε_{eq} is the equivalent strain and ε_{do} is the tensile damage threshold and it is equal to $\frac{f_t}{E}$.

Fichant (Fichant, 1996) developed two damage models: an isotropic one to solve unilateral problems and an orthotropic one for solving more complex loadings. In these models, the damage development is controlled by the cracking energy. These models could take into account the plasticity and the lateral effect. In this study, the isotropic model was chosen because the idea of mesoscopic simulations is to use simple behavior laws for each constituent associated with a complex geometry.

In this model, damage affects the elastic part of the stress-strain relation behavior (Fichant et al., 1999):

$$\sigma_{ij} = (1-D)\langle\tilde{\sigma}_{ij}\rangle^{+} + (1-D)^{\alpha}\langle\tilde{\sigma}_{ij}\rangle^{-} \tag{3.3}$$

$$\sigma_{ij} = C_{ijkl}^{damage}\,\varepsilon_{kl} \tag{3.4}$$

where α is a parameter control the contribution of damage in compressive part, C_{ijkl}^{damage} is the stiffness of the damaged material whereas σ_{ij} and ε_{kl} represent the components of the stress tensor and elastic strain tensor, respectively.

The equivalent strain (ε_{eq}) is calculated from the elastic strain (ε_e) of Mazars (Mazars, 1984) and the damage affects the elastic portion of stress-strain behavior law. The damage evolution law is expressed as follows:

$$D = 1 - \frac{\varepsilon_{d0}}{\varepsilon_{eq}} exp(B_t(\varepsilon_{d0} - \varepsilon_{eq})) \quad \text{with} \quad 1 \geq D > 0 \tag{3.5}$$

The parameter B_t is calculated as a function of the cracking energy G_f and of the element size h by the following equation:

$$B_t = h\, f_t / G_f \tag{3.6}$$

where f_t is the tensile fracture stress of the material. This regularised technique based on the proposition of Hillerborg et al. (Hillerborg et al., 1976) allows avoiding strong mesh dependency. In this technique, the analysis can be performed with a rather coarse mesh because there are no stress singularities and the amount of absorbed energy is not very sensitive to the mesh size (Hillerborg et al., 1976).

The basic creep model used is composed of three chains Kelvin Voigt (KV) combined in a series with a dashpot (see Figure (3.2)).

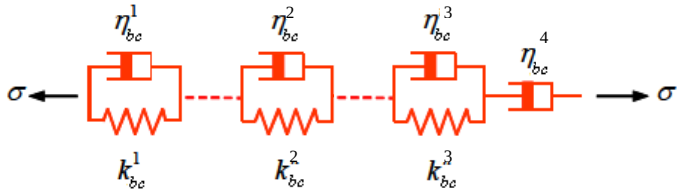

Figure (3.2): Kelvin-Voigt elements for predicting creep strain (Benboudjema and Torrenti, 2008)

This model could take into account the effects of hydration (ξ is the hydration degree). The deformation of one KV chain can be obtained by solving the following differential equation (Benboudjema and Torrenti, 2008):

$$\tau_{bc}^i \ddot{\varepsilon}_{bc}^i + \left(\tau_{bc}^i \frac{\dot{k}_{bc}^i(\xi)}{k_{bc}^i(\xi)} + 1 \right) \dot{\varepsilon}_{bc}^i = \frac{\ddot{\sigma}}{k_{bc}^i(\xi)} \quad \text{and} \quad \tau_{bc}^i = \frac{\eta_{bc}^i}{k_{bc}^i} \tag{3.7}$$

where τ_{bc}^i is the characteristic time (constant), k_{bc}^i and η_{bc}^i are the stiffness of the springs and the viscosities respectively (function of the degree of hydration).

The stiffness parameters for each chain are calculated from the following equations (De Schutter, 1999):

$$k_{bc}^{i}(\xi)=k_{bc\_\infty}^{i}\frac{0.473}{2.081-1.608\bar{\xi}}\bar{\xi}^{\psi} \quad \text{and} \quad \eta_{bc}^{j}(\xi)=\eta_{bc\_\infty}^{j}\frac{0.473}{2.081-1.608\bar{\xi}}\bar{\xi}^{\psi} \tag{3.8}$$

3.2.3 Compressive Creep Results

The experimental compressive creep results of Roll (Roll, 1964) for four loading levels (25%, 35%, 50% and 65% of the compressive strength) were simulated. The creep law parameters were calibrated for the lowest loading level whereas the mechanical properties were calibrated with ordinary cement paste values (Nguyen et al. 2010) and to obtain no damaged element after creep loading of level 25%. It is mentioned here that according to the concrete properties the loading levels which correspond to the above loading levels are 7.5 MPa, 10.5 MPa, 15 MPa and 19.5 MPa, respectively. The parameters used in the numerical model are illustrated in Table (3.1).

Table (3.1): Set of parameters used for viscoelatic damage models to reproduce (Roll, 1964) and (Illston, 1965) creep test; $_{agg}$ and $_{cp}$ stands respectively for aggregate and cement paste

Parameter	Unit	Value
E_{agg}	Pa	6e10
Ft_{agg}	Pa	6e6
$G_{f\ agg}$	J/m²	60
$\alpha 1_{agg}$	-	30
ν_{agg}	-	0.2
E_{cp}	Pa	2.5e10
$F_{t\ cp}$	Pa	2.5e6
$G_{f\ cp}$	J/m²	20
$\alpha 1_{\ cp}$	-	10
ν_{cp}	-	0.2
$k^{1}_{bc,cp}$	Pa	2e9
$k^{2}_{bc,cp}$	Pa	1.2e9
$k^{3}_{bc,cp}$	Pa	0.18e9
$\tau^{1}_{bc,cp}$	days	5
$\tau^{2}_{bc,cp}$	days	50
$\tau^{3}_{bc,cp}$	days	500

A comparison between the experimental results and the mesoscopic approach with and without damage are presented in Table (3.2) and Figure (3.3). It is observed from Table (3.2) that in the case where there is no damage, the relation between the stress and the creep remains as expected linear. Figure (3.3) highlights that the simulations of creep evolution with

damage due to strain incompatibilities are closer to the experimental ones than the simulation curves without damage. Assuming that creep of concrete occurs without damage means that there are no microcracks at the interface between cement paste and aggregate. Consequently, there is no additional creep strain that occurs due to these microcracks.

By comparing the field of damage for two loading levels 25% and 65%, it is remarked that the damage amount is higher for 65% than that for 25% as strongly expected. The increasing of the damage amount is related to incompatible strains between the cement paste which creeps throughout the loading, and the aggregate which act as an obstacle to this creep because of their higher stiffness. Thus, tensile stresses develop at the cement paste-aggregate interface leading to the cracking development. As creep strain of cement paste is directly related to loading level, the damage at the interface between cement paste and aggregate increases.

Table (3.2): Comparison of the experimental compressive creep results (Roll, 1964) with those of mesoscopic approach with and without damage

Loading level		Exp. results (ε_{exp}) 10^{-6}	With damage		Without damage		Nonlinearity %
MPa	$\sigma/\ \sigma_{7.5}$		Sim. results (ε_{wd}) 10^{-6}	sim/ $sim_{7.5}$	Sim. results (ε_{wod}) 10^{-6}	sim/ $sim_{7.5}$	
10.5	1.4	1153 at 210 days	1026	1.65	594	1.39	77.2
15	2	2108 at 209 days	1719	2.77	836	1.97	69.4
19.5	2.6	3183 at 209 days	2476	3.99	1087	2.56	66.3
Nonlinearity% = 100 (ε_{wd} - ε_{wod}) / (ε_{exp} - ε_{wod})							

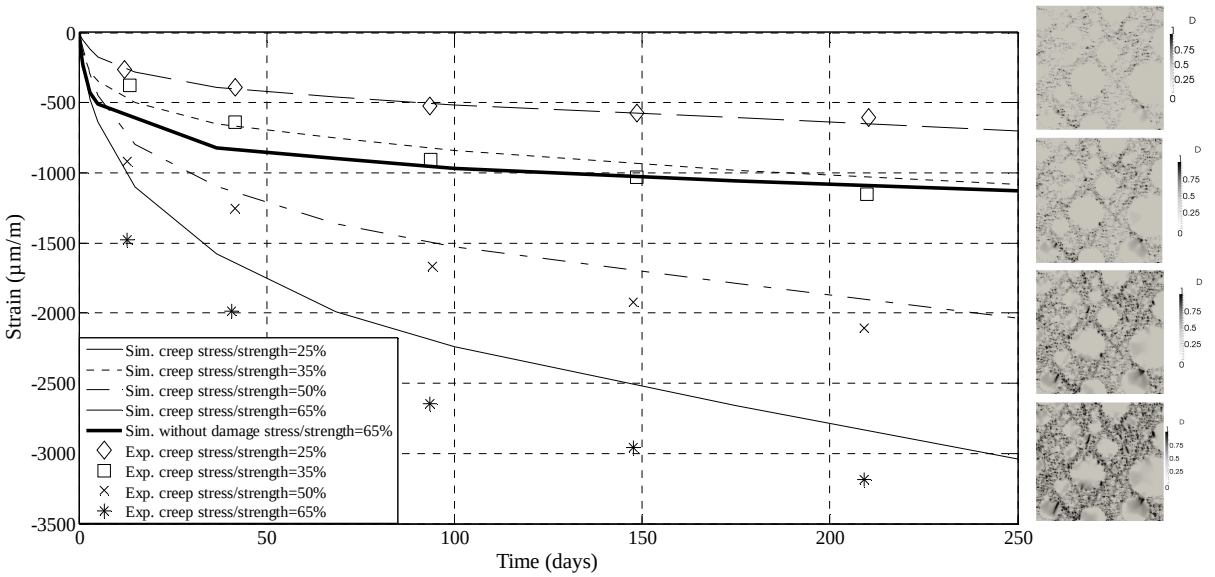

(a) (b)

Figure (3.3): (a) Compressive creep strain evolution: comparison between experimental data and mesoscopic approach with and without damage, (b) Field of damage

The linear models propose that the creep strain is directly proportional to the applied load and develops in the same percentage. This proposal is not like the reality where the creep strains increase in a higher percentage (due to the microcracks) than that of the applied load. As the mesoscopic simulation represents the microcracks occurrence, the linearity between the applied load and the creep strains is decreased. So, for representing the shift between the mesoscopic model and the linear models, the mesoscopic creep value is subtracted from that of linear. When the obtained result is divided by the difference between the experimental and the linear creep values, the nonlinearity is attained thanks to the misoscopic model. So, the percentages of the nonlinearity predicted by the mesoscopic approach are equal to 77.2%, 69.4% and 66.3% for the loading levels of 10.5 MPa, 15 MPa and 19.5 MPa, respectively.

Figure (3.3) shows that, a difference between the mesostructure simulation results and the experimental results still remains. This difference could be attributed to three facts. Firstly, when concrete is loaded in compression, the microcracks occur due to shear stress and tensile stress (Poisson ratio effect). As the adopted model Benboudjema and Torrenti (Benboudjema and Torrenti, 2008) does not compute the development of shear damage till the failure, there will still be a part of microcracks effect on increasing creep which does not be taken into account. Secondary, assuming an elastic damage model (damage due to expansion) is perhaps not sufficient. So, the plastic strains that probably occur could also explain the remaining difference in creep strains amplitude. The third reason is related to that the simulation was achieved in two dimensions. For the case of tensile creep, modelling in two

dimensions is appropriate because cracks are globally perpendicular to the loading axis, inversely in compression case, the crakes pattern occurs in three dimensions. Nevertheless, simulating creep in three dimensions by using viscoelastic and damage models is very heavy with applying fine mesh. The problem could be solved by using coarse mesh but in this case, representation of the fine aggregate becomes impossible.

It is worth noting that the use of a mesoscopic mesh allows retrieving a part of the nonlinearity with respect to loading level without having to introduce coupling between creep and damage. Although these mesoscopic simulations are based on simple assumptions as the form of aggregate (circular), a 2D plane strain state and the absence of Internal Transition Zone (ITZ), it is observed that for the loading level of 65% the percentage of nonlinearity due to the strain incompatibilities and associated damage is about 66%.

3.2.4 Direct Tensile Creep Results

Figure (3.4) represents numerical and experimental results of Illston (Illston, 1965) for two levels of stress/strength ratio in tension (50% and 75%). As for creep in compression, the parameters of the numerical model were calibrated for the lowest loading level and the mechanical properties were calibrated with the ordinary cement paste values of Nguyen et al. (Nguyen et al., 2010). According to the concrete properties the loading levels which correspond to the above loading levels are (1.4 MPa and 2.1 MPa).

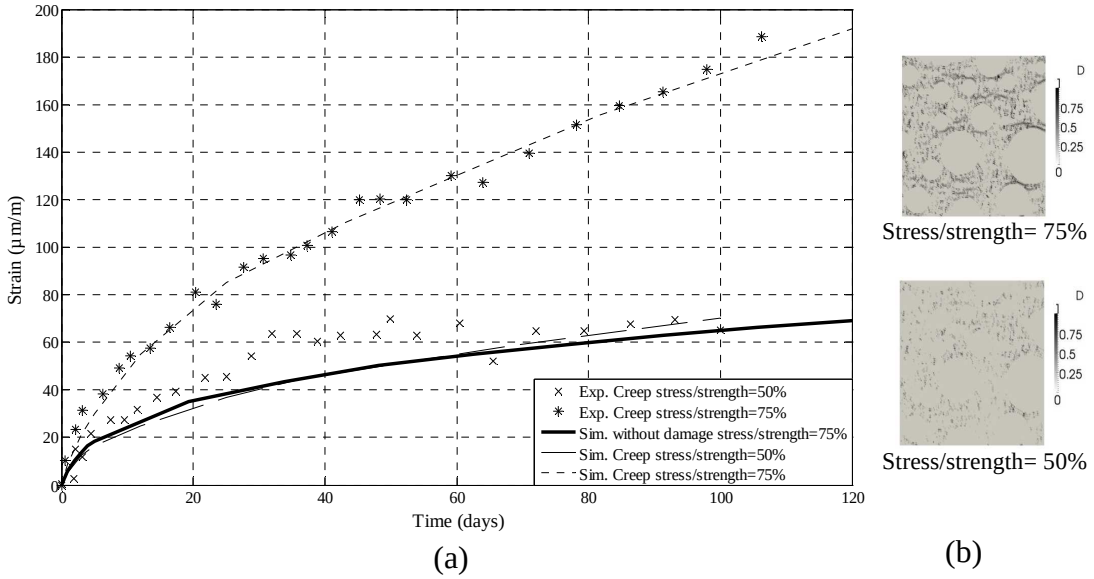

Figure (3.4): (a) Direct tensile creep throughout the time, (b) Field of damage

Figure (3.4) and Table (3.3) show that for the same tensile loading level, results of creep simulation without damage are much lower from those of experiments while the results of simulation with damage are close to the experimental ones.

Table (3.3): Comparison of the experimental tensile creep results (Illston, 1965) with those of mesoscopic approach with and without damage

Loading level		Exp. results (ε_{exp}) 10^{-6}	With damage		Without damage		Nonlinearity %
MPa	$\sigma/\sigma_{1.42}$		Sim. results (ε_{wd})	sim/ $sim_{1.42}$	Sim. results (ε_{wod})	sim/ $sim_{1.42}$	
2.13	1.5	190 at 112 days	184	2.62	76	1.54	95.3
Nonlinearity% = $100 \times (\varepsilon_{wd} - \varepsilon_{wod}) / (\varepsilon_{exp} - \varepsilon_{wod})$							

As for compressive creep, in the case where there is no damage, the relation between the stress and the creep is linear. The mesoscopic approach reveals the nonlinearity between the creep strain and the applied load. The percentage of the nonlinearity due to the mesoscopic approach increases up to 95.3% for a loading level of 75%.

3.2.4 Stress-Strain Results

Figures (3.5), (3.6), (3.7) and (3.8) show the relationship between strain and stress obtained from the tensile or compressive strength test on a mesostructure for 3 situations in tension and 5 in compression as presented in Table (3.4).

Table (3.4): Stress/strength ratios used in a mesostructure simulations that are presented in section 3.2.3 and 3.2.4

Type of the test	Tensile strength			Compressive strength				
Creep loading level (%)	Before creep	50	75	Before creep	25	35	50	65
Creep loading duration (days)	-	100	120	-	250	250	250	250

The initial damage fields of simulations “after creep” are the damage fields obtained at the end of creep simulations. The mechanical model presented before does not allow failure due to shear stress because the residual shear stress does not tend to 0 MPa. Thus, for simulating the stress-strain relation for concrete before and after creep, the damage model

developed by Fichant et al. (Fichant et al., 1999) is used. This model with the parameters used allows obtaining shear stress which tends to zero when the deformation reaches to the value corresponding to the maximum shear strength. Moreover, this model is based on damage enabling the use of the damage field, displacement field and stress field identified at the end of numerical creep test.

Figure (3.5) displays the constitutive law for tensile behavior, both before and after creep in compression for several percentages of loading levels (from 25% to 65% of the compressive strength). That means the initial value of damage and displacement of the instantaneous behavior is the one of the last time step of the creep simulations to a stress level of 25% or 65%.

Figure (3.5) and Table (3.5) reveal that the maximum resistance and that the Young's modulus for the specimens under higher loading levels is lower than those which were under lower loading levels. As it is presenting in Table (3.5), the decrease in the resistance varies from 15.5% (for the loading of 7.5 MPa) to 40.6% (for 19.5 MPa) relatively to the specimens that were not subjected to the creep test. Likewise, the Young modulus decrease varies from 17.3% (for the loading of 7.5 MPa) to 78.2% (for the loading of 19.5 MPa), with respect to the specimens which were not subjected to the creep test. That result is related to the damage which occurs during the creep loading and increases with increasing the level of this loading.

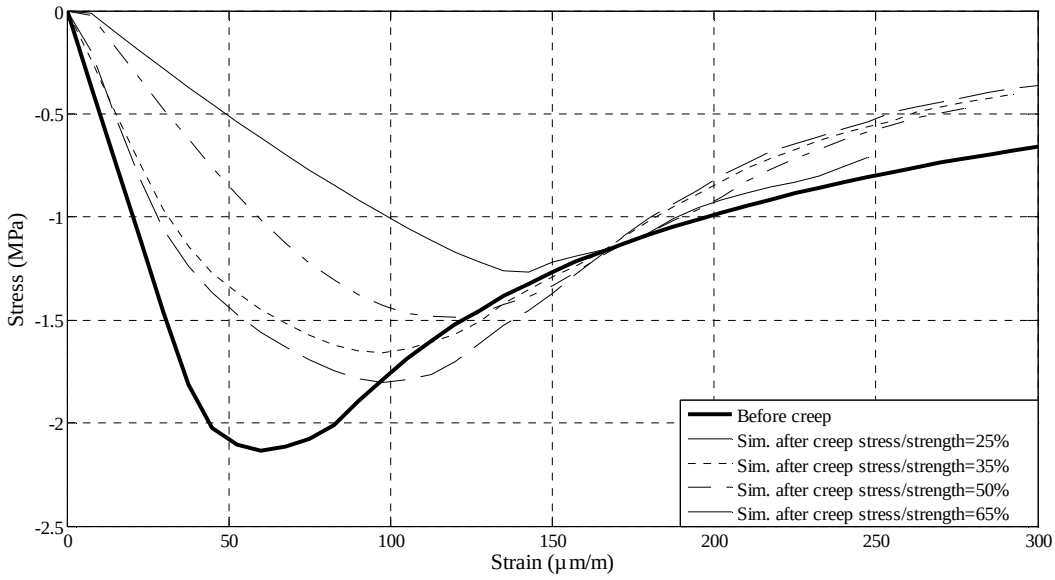

Figure (3.5): Mesoscopic unilateral behavior in tension before and after creep in compression

Table (3.5): Changes of the mechanical properties after creep test

Loading level for creep test		Loading in tension after creep test				Loading in compression after creep test			
		Ft_{max} MPa	Ft % (*)	Et GPa	Et % (*)	Fc_{max} MPa	Fc % (*)	Ec GPa	E % (*)
Creep in compression	Before creep	2.1	----	48.8	----	34.4	----	48.7	----
	7.5MPa	1.8	15.5	40.4	17.3	34.2	0.7	48.6	0.3
	10.5MPa	1.7	22.3	32.7	32.9	33.7	2.1	48.1	1.2
	15MPa	1.5	30.3	19.2	60.7	32.7	4.8	44.3	9.0
	19.5MPa	1.3	40.6	10.8	77.9	29.8	13.4	36.5	25.1
Creep in tension	Before creep	2.1	----	48.8	----	34.4	----	48.7	----
	1.4MPa	2.1	0.2	47.7	2.4	35.1	-2.0	48.7	0.1
	2.1MPa	2.1	1.8	43.0	12	34.9	-1.5	48.7	0.01
(*) % of decrease (Ft, Fc, Et, Ec) = 100× (value before creep - value after creep)/ value before creep									

Figure (3.5) shows that, the ductility increases as the compressive creep loading level increases. This result is in accordance with the results obtained by Heinfling et al. (Heinfling et al., 1998) and Briffaut et al. (Briffaut et al., 2013). This increase is explained by the fact that the damage location is distributed in the whole mesostructure during the creep test whereas the tensile strength test generates mainly a localised macrocrack. As the amount of damage is directly related to the loading level, the concrete which was under higher creep loading level includes more damage than that which was under lower one. As a result, the amount of cracking energy that is released during tensile strength test is higher for the concrete specimens that were under higher creep loading levels.

Figure (3.6) shows the effect of creep in tension on the evolution of the tensile behavior. It represents the behavior law of the tensile strength test after creep in tension had taken place for different creep loading levels. From Table (3.5) it could be remarked that the maximum

resistance is about the same before and after loading. Even though, the specimens that were under high creep loading levels, the Young modulus is slightly lower than the others. Compared to the specimens that were not subjected to any creep test, the percentage of decrease in resistance is 0.2% for the loading level of 1.4 MPa and 1.7% for the loading level of 2.1 MPa while the decrease in Young modulus is 2.4% and 12%, respectively.

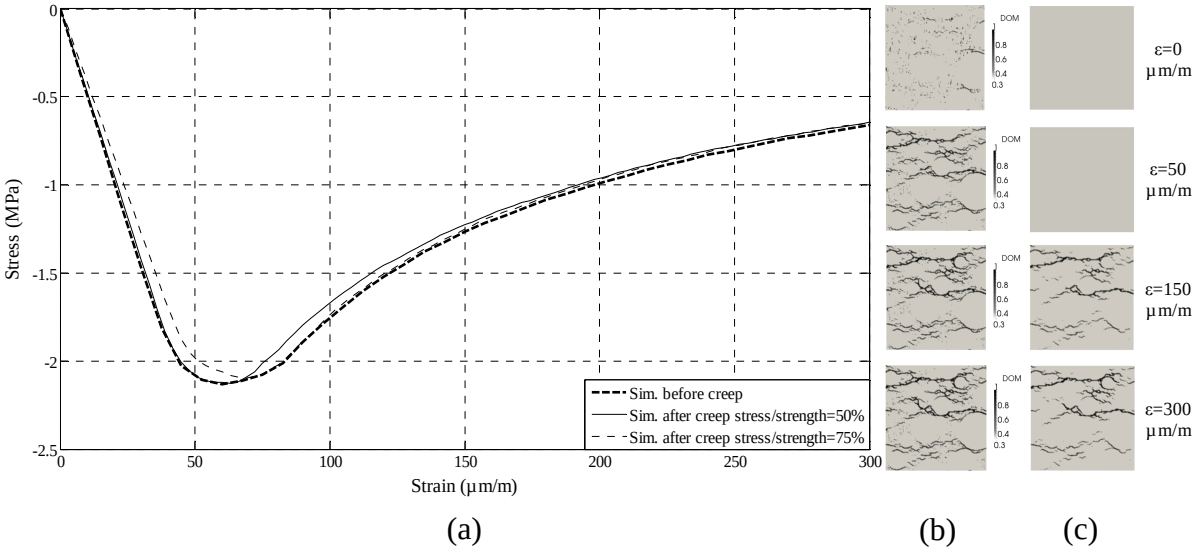

Figure (3.6): (a) Mesoscopic unilateral behavior in tension before and after creep in tension, (b) Field of damage after creep of level 75%, (c) Field of damage before creep

Figure (3.7) represents the compressive behavior both before and after creep in compression had taken place. This figure and Table (3.5) reveal that the maximum strength and the Young modulus are lower for the concrete specimens that were under high creep loading levels. Comparing with the specimens that were not subjected to creep test, the decrease in the resistance for specimens that were under creep loading of 7.5 MPa and 19.5 MPa is equal to 0.7% and 13.4% while the decrease in the Young modulus is equal to 0.4% and 25.1%, respectively.

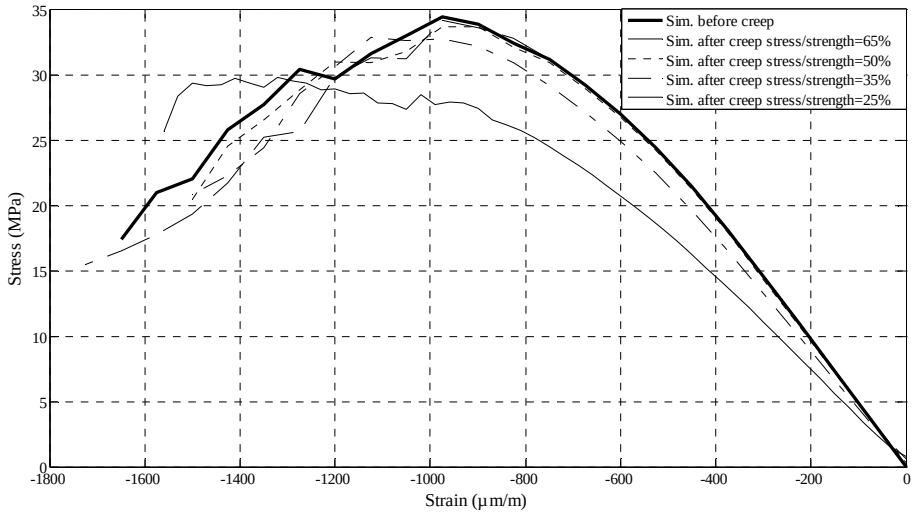

Figure (3.7): Mesoscopic unilateral behaviour in compression before and after creep in compression

Figure (3.8) shows the behavior law of a compressive test both before and after creep in tension had taken place. It is noticed that the maximum resistance in compression and Young modulus are almost the same for all the creep loading levels (see Table (3.5)).

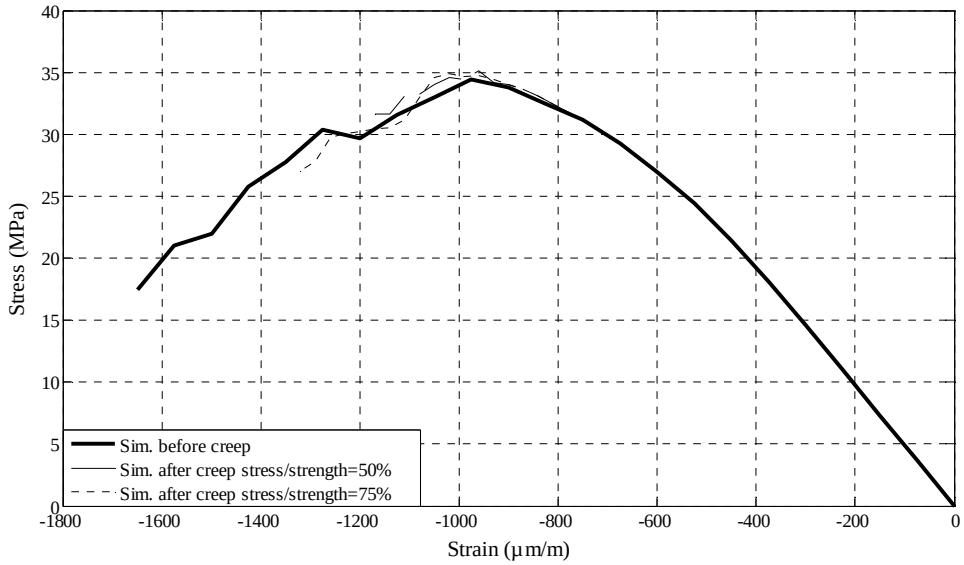

Figure (3.8): Constitutive law - compressive test before and after creep in tension had taken place

3.3 Simulation and Results of Indirect Tensile Creep test (Brazilian Creep)

To evaluate the magnitude of indirect tensile creep stains that were experimentally measured, the Brazilian creep strains were simulated and then the results were compared with the experimental ones. Firstly, the stress-strain relation of Brazilian test was simulated and the materials parameters were changed to obtain a tensile strength value that is close to the value

obtained in the experimental work. The average value of ultimate tensile strength of indirect tensile tests that achieved thought out the experimental work on the sound concrete and at age of 1 month was 3.5MPa. Obtaining the value of 4.2MPa from the numerical simulation model is satisfied since the results of the Brazilian test is very scattered (from 2.7MPa to 4.7MPa).

The second step was to calibrate the creep parameters. The compressive creep strain of the concrete used in experimental work of this study was simulated using the model of Benboudjema and Torrenti (Benboudjema and Torrenti, 2008). Then parameters of creep were calibrated by comparing the compressive creep simulation results with those of experimental for loading level of 80% applied at the age of 3 months (see Figure (3.9)). Figure (3.10) represents the field of damage at the end of compressive creep test.

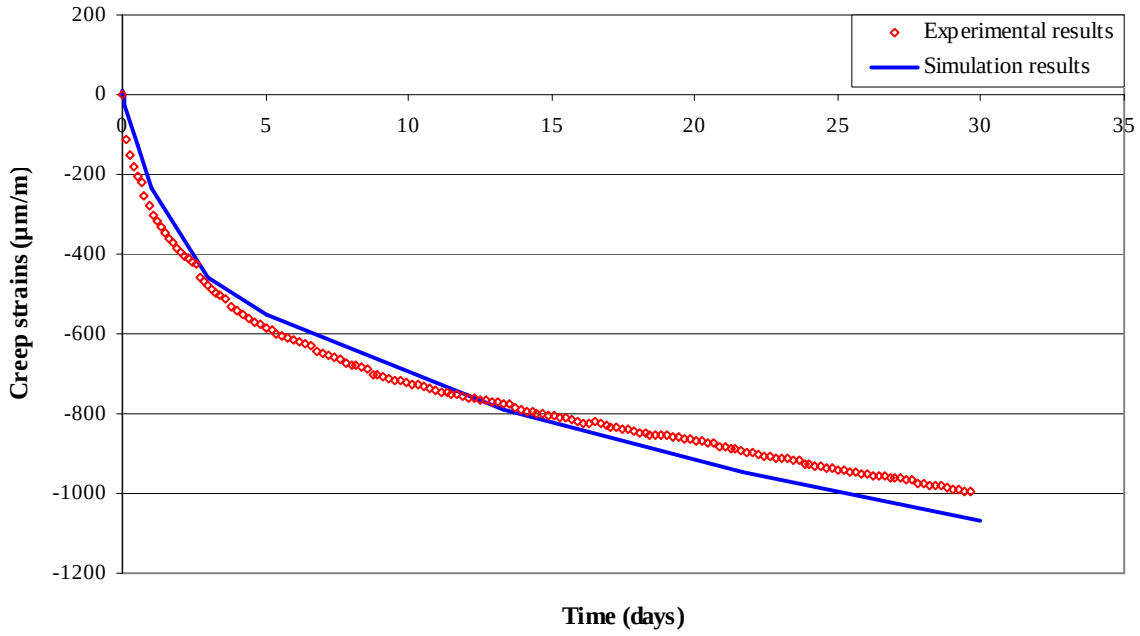

Figure (3.9): Calibrating the compressive creep simulation with those of experimental

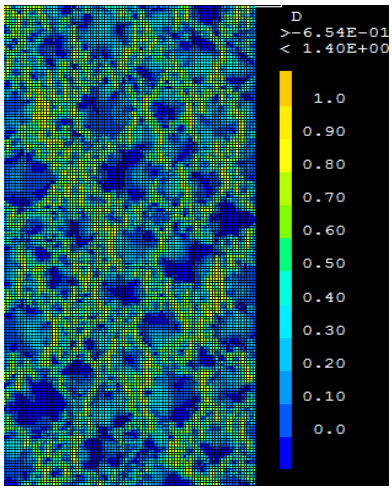

Figure (3.10): Field of damage due to compressive creep

Thereafter, the obtained creep and material parameters were used for simulating the indirect tensile creep (Brazilian creep) by using the model of Benboudjema and Torrenti (Benboudjema and Torrenti, 2008). Figure (3.11) represents the numerical and experimental results of Brazilian creep for loading levels of 50% and 80%.

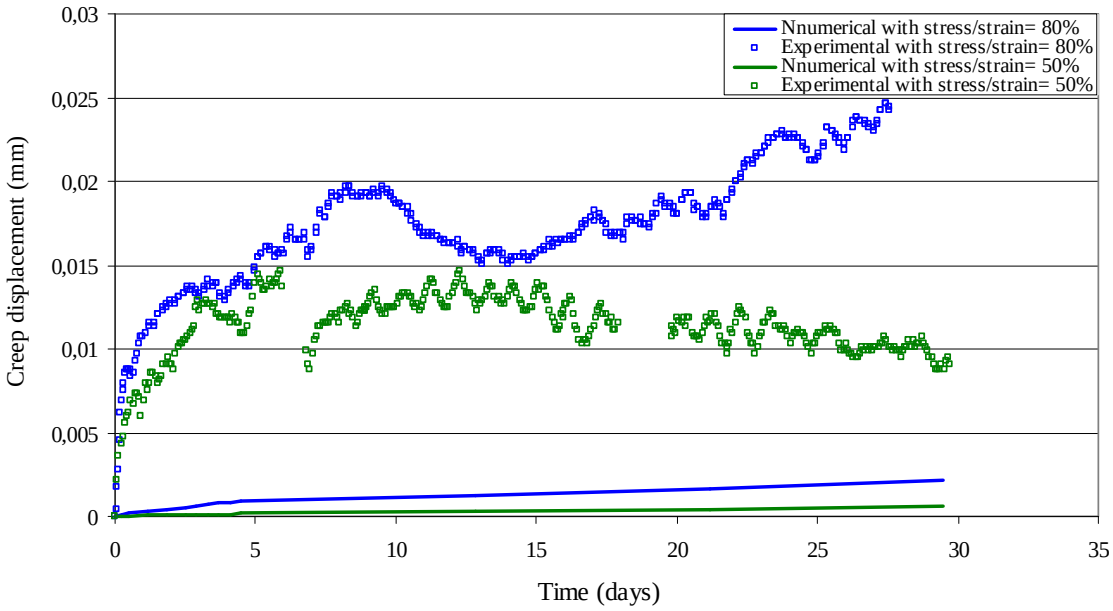

Figure (3.11): Numerical and experimental results of Brazilian creep vs. time for loading levels of 50% and 80%

It is clear that for the both loading levels (50% and 80%) the difference between the simulation and the experimental results is important. This difference may be due to experimental and/or numerical defects. The load in the Brazilian strength test is applied on a cylindrical specimen arranged laterally (its axis is perpendicular to the applied load). This test is considered delicate as there is an occasion that the cylindrical specimen roles. Therefore,

for the Brazilian creep test where 3 cylindrical specimens are used, the test is much more sensitive. In addition, the defect may be related to the displacement transducer used to measure the displacement during the creep Brazilian test. In this apparatus, a strain gauge is fixed on a metal which has an arch shape and its two ends are glued on the concrete i.e. the strain gauge is not glued directly on the concrete (see Figure (2.34) in chapter two). The arch metal, on which the strain gauge is fixed, is sensitive to the temperature which is clear from the zigzag observed on the experimental results in spite of performing the test in a control room. Numerically, the principal of creep model used in this study depends on applying stress on the series of Kelvin-Voigt for obtaining creep strain. Consequently, the same strain magnitude is obtained if the stress is applied in compressive or in tensile direction and so that may be not completely right. In addition, as the simulation was achieved in two dimensions, the microcracks that occur in the third direction could not be taken into account. So, for the Brazilian creep test where a compressive load is applied, simulating the indirect creep strain is not precise.

Figure (3.12) represents the numerical simulations of the Brazilian creep for the both loading levels (50% and 80%). Figures (3.13) and (3.14) show the field of damage at the end of Brazilian creep test for the loading levels of 50% and 80%, respectively.

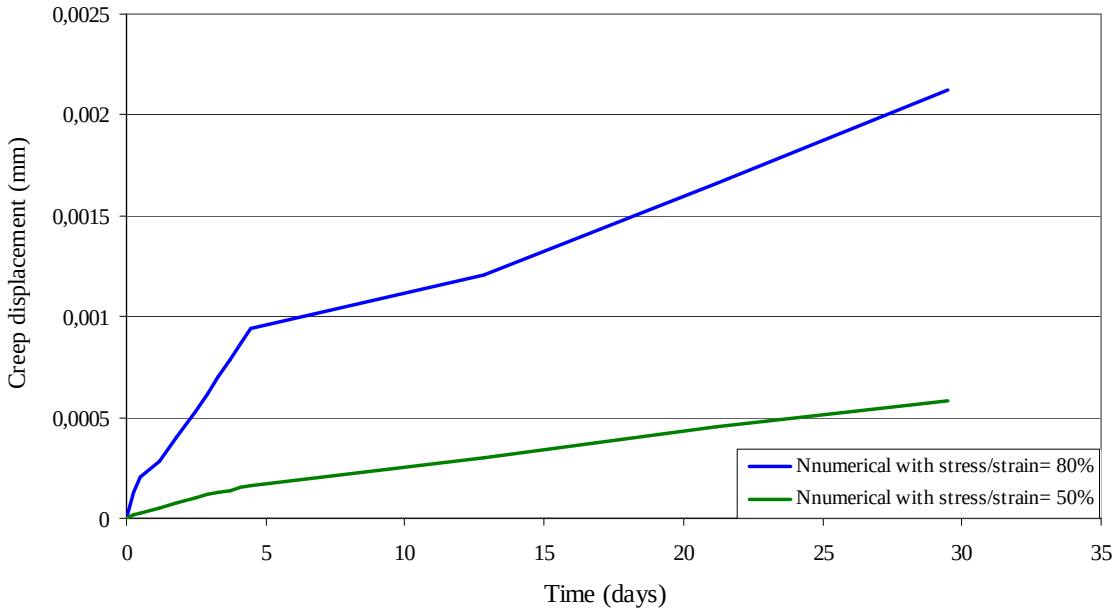

Figure (3.12): Numerical results of Brazilian creep vs. time for loading levels of 50% and 80%

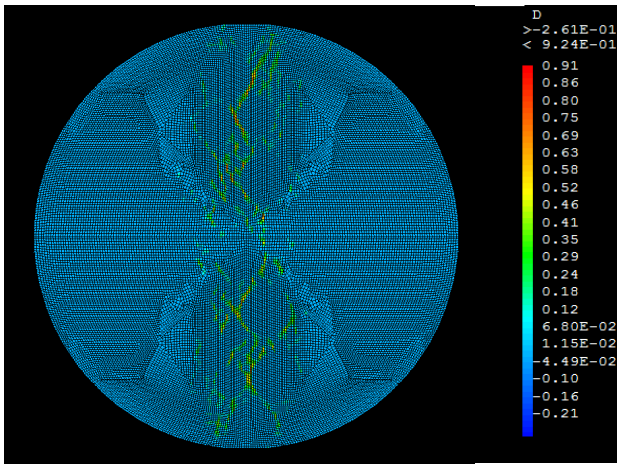

Figure (3.13): Field of damage due Brazilian creep for loading level of 50%

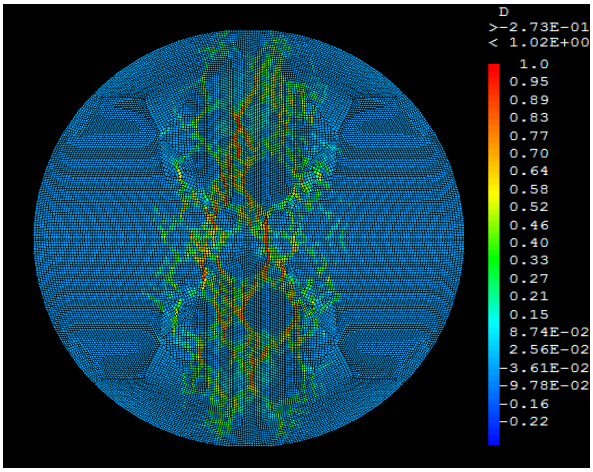

Figure (3.14): Field of damage due Brazilian creep for loading level of 80%

It is clear from Figure (3.12) that the creep values are not linear with respect to the loading levels. That means that the model is able to simulate the nonlinearity that occurs due to the increase of damage at the aggregate-cement paste interface. Figures (3.13) and (3.14) give the evidence that the damage due to loading level of 80% is much larger than that of 50%.

In this chapter, mesoscopic model was developed for simulating creep strain in compression and tension for different loading levels. In addition, for verifying creep effect on the residual mechanical properties, these the last were simulated before and after creep. The aim from these simulations was to represent effects of microcracks that generate due to the local incompatible strain between cement paste and aggregate. The results of mesoscopic simulations that were used are as follows:

- Significant nonlinearity between the creep strains and stress rate. For compressive creep strain the nonlinearities were 77.2%, 69.4% and 66.3% for loading levels 35%, 50% and 65%, respectively (see Table (3.2)). As well, nonlinearity for loading level of 75% was 95.3% (see Table (3.3)).
- This microcracks appear to have an impact on the residual mechanical properties of concrete. The decrease in the compressive strength due to compressive creep, comparing with the unloaded specimens, was varied from 0.7% to 13.4% while the elastic modulus was ranging from 0.4% to 25.1%, for compressive creep loading level of 35% and 65%, respectively. As well, the decrease in the tensile strength due to compressive creep load was ranging from 15.5% to 40.6% and elastic modulus was from 17.3% to 78.2% for loading level of 35% and 65%, respectively (see Table (3.5)).
- It could say that, the tensile creep strain result has almost no effect on the residual mechanical properties of concrete except for loading level of 75%, the decrease in the elastic modulus was 12% (see Table (3.5)).
- After calibrating the creep and the material parameters according to the experimental results, a numerical simulation of Brazilian creep test was done and the results were compared with those of experimental Brazilian creep tests. For both loading levels (50% and 80%), it was clear that the numerical results are very far from the experimental ones (see Figure (3.11)). The reason may be related to the fact that the Brazilian creep test is difficult to control. The reason may be also related to the numerical model that assumes the deformation due to the applied stress is the same if the stress is applied in the tensile or in the compression direction. Moreover, the simulation was done in two dimensions, so the microcracks that occur in the third direction could not be taken into account. Therefore, for the Brazilian creep test where a compressive load is applied, simulating the indirect creep strain is not precise.

CONCLUSION

The aim of this thesis is to study the change of mechanical properties of concrete due to creep effect, experimentally and numerically. The experimental work was carried out to overcome the lack of available information on this topic in literatures. Chapter two which concerns experimental work includes creep tests in tension and in compression at different loading levels and at different concrete ages. At the end of each test, either a compressive strength test or an indirect tensile strength test (Brazilian test) was done both on creep and control specimens for highlighting the creep effect on the residual mechanical properties of concrete. The following points were concluded from the obtained results:

- For the same compressive relative loading level, creep strains increase with increasing the age of loading.
- For young age of loading (1 month), the compressive strength and the modulus of elasticity of creep specimens are larger than those of control specimens. Inversely, for late age of loading (3 months), creep specimens have lower compressive strength than those of control specimens while the modulus of elasticity value is about the same for creep and control specimens.

The justification given for the both previous conclusions was related to the age of loading linked to the continuity of the hydration process. With the availability of free water the hydration process continue, resulting in filling up the pores of cement paste by cement hydrated products. Therefore, when concrete is loaded at late ages, there will not be enough spaces for the water and the cement gel to diffuse from their narrow places to wider spaces inside the cement skeleton. Thus, the energy induced by these moving particles on the hardened cement paste will provoke microcracks. Due to these microcracks, there will be an increasing in creep strains, and decreasing both in compressive strength and in elastic modulus. On contrary, when concrete is being loaded at young ages, the applied load promotes the cement gel to move from its place to a wider place to fill up the pores inside the cement paste. Consequently, the size of concrete specimen becomes smaller and denser than that which was not subjected to creep loading. As a result, the dense specimens (creep specimens) reveal higher resistance than those which are less dense (control specimens).

In addition, in concrete under sustained loading levels, cement paste creeps while aggregate acts as an obstacle. So, tensile stresses arise at aggregate-cement paste interface leading to microcracks at this zone that participate in decreasing the compressive strength of creep specimens. At mesoscopic scale, as the flow of cement gel and water is more accessible

at young age than that at late age, the concentration of stresses at the aggregate-cement paste interface for new concrete may be relaxed faster than those for old concrete. Therefore, the microcracks at the aggregate-cement paste interface for new concrete are expected to be less than those for old concrete.

It could be added that, the microcrack that occur due to creep will generates new path for the hydration process to continue and that may decrease the width of the microcrack. As the unhydrated cement in new concrete is expected to be more than in old concrete, the hydration process is more active in new concrete. That leads to, that the concrete loaded at young age has less microcracks (or at least thinner width of microcracks) comparing with the concrete loaded at late ages.

The tomographic scan gave evidence that creep specimens that were loaded at age of 1 month with loading level of 65% are sound and free from visible cracks.

Furthermore, a Brazilian strength test was carried out at the end of compressive creep test in which the loading level was 80%. This test was achieved to simulate the tensile zone of structural beam that is subjected to prestress loading. When the prestress load is applied, the main part of the section of a beam is under compressive stress. Afterward, due to the stress relaxation and to the applied load, tensile stresses could take place. The results revealed that the compressive creep has no significant effect on the tensile strength as the creep and the control specimens have about the same tensile strength.

To check the effect of compressive creep on the tensile strength and distinguish this effect from that of quasi-instantaneous loading, 3 tests of quasi-instantaneous preloading in compression were carried out up to three different specified loading levels. The results revealed that, the compressive preloading level of 80% has no effect on the concrete tensile strength while higher preloading levels have negative effects on the concrete tensile strength. When the compressive load is applied up to a high loading level, microcracks will appear in the direction parallel to the applied load. Intuitively, these microcracks increase as the applied loading level is increased until it reaches the level of failure (loading level equal to 100%). So, when the specimen is subjected to the Brazilian test after the quasi-instantaneous compressive loading test, the preloaded specimens show lower resistance than the unloaded specimens.

In addition, the apparent Poisson’s ratio was calculated throughout compressive creep tests. Among the results of the creep Poisson’s ratio which are inhomogeneous, results of two cases become stable after several days of loading to have about the same value (0.2 for loading at age of 1 month at level 65% and 0.18 for loading at age of 3 months at level 80%).

These values of creep Poisson's ratio are similar to those of Poisson's ratio (calculated within the elastic range) of current work (between 0.18 and 0.23).

Finally, indirect tensile creep tests were carried out by applying the load on three specimens together. The application of load on the specimens is similar to the Brazilian test by replacing the one cylindrical specimen with three specimens. So, an apparatus was designed and fabricated in 3SR laboratory for holding the three specimens together throughout the creep test and for preventing eccentricity between them. The test was very sensitive and needed to a lot of accuracy. It was very difficult to prevent errors coming from the slip of specimens after the loading application and from the release of the screws of the apparatus that were holding them. The displacement transducer used for measuring the displacement throughout the test is not sensitive enough as it is not glued directly on the concrete but it is fixed on an arch shape metal, which is sensitive to the temperature, and their two ends are glued on the concrete.

The effect of tensile creep on the tensile strength evolution was measured as follows:

- For low loading level (50%), the creep specimens have higher tensile strength than those of control specimens while for loading level of 80% and 90%, the tensile strength was about the same for the creep and control specimens.

As it was justified for the effect of compressive creep, at rather low tensile loading level the applied sustained load works on moving the cement gel particles from their narrow spaces to larger spaces resulting in concrete more dense. At the same time, microcracks could appear in the direction of tensile stress i.e. in the lateral direction (due to Poisson's ratio). So, when concrete is being loaded at a higher level, the negative effect of microcracks perhaps becomes equivalent to the useful effect of gel flow inside the pores.

Numerically, a mesoscopic model was used to show the effect of microcracks at the aggregate-cement paste interface with increasing creep strain values and to show that the heterogeneity of concrete could be the main cause of nonlinearity between creep strain and loading level. Another objective was to represent the participation of these microcracks in the decrease of the elastic modulus and of the concrete strength. Creep in tension as well as in compression were simulated then the residual mechanical properties before and after creep were also simulated. The following could be concluded from the mesoscopic simulations results:

- Considerable nonlinearity is remarked between stress rate and creep strains whether in tension or in compression.

- For numerical point of view, damage appears to have a negative effect on the residual mechanical properties of concrete as the compressive strength, the tensile strength and the elastic modulus were decreased after compressive creep. However, tensile creep has nearly no effect on the residual mechanical properties of concrete except for the higher loading level (75%), the elastic modulus was slightly decreased (12%).

  These results are not conformed with the experimental ones and that may be related to that the aggregate was supposed to be round in the mesoscopic simulation which is not similar to the experimental work where the angular aggregate was used. In addition, the simulation used in this study depends on the deformation in two directions. The simulation is acceptable for tensile case as the cracks occur in the direction perpendicular to the applied load but for compressive case the model is not adequate, as the cracks may occur in three directions. Therefore, the simulation needs to be modified.
- The creep and the material parameters were calibrated according to the experimental results of this study. After that, the numerical simulation of Brazilian creep was achieved and then the results were compared with those of experimental Brazilian creep tests. The numerical results are very far from those of experimental. The reason could be related to the fact that the Brazilian creep test is very difficult to control perfectly and depends a lot on boundary conditions.

Perspectives

The actual study includes two parts; experimental and numerical. The recommendations that are given here could enrich the present subject in the future.

1. Experimental recommendations

- It had been planned that creep tests are carried out at two loading ages (1 month and 3 months) for each loading level. Due to an experimental error, the high loading level of 80% at age of 1 month was replaced by 65%. So, it is better to carry out the creep test for the same high loading level at different ages of loading to better compare the results.
- To check the soundness of concrete after creep test, it is valuable to use both, the tomographic technique and the permeability test.
- The results of indirect strength test (Brazilian test) are very scattered so more tests should be achieved to check the results obtained from this actual work.

- The designed apparatus for holding the specimens throughout the Brazilian creep test must be improved to obtain more accurate results. For instance, make a slot along and at the middle the bottom plate in which, one of the plywood pieces used for the Brazilian creep test could be placed. Hence and at least, it becomes sure that the plywood piece that is placed at the base, still fixed during the test.
- Only one test was carried out to check the effect of compressive creep on the tensile strength (by using the Brazilian test). So, more tests are needed with different ages of loading and different loading levels.
- It will be useful to make an experimental test for new and old concrete that were unloaded in creep and that were subjected to creep loading to calibrate the amount of hydrated cement. If the difference in the amount of hydrated cement between unloaded concrete and the loaded one for concrete loaded at young age is more than that for concrete loaded at late age, the proposal of that microcracks provide a new path for continuing the hydration process is more active in new creep concrete than that for the old one would be confirm.

2. Numerical recommendations

- Simulation creep and stress/strain relation in tension could be done in 2 dimensions because cracks are globally perpendicular to the loading axis. For the case of compression, the cracks pattern is of 3 dimensions. So, there will be an error if it is calculated in 2 dimensions. Nevertheless, 3 dimensions simulation with viscoelastic model and damage are very heavy with a fine mesh. With a coarse mesh, it is possible but the representation of the finer aggregate becomes impossible. Therefore, the model could be developed by taking into account the 3 dimensions if there is enough computer power.
- An explicit representation of the aggregate strongly increases the number of element for representing correctly fine aggregate. As it is presented in Nguyen et al. (Nguyen et al., 2011), the representation of fine aggregate is essential when simple behavior law is considered for cement paste and aggregate. Even though, an aligned mesh i.e. the elements lines are located at the interface, should be simulated and then compare the results with those of a regular grid.
- The mesoscopic model must be developed to take into account the effect of creep loading age on the development of residual mechanical properties of concrete.
- The mesoscopic simulation should be developed for angular aggregate (as it is used in the actual experimental work) and compare the results with perfectly round aggregate. This step is important to check the effect of shape on the stresses concentration at the aggregate-cement

paste interface and subsequently the opportunity of microcracking occurrence at this zone. In addition, different arrangements of aggregate inside the cement paste is recommended to be studied, to know their effect on creep magnitude and on the residual mechanical properties of concrete.

REFERENCES

ACI Committee 209, “Effect of Concrete Constituents, Environment and Stress on Creep and Shrinkage in Concrete Structures”, Paper SP 27-1,in ACI Special Publication SP-27, “Designing for Effect of Creep and Shrinkage in Concrete Structures”, 1992.

Al-Rawi, R.S. and Al-Qassab, F.F., “Control of Shrinkage Cracking in Continuously Reinforced Concrete Pavements”, Presented at ACI Fall Convention, Vancouver, September, 1986.

Asamoto, S., Kato, K. and Maki, T., “Effect of creep induction at an early age on subsequent prestress loss and structural response of prestressed concrete beam”, Construction and Building Materials Vol. 70, November 2014, pp. 158-164.

Atrushi, D.S., “Tensile and Compressive Creep of Early Age Concrete: Testing and Modeling”, Thesis Submitted to The Norwegian University of Science and Technology for Ph.D. Degree, Trondheim, Norway, March 2003.

Bazant, Z. P., ‘‘Viscoelasticity of solidifying porous material concrete’’, Journal of the Engineering Mechanics Division, Vol. 103, No. 6, 1977, pp. 1049-1067.

Bazant, Z.P. and Panula L., “Practical Prediction of Time-Dependent Deformations of Concrete”, Materials and Structures, RILEM, Part (1)- Shrinkage and Part (2)-Basic Creep: Vol.11, No.65, Sep.-Oct. 1978, pp. 307-328; Part (3)-Drying Creep and Part (4)-Temperature Effect on Basic Creep: Vol. 11, No.66, 1978, pp. 415-434; Part (5)-Temperature Effect on Drying Creep: Vol.12, No.69, 1979, pp. 169-182.

Bazant, Z.P. and Prasannan, S., “Solidification Theory for Concrete Creep. I: Formulation”, Journal of Engineering Mechanics, ASCE, Vol. 115, No. 8, August 1989, pp. 1691-1703.

Bazant, Z., Hauggaard, A., Baweja, S., and Ulm, F., “Microprestress-Solidification Theory for Concrete Creep. I: Aging and Drying Effects”, Journal of Engineering Mechanics, Vol. 123, No. 11, November 1997, pp. 1188-1194.

Benboudjema, F., “Modelisation des deformations differees du beton sous sollicitations biaxiales.application aux enceintes de confinement de batiments reacteurs des centrales nucleaires”, Thesis Submitted to University of Marne la Vallée for Ph.D. Degree, France, 2002.

Benboudjema, F., Torrenti and J.-M., “Early-age behavior of concrete nuclear containments, Nuclear Engineering and Design”, Nuclear Engineering and Design, Elsevier, 2008, pp. 2495-2506.

Bentz, D., “Three-dimensional computer simulation of portland cement hydration and microstructure development”, Journal of the American Ceramic Society, Vol. 80, No. 1, 1997, pp. 3-21.

Bissonnette, B., Pigeon, M. and Vaysburd, A. M., “Tensile Creep of concrete study of its sensitivity to basic parameters”, ACI Materials Journal, Vol. 104, No. 4, July-August 2007, pp. 360-368.

Briffaut, M., Benboudjema, F., Torrenti, J.-M. and Nahas, G., “Numerical analysis of the thermal active restrained shrinkage ring test to study the early age behavior of massive concrete structures”, Engineering Structures, Vol. 33, No. 4, April 2011, pp. 1390-1401.

Briffaut, M., Benboujema, F., Torrenti, J.-M. and Nahas, G., “Concrete early age basic creep: Experiments and test of rheological modelling approaches”, Construction and Building Materials, Vol. 36, 2012, pp. 373-380.

Briffaut, M., Benboudjema, F., Laborderie, C. and Torrenti, J.-M., “Creep consideration effect on meso-scale modeling of concrete hydration process and consequences on the mechanical behavior”, Journal of Engineering Mechanics, Vol. 139, No. 12, December 2013, pp. 1808–1817

Brooks, J. J. and Neville, A. M., “A comparison of creep, elasticity and strength of concrete in tension and in compression”, Magazine of Concrete Research, Vol. 29, No. 100, September 1977, 131-141.

Browne, R. D. and Blundell R. , “ The influence of loading age and temperature on the long term creep behavior of concrete in a sealed, moisture stable, state”, Material and Construction, March-April 1969, Volume 2, No. 8, pp. 133-143.

Bryant, A.H. and Vadhanavikkit, C., “Creep, Shrinkage,- Size and Age at Loading Effects”, ACI Materials Journal, Vol.84, No.2, March-April 1987, pp. 117-123.

Cast3M finit element code, Commissariat à l'Energie Atomique CEA-DEN/DM2S/SEMT, available at http://www-cast3m.cea.fr/

CEB-FIP, “Model Code for Concrete Structures”, Comité Euro-International du Béton, Paris, 1998.

Cervera, M., Oliver, J. and Prato, T., “Thermo-chemo-mechanical model for concrete. I: hydration and aging”, Journal of Engineering Mechanics, Vol. 125, No. 9, September 1999, pp. 1018-1027.

Charpin, L., Le Pape, Y., Coustabeau, E., Masson, B. and Montalvo, J., “EDF Study of 10-years concrete creep under unidirectional and biaxial loading: evolution of poisson coefficient under sealed and unsealed conditions”, Paper of Concreep Conference, September 2015.

Counto, U. J., "The effect of the elastic modulus of the aggregate on the elastic modulus, creep and creep recovery of concrete", Magazine of Concrete Research, Vol. 16, No. 48, September 1964, pp. 129-138.

De Larrard, T., “Variabilité des propriétés du béton : caractérisation expérimentale et modélisation probabiliste de la lixiviation” , Thesis Submitted to ENS Cachan for Ph.D Degree, Paris, France, 2010.

De Sa, C., Benboujema, F., Thiery, M. and Sicard, J, “Analysis of microcracking induced by differential drying shrinkage”, Cement and Concrete Composites, Vol. 30, No. 10, November 2008, pp. 947-956.

De Schutter, G. and Taerwe, L., “Towards a more fundamental non-linear basic creep model for early age concrete”, Magazine of Concrete Research, Vol. 49, No. 180, September 1997, pp. 195-200.

De Schutter, G., “Degree of hydration based Kelvin model for the basic creep of early age concrete”, Materials and Structures, Vol. 32, May 1999, pp. 260-265.

Domone, P. L, “Uniaxial tensile creep and failure of concrete”, Magazine of Concrete Research, Vol. 26, No. 88, September 1974.

E. Cinlar, “Probabilistic approach to deformations of concrete”, in: Bazant Z.P., Wittmann F.H., “Creep and Shrinkage in concrete Structures”, Wiley, 1982, pp. 51-85.

Feyel, F., “A multilevel finite element method (FE2) to describe the response of highly non-linear structures using generalized continua”, Computer Methods in Applied Mechanics and Engineering, Vol. 192, No. 28-30, July 2003, pp. 3233-3244.

Fichant, S., “Endommagement et Anisotropie Induite du Béton de Structures: Modélisations Approchées”, Thesis Submitted to ENS Cachan for Ph.D Degree, Paris, France, 1996.

Fichant, S., La Borderie, C. and Pijaudier-Cabot, G., “Isotropic and anisotropic descriptions of damage in concrete structures”, Mechanics of Cohesive-Frictional Material, Vol. 4, No. 4, July 1999, pp. 339-359.

Galenne E., Foucault A., Hamon F., “Prediction of Delayed Strain of Nuclear Containment Building: from laboratory tests to an industrial mock-up”, International Conference on Technological Innovations in Nuclear Civil Engineering, Paris, 2013.

Giaccio, G., Rocco, C., Violini, D., Zappitelli, J. and Zerbino, R., “High-strength concretes incorporating different coarse aggregates”, ACI Materials Journal, Vol. 89, No. 3, May-Jun1992, pp. 242-246.

Grasley, Z. C. and Lange, D. A., “The viscoelastic response of cement paste to three-dimensional loading”, Mechanics of Time-Dependent Materials, Vol. 8, No. 1, 2007, pp. 27-46.

Grassl, P., Wong, H.S. and Buenfeld, N.R., “Influence of aggregate size and volume fraction on shrinkage induced micro-cracking of concrete and mortar”, Cement and Concrete Research, Vol. 40, No. 1, January 2010, pp. 85-93.

Grassl, P. and Pearce, C., “Mesoscale Approach to modeling concrete subjected to thermomechanical loading”, Journal of Engineering Mechanics, Vol. 136, No. 3, March 2010, pp. 322-328.

Grondin, F., Dumontet, H., Ben Hamida, A. and Boussa, H., “Micromechanical contributions to the behavior of cement-based materials: Two-scale modelling of cement paste and concrete in tension at high temperatures”, Cement and Concrete Composites, Vol. 33, No. 3, March 2011, pp. 424–435.

Gudmundsson J. G. “Long-term creep and shrinkage in concrete using porous aggregate – the effects of elastic modulus”, Master of Science in Civil Engineering, January 2013

Hansen, T. C. “Creep of Concrete. The Influence of Variations in the Humidity of the Ambient Atmosphere”, sixth IABSE congress report, Research Engineer, Swedish Cement and Concrete Research Institute at the Royal Institute of Technology, Stockholm, 1960.

Hansen, T. C. and Mattock, A. H., "Influence of size and shape of member on the shrinkage and creep of concrete", Journal of the American Concrete Institute, February 1966.

Hauggaard, A.B., Damkilde, L., Hansen and P.F., "Transitional thermal creep of early age concrete", Journal of Engineering Mechanics, Vol. 125, No. 4, April 1999, pp. 458- 465.

Heinfling, G., Stabler, J., Baker, G. and Reynouard, J.M., "Effects of high temperatures on the fracture energy of concrete", International Conference on Fracture Mechanics of Concrete Structures, FRAMCOS 3 (3rd), 1998.

Hilaire, A., "Étude des déformations différées des bétons en compression et en traction, du jeune âge au long terme", Thesis Submitted to the Superior College of Cachan for Ph.D. Degree, Cachan, France, 2014.

Hillerborg, A., Modeer, M. and Petersson, P. E, "Analysis of crack formation and crack growth in concrete by means of fracture mechanics and finite elements", Cement and Concrete Research, Vol. 6, No. 6, November 1976, pp. 773-781.

Hobbs, D.W., "The dependence of the bulk modulus, Young's modulus, creep, shrinkage and thermal expansion of concrete upon aggregate volume concentration", Materials and constructions, Vol. 4, No. 20, 1971.

Illston, J. M., "The creep of concrete under uniaxial tension", Magazine of concrete Research, Vol. 17, No. 51, June 1965, pp. 77-84.

Illston, J.M.. and Sanders, P.D., "The effect of temperature change upon the creep of mortar under tensional loading", Magazine of Concrete Research, Vol. 25, No. 84, September 1973, pp. 136-143.

Jordaan, I.J. and Illston J.M., "The creep of sealed concrete under multiaxial compressive stresses", Vol. 21, No. 69, December 1969, pp. 195-204.

Kammouna, Z., "Development of a mathematical model for creep of concrete with reference to Baghdad Climate", Thesis Submitted to University of Baghdad for M.Sc. Degree, Baghdad, Iraq, December 2001.

Kennedy, T., "An evaluation and summary of a study of the long-term multiaxial creep behavior of concrete", Department of Civil Engineering, University of Texas at Austin, 1975.

Kim, J. K., Kwon, S. H., Kim, S. Y. and Kim, Y. Y., “Experimental studies on creep of sealed concrete under multiaxial stresses”, Magazine of Concrete Research, No. 10, Vol. 57, December 2005, pp. 623-634.

Klinkenberg, L. J., “The permeability of porous media to liquid and gases”, in: Drilling and Production Practices, American Petroleum Institute, January 1941, pp. 200-211.

Lagier, F., Jourdain, X., De Sa, C., Benboudjema, F. and Colliat, J.B., “Numerical strategies for prediction of drying cracks in heterogeneous materials: comparison upon experimental results”, Engineering Structures, Vol. 33, No. 3, March 2011, pp. 920-931.

Lea, F. M. and Lee, C.R., “Shrinkage and creep in concrete”, Symposium on the Shrinkage and Cracking of Cementive Materials, Society of Chemical Industry, London, 1947, pp. 7-17.

Liniers A.D., “Microcracking of concrete under compression and its Influence on tensile strength”, Materials and Structures, 1987, Vol. 20, No. 2, pp. 111-116.

Liu, G.T., Gao, H. and Chen, F.Q., “Microstudy on creep of concrete at early age under biaxial compression”, Cement and Concrete Research Vol. 32, No. 12, December 2002, pp. 1865-1870.

Lohtia R.P., “Mechanism of creep in concrete”, Roorkee University Research Journal, 1-2 (12), 1970, pp. 37-47.

Loo, Y H and Base, G D, “Variation of creep poison’s ratio with stress in concrete under short-term uniaxial compression”, Magazine Of Concrete Research, Vol. 42, No. 151, 1990, pp. 67-73.

Mazars, J., “Application de la mécanique de l'endommagement au comportement non linéaire et à la rupture du béton de structure”, Thesis Submitted to ENS Cachan for Ph.D Degree, Paris, France,1984.

Mazars, J., “A description of micro- and macroscale damage of concrete structures”, Engineering Fracture Mechanics, Vol. 25, No. 5-6, 1986, pp. 729-737.

Mazars, J., and Pijaudier-Cabot, G., ‘‘Continuum damage theory-application to concrete.’’ Journal of Engineering Mechanics, Vol. 115, No.2, February 1989, pp. 345-365.

Mazzotti, C. and Savoia, M., "Nonlinear creep damage model for concrete under uniaxial compression", Journal of Engineering Mechanics, Vol. 129, No. 9, September 2003, pp. 1065-1075.

Meyers, B.L. and Slate, F.O., "Creep and creep recovery of plain concrete as influenced by moisture conditions and associated variables", Magazine of Concrete Research, Vol. 22, No. 70, March 1970, pp. 37-41.

Mortensen, C., Saiidi, M. and Ladkany, "Creep and Shrinkage Losses in Prestressed Concrete Bridges in Highly Variable Climates", WordTRB Annual Meeting CD-ROM, 2003.

Neville, A.M., Discussion of "The design, construction, and testing of a prestressed concrete reactor pressure vessil model", by Baker, A.L.L., et al., Proceeding, Institution of civel Engineers, London, Vol. 23, November 1962, pp. 495-496.

Nasser, K.W. and Neville, A.M., "Creep of Concrete at Elevated Temperature", ACI Journal, Proceedings, No.12, Vol.62, December, 1965, pp. 1567-1579.

Neville, A.M. and Diliger, W., "Creep of Concrete Plain, Reinforced and Prestressed", North-Holland, Publishing Company-Amsterdam, 1970.

Neville, A.M. and Brooks, J.J., "Concrete Technology", Pearson Educated Limitted, 2nd Edition, London, 2010.

Neville, A.M., "Properties of Concrete", Pearson Educated Limitted, 5th Edition, London, 2011.

Nguyen, T., Lawrence, C., La Borderie, C., Matallah and M., Nahas, G., "A mesoscopic model for a better understanding of the transition from diffuse damage to localized damage", European Journal of Environment and Civil Engineering, Vol. 14, No. 6-7, August 2010, pp. 751-776.

Omar, M., Loukili, A., Pijaudier-Cabot, G. and Le Pape, Y., "Creep damage coupled effects : experimental investigations on bending beams of different sizes", Advanced Engineering Materials, Vol. 21, No. 2, February 2009, pp. 65-72.

Orchard, D.F., "Concrete Technology Vol. 1: Properties of Materials", Applied Science Publishers Ltd., England, 1979.

Pijaudier-Cabot G. and Bazant, Z.P., "Nonlocal damage theory". Journal of Engineering Mechanics, Vol. 113, No. 10, October 1987, pp. 1512-1533.

Pijaudier-Cabot, G. and Reynouard, J.-M, "Comportement mécanique du béton", Lavoisier, 2005.

Polivka M., Pirtz D. and Adams R.F., "Studies of creep in mass concrete", Symposium on Mass Concrete, ACI Special Publication, Vol. 6, 1963, pp. 257-286.

Powers, T.C., "The Thermodynamics of Volume Change and Creep", Materials and Structures, RILEM,Vol.1, No. 6, November-December 1968, pp. 487-507.

Ranaivomanana, N., Multon, S. and Turatsinze, A., "Tensile, compressive and flexural basic creep of concrete at different stress levels", Cement and Concrete Research, Vol. 52, October 2013, pp. 1–10

Reviron, N., Benboudjema, F., Torrenti, J.M., Nahas, G., Millard, A., "A Coupling between creep and cracking in tension", FraMCos 6 - 6th International Conference on Fracture Mechanics of Concrete and Concrete Structures, 2007.

Reviron, N., "Etude du fluage en traction. Application aux enceintes de confinement des centrales nucléaires à eau sous pression", Thesis Submitted to ENS Cachan for Ph.D Degree, Paris, France, 2009.

Roll, F., "Long time creep-recovery of highly stressed concrete cylinders", ACI Special Publication, Vol. 9, 1964, pp. 95-114.

Rossi, P., Tailhan, J.L. Tailhan and F., Le Maou, "Creep strain versus residual strain of a concrete loaded under various levels of compressive stress", Cement and Concrete Research, Vol. 51, 2013. pp. 32-37.

Rots, J.G. "Computational modeling of concrete fracture", Thesis Submitted to Delft University of Technology for Ph.D. Degree, Netherlands, 1988.

Saliba, J., Grondin, F., Matallah, M., Loukili, A. and Boussa, H., "Relevance of a mesoscopic modeling for the coupling between creep and damage in concrete", Mechanics of Time-Dependent Materials, Vol. 17, No. 3, August 2012, pp 481-499.

Saliba, J., Loukili, A., Grondin, F. and Regoin, J.-P., "Experimental study of creep-damage coupling in concrete by acoustic emission technique", Materials and Structures, Vol. 45, No. 9, February 2012, pp. 1389-1401.

Schapery, R.A., "Correspondence principles and a generalized J integral for large deformation and fracture analysis of viscoelastic media", International Journal of Fracture, Vol. 25, No. 3, 1984, pp. 195-223.

Scrivener, K.L., Crumbie, A.K. and Laugesen, P., "The interfacial transition zone (ITZ) between cement paste and aggregate in concrete", Interface Science Journal, Vol. 12, No. 4, October 2004, pp. 411–421.

Sellier, A. and Buffo-Lacarrière, L, "Vers une modélisation simple et unifiée du fluage propre, du retrait et du fluage en dessiccation du béton", European Journal of Environmental and Civil Engineering, Vol. 13, No. 10, ,2009, pp. 1161-1182.

Smadi, M.M., State, F.O. and Nilson, A.M., "Shrinkage and Creep of High-, Medium-, and Low-Strength Concrete, Including Overloads", ACI Materials Journal, Vol. 84, No. 3, May-June 1987, pp. 224-234.

Thai, M.-Q., Bary, B. and He, Q.-C., "A homogenization-enriched viscodamage model for cement-based material creep", Engineering Fracture Mechanics, Vol. 126, August 2014, pp. 54-72.

Torrenti, J.-M. and Benboudjema, F. "Sur les déformations à très long terme des structures en béton précontraint", 32nd Meetings of AUGC, Polytech Orleans, from 4 to 6 of June, 2014.

Troxell, G. E., Raphael, J. M. and Davis, R. E., "Long-time creep and shrinkage test of plain and reinforced concrete", ASTM Proceeding, Vol. 58, 1958, pp. 1101-1120.

Ulm, F.-J. and Acker, P., "Le point sur le fluage et la recouvrance des bétons. Bulletin des Laboratoires des Ponts et Chaussées", 1998, pp. 73-82.

Vidal, T., Sellier, A., Ladaoui, W. and Bourbon X., "Effect of temperature on basic creep of high performance concretes heated between 20°C and 80°C", Third International Conference on Sustainable Construction Materials and Technologies, Japan, August 2013

Wagner, O. and Kriechen, D., " Unbewehrten beton", German Committee for Reinforced Concrete, No. 131, Berlin, 1958, P. 74.

Ward, M. A. and Cook, D. J. “The mechanism of tensile creep in concrete”, Magazine of concrete Research, Vol. 21, No. 68, September 1969, pp 151-158.

Wittmann, F.H., “Einfluss des feuchtigkeitsgehaltes auf das kriechen des zementsteines”, Rheologica Acta, Vol. 9, No. 2, April 1970, pp. 282–287.

Wittmann, F.H., “Interaction of hardened cement paste and water”, Journal of The American Ceramic Society, No. 8, Vol. 56, August 1973, pp. 409-415.

Wittmann F.H., “Creep and shrinkage mechanisms”, in: Bazant Z.P., Wittmann F.H., “Creep and Shrinkage in concrete Structures”, Wiley, 1982, pp. 129-161.

Zongjin, Li., “Advanced concrete Technology”, John Wiley and Sons, Inc., Hoboken, New Jersey, 2011.

Zou, D., Liu, T., Teng J., Du, C. and Li, B., “Influence of creep and drying shrinkage of reinforced concrete shear walls on the axial shortening of high-rise buildings”, Construction and Building Materials, Vol. 55, No. 31, March 2014, pp. 46-56.